GLUED-IN RE-BAR CONNECTION

by

Robert Malczyk

M.Sc.(Civ.Eng), Warsaw Technical University, Warsaw, Poland,1990.

A THESIS SUBMITTED IN PARTIAL FULFILLMENT OF
THE REQUIREMENTS FOR THE DEGREE OF
MASTER OF APPLIED SCIENCE

in

THE FACULTY OF GRADUATE STUDIES
DEPARTMENT OF CIVIL ENGINEERING

We accept this thesis as conforming
to ~~the~~ required standard

THE UNIVERSITY OF BRITISH COLUMBIA

October 1993

In presenting this thesis in partial fulfilment of the requirements for an advanced degree at the University of British Columbia, I agree that the Library shall make it freely available for reference and study. I further agree that permission for extensive copying of this thesis for scholarly purposes may be granted by the head of my department or by his or her representatives. It is understood that copying or publication of this thesis for financial gain shall not be allowed without my written permission.

(Signature)

Department of CIVIL ENGINEERING

The University of British Columbia
Vancouver, Canada

Date 14/10/94

DE-6 (2/88)

Abstract

The aim of this research was to develop a reliable structural timber connection, which would break by failure of its steel components, thus taking advantage of the lower variability and higher strength of steel.

The basic concept of the joint was to glue the reinforcing bars in pre-drilled holes and develop a bond strength stronger than tensile resistance of the bar.

This report describes the testing and design of such connections. The joints consist of re-bars and steel plates. Weldable #10 and #20 re-bars were used. The steel plates were cut from flat bar. The re-bars are welded to the steel plates and inserted into the holes, and fixed to the wood by epoxy glue. The holes are drilled on an angle to the grain; 30 degree angle was found to be the most effective.

The testing consisted of preliminary pull-out tests used to establish the embedment length needed to induce steel failures. Additional testing examined the behavior of glued-in rod joints used as a beam splice connection, a column foundation joint loaded with horizontal forces, and knee joints as used in a portal frame, loaded with positive and negative moment. Steel failures were observed consistently.

A typical portal frame was designed in order to tie the research to practical applications. Internal forces from this analysis were then used as a guide to the magnitude of the forces that can be expected in real life situations.

In the last part of this report the necessary design steps for two configurations of glued-in rod joints are presented :

1. Column foundation or beam splice joints.
2. Knee joints.

This was performed in order to inform structural engineers how glued-in rod joints

work under load, and how they should be designed.

Glued-in rod connections have several advantages over presently used systems. They can be manufactured in the glulam plant, using conventional tools, reducing the field work to merely bolting of the joints. The construction method becomes very similar to the erection methods of the steel structures. The elements are connected by bolts or welding. Glued-in rod connections have a great potential to become a safe connection method for the statically indetermined structures.

The testing of knee joints showed the possibility of developing a moment resisting connection, which would make glulam more competitive against steel in the area of portal frames widely used for commercial buildings.

TABLE OF CONTENTS

Table of Figures

List of Tables

Table of Photographs

Acknowledgement

The author is very grateful to his supervisor Professor Borg Madsen for his guidance, valuable suggestions, and encouragement throughout this research.

The author express his gratitude to Professor R.O. Foschi for theoretical input and for reviewing the manuscript, and Professor R. Sexsmith for reviewing the manuscript.

Appreciation is extended to Mr. H. Kulmann, Mr. P. Symons, and Mr. R. Wiktor for the helpful participation in preparing and maintaining instrumentation used in the experimental part of this research, and for necessary assistance during the various investigations.

Research grant from British Columbia Science Council is gratefully acknowledged.

Extensive testing described in this report was possible with the help of the following companies: Industrial Formulators of Canada, Structurlam, Surrey Laminaters, and Truss Joist MacMillan.

The author wish to thank his family and friends for their support throughout his graduate career.

CHAPTER 1

INTRODUCTION AND LITERATURE REVIEW

1.1 INTRODUCTION

In today's construction market timber structures are less developed than steel and concrete structures. There are several reasons for this. For years timber buildings were designed as statically determined structures, because there were no tools to calculate indeterminate structures accurately. Because of wide use of computers, this is no longer valid.

The real reason however for timber structures being less developed than structures made from steel and concrete is a lack of reliable connections.

In indeterminate structures the efficient use of material depends on the availability of rigid connections. To make timber more competitive new kinds of rigid joints are under development. There are several approaches to this problem and many research programs are presently under way dealing with rigid joints.

One technique is to make a connection where the failure is forced to occur in the steel thus utilizing its small variability. Properly designed connections will fail by tension failure in the steel dowel, without affecting the wood.

The idea originated in Scandinavia where steel rods, were inserted in holes drilled parallel to grain and fixed to the wood by adhesives. Research modifying this method is presented in the following literature review.

1.2 LITERATURE REVIEW

1.2.1 GENERAL COMMENTS

A comprehensive overview of research related to the topic of this thesis is presented in chronological order. Studies on glued-in rod connections are presently performed (October, 1993) in Canada, Finland, Russia, Australia and New Zealand.

Two different approaches are represented. Russian and Finnish researchers are using reinforcing bars glued in to glulam at an angle. In New Zealand and in Australia rigid connections using rods glued parallel to grain are being tested.

The first research on glued-in steel rods in laminated timber was performed in Sweden around 1965.

1.2.2 RIBERHOLT.

The first major work on dowels glued in glulam was performed by Riberholt (1980, 1986, 1988.) In Denmark. Riberholt used threaded rods, glued parallel to grain.

His report covers testing with pull-out tests where axial loads were applied for both short and long term period. In addition rods subjected to lateral loads were mentioned. This information is then applied to spliced beams tested under both wet and dry service conditions. Column foundation joints were also developed, which could transmit moments and shear forces in addition to axial loads. Finally the experience was applied to connections where moment resistant joints were required.

In order to achieve this it was necessary to establish the minimum embedment lengths that would cause yielding in the steel rather then bonding failure in the glue when subjected to an axial tension load.

The effect of the rod diameter was also investigated as well as the influence of the hole size. The importance of the density of the glulam was also investigated.

The physical dimensions such as end distances were established such that the failure

would take place in the wood. Several glue types were investigated, and while some differences were observed both Polyurethane and Araldite glue were found to be acceptable.

From his tests with the effect of moisture content it was found that wet specimens were generally 15 percent weaker than the dry ones.

Riberholt also noted that long term pull-out tests specimens exposed to outdoor conditions have half the strength of the matching specimens tested under dry conditions.

Summary :

1. Equations for maximum pull out force depending on hole diameter, embedment length, and specific density were determined.
2. An edge distance of 1.5 times dowel diameter was found to be sufficient to secure full strength of glued in dowel.

Figure 1.1 shows the moment resistant column foundation joint that was investigated by Riberholt.

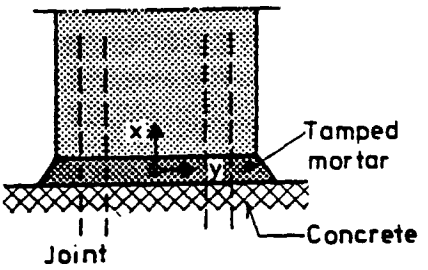

Figure 1.1 Moment resisting column foundation joint. Riberholt, (1986).

In 1986 Riberholt started testing of moment resisting knee joint connection. Figure 1.2 presents moment resistant knee joint tested in this program. The capacity of the joint reached 80% of the glulam cross-section capacity.

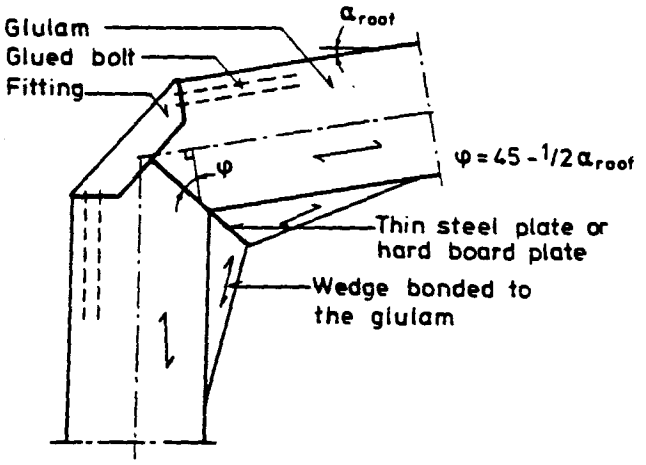

Figure 1.2 Moment resisting knee joint. Riberholt, (1986).

1.2.3 TURKOWSKIJ.

Connections using reinforcing bars glued into glulam on an angle to grain have been introduced in Russia in 1975, Turkowskij, (1991). Re-bars were glued into pre-drilled holes 4 mm larger than their diameter. Epoxy was used as the adhesive. The re-bars were then welded to the slotted steel plate, connecting to the next element.

Several tests were performed, checking the behavior of these joints in tension, compression, bending, and shear.

Several buildings have been completed using this connection method. The list includes sport centre, where glued-in re-bars were used as knee and column foundation joints. See Figure 1.3 This method was also used for reinforcing existing glulam structures.

For architectural reasons Canadians would find this connection unacceptable because of the appearance and the welding up against glulam. However the concept of glueing dowels on an angle to grain was used in the connection presented in this thesis.

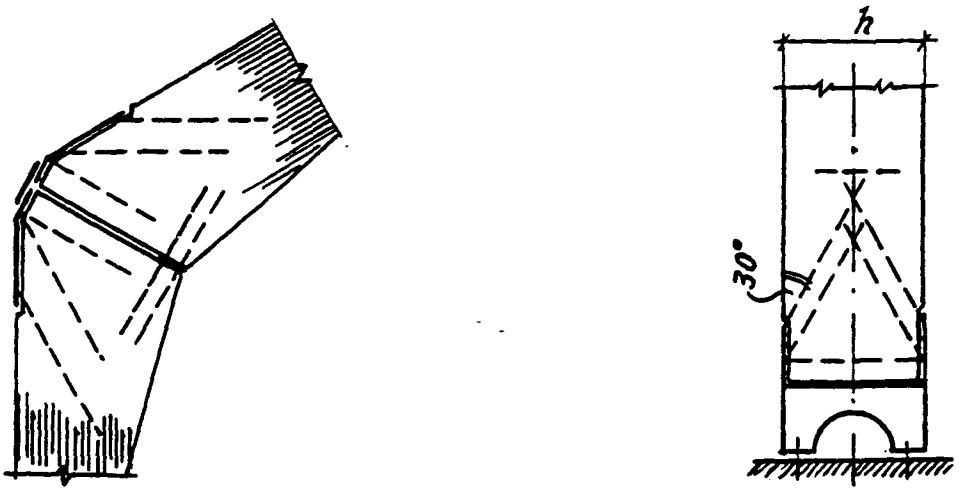

Figure 1.3 Knee and column-foundation joint, Turkowskij (1991)

1.2.4 TOWNSEND AND BUCHANAN.

An extensive program of glued in dowels testing was carried out by Townsend and Buchanan, (1990), in New Zealand. It should be noted that they used high strength reinforcing bars glued parallel to grain.

Their testing program duplicates the experiments conducted by Riberholt but using radiata pine wood. Unlike Riberholt, Townsend and Buchanan used reinforcing bars as well as threaded rods.

During the next series of tests, Townsend examined the behaviour of several beam splice joints using reinforcing bars. See Figure 1.4. The capacity of the connection was higher than the capacity of the glulam cross-section. The beam splice used in this program is shown on Figure 1.4

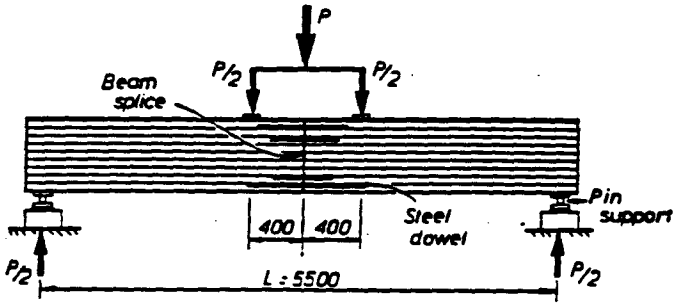

Figure 1.4 Beam splice joint, Townsend, Buchanan, (1990)

Several types of knee joints were tested by Buchanan and Townsend. The most successful one, using structural steel bracket is already patented. See Figure 1.5

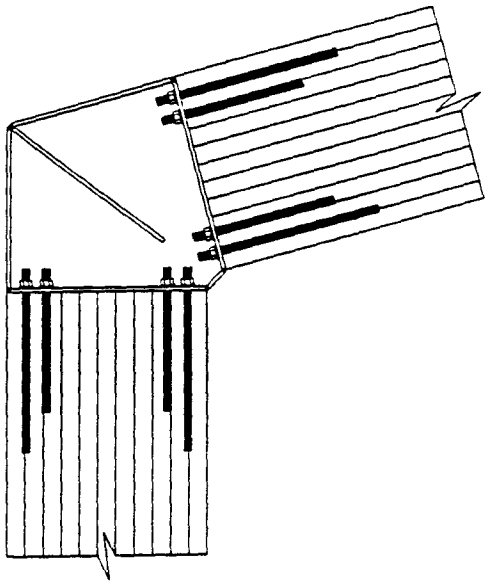

Figure 1.5 Knee joint using structural steel bracket, Townsend, Buchanan (1990)

Conclusions :

1. Equations for the maximum pull-out force were established in the function of : bar

diameter, embedment length, ratio of hole diameter to bar diameter, ratio of edge distance and bar diameter. The equations developed by Riberholt were confirmed during Townsend and Buchanan tests.

2. In dry wood specimens, adhesive Araldite K-2005, (similar to polyurethane used by Riberholt), behaved similar to Araldite K-80 (more rigid epoxy).

3. The resistance of the specimens with K-80 epoxy, tested after wet and dry cycles was 20% weaker than the ones with K-2005 adhesive.

4. In over 300 tests there was no glue failure of the adhesive bond between the epoxy and the wood surface. Pull out failures, when they did occur were caused by a shear failure in the surrounding wood, away from glue line.

1.2.5 CONCLUSIONS

1. The number of research programs presently under way using glued-in dowels testifies to the need for better connection methods.

2. Reinforcing bars can be used for the glued-in rod connections. A cost comparison of re-bars and threaded rods favours the re-bars.

3. Inclined bars engage more of the glulam cross-section, than parallel glued ones, which behave more like skin connectors. The re-bars also increase the shear capacity of the glulam cross-section.

4. Another advantage of the inclined bars is that in contrast to parallel bars they do not cause air pockets during the gluing operation, so they are easier to make and more reliable.

5. Holes 4 mm larger, than the re-bar diameter were found acceptable by mentioned researchers.

CHAPTER 2

PRELIMINARY ANALYSIS

2.1 INTRODUCTION

The aim of this chapter is to establish what internal forces can be expected in a heavily loaded portal frame. The span of the frame was chosen to be 12 m, spacing - 6 m. A 175 mm wide, 20f-EX glulam sections were used. Roof slope was selected to be 8 degrees to check a demanding geometry resulting in high bending moments at the knee joints.

Three frame types with different hinge locations were analyzed:

1. Fixed frame.
2. Two hinged frame - foundation hinges.
3. Three hinged frame.

The frame with foundation hinges, rigid knee joints and rigid apex joint was found to be the most effective. This frame was subsequently designed according to CAN/CSA 086.1-M89. Several load cases were checked including snow, wind, earthquake, as well as their combinations. Bending moment and shear force envelopes were established. The knowledge of internal forces found in this chapter was used as background for the experimental part of this thesis. Four full size tests of the knee joints, from the designed frame were tested, as final experiments described in this report. See Chapter 7.

2.2 FRAME GEOMETRY

Many commercial buildings need portal frames with clear span of 10 to 15 m. The shape of the frame was selected to be a demanding one, where high values of internal forces are present. The spacing was chosen to be 6 m for the snow loads in Vancouver. For other areas, where the snow load is higher, the spacing should be proportionally decreased.

The final geometry, see Figure 2.1, was developed in conjunction with the glulam manufacturers. In their opinion there is a great need for development of this type of joints

for these structural frames.

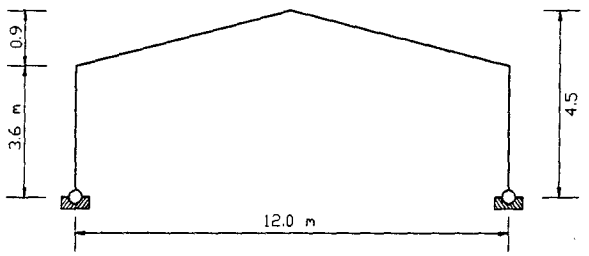

Figure 2.1 Frame geometry.

2.3 LOADING

Vancouver B.C. was chosen for the location of the building. The climatic data was established according to Canadian Building Code.

1. Snow load : Ss = 2.5 kPa, Sr = 0.3 kPa.
2. Wind load : q = 0.55 kPa
3. Earthquake load : v = 0.2

The frame was loaded with four load combinations.

- dead load + full snow load
- dead load + wind load
- dead load + earthquake load
- dead load + wind load + 1/2 snow load

The limit states load factors were used according to CAN/CSA 086

2.4 SUMMARY OF THE ANALYSIS

A two hinge glulam frame of the geometry shown on Figure 2.1 was designed for an industrial building in Vancouver. Appendix A presents the loads, and the design of decking and purlins, as well as design of the frame.

The following table presents the maximum internal forces obtained during analysis at knee joint for all load combinations.

Load combination	Bending moment kNm	Shear force kN	Axial force kN
1. Full snow	219.5	111.4	147.9
2. Wind	51.6	26.5	18.5
3. Earthquake	-22.6	3.3	22.9
4. Wind + half snow	76.6	24.4	25.3

Table 2.4 Internal forces obtained during analysis.

The maximum bending moment occurred during full snow load - positive moment resulting in tension on outside of the frame, and during earthquake load - negative bending moment resulting in tension on the inside part of the knee joint area. Negative moment from earthquake load was around 10% of the positive moment from full snow load. Maximum shear and axial forces were found during full snow load.

2.5 PRELIMINARY CONNECTION DESIGN

The analysis provided the external forces that can be expected in the heavily loaded portal frame. Maximum bending moment under full snow load was 219.5 kNm. This results in a tension force in re-bars Fr = 391.4 kN. The following figure shows the forces in glued-in rod connection, and the free body diagram, for a very simple concept of joint behaviour, used as a first approximation.

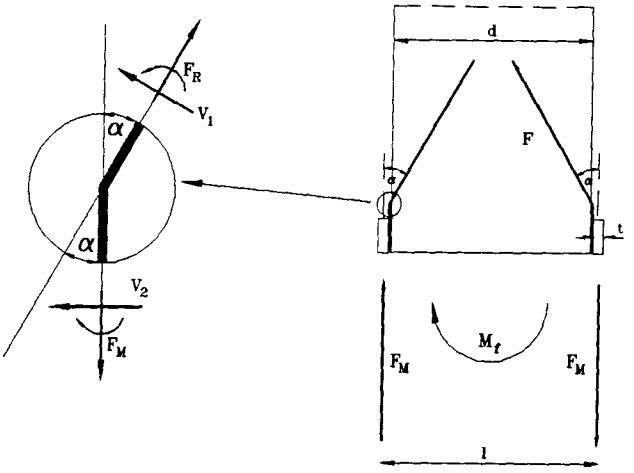

Figure 2.2 Forces in the glued-in re-bar connection.

$$F_M = \frac{M_f}{l} = \frac{219.4}{0.646} = 339.6kN$$

$$F_R = F_M \times \cos(\alpha) = 339.6 \times \cos(30) = 295.6kN$$

In the calculation of force Fr the following assumption was made :

Shear force V2 is assumed small in comparison to Fm and it was neglected.

Assuming standard variation - 15%, increase for the fifth percentile equals to 1.33

$$F_R^{'} = 1.33 \times 295.6 = 392.4kN$$

Therefore the embedment length of the re-bars during the pull-out tests has to be enough to ensure the tension failure of the re-bars, at the pull out force above 400 kN . Assuming that the re-bars would yield at stress of 400 MPa, and #20 re-bars will be used in the joint the required re-bar area can be calculated.

$$A_{reb}^{req} = \frac{F_R^{'}}{F_v} = \frac{400 \times 10^3}{400} = 1000mm^2$$

$$n_{reb} = \frac{A_{reb}^{req}}{A_{reb}} = \frac{1000}{300} = 3.3$$

Four #20 re-bars are needed at the knee joint connection. The re-bars will be stressed to

83% of the yield stress.

2.6 SUMMARY

1. This chapter has established that a suitable joint being able to resist the bending moment of 219.4 kNm requires four #20 re-bars.

CHAPTER 3

MATERIALS USED FOR TESTING

3.1 INTRODUCTION

This chapter describes the types of materials used in this program for making specimens. The test types were :

- pull-out tests (embedment length)
- beam test (splice joint)
- racking tests (column foundation joint)
- knee joint tests (frame structures)

Materials readily available in the building supply trade were chosen.

3.2 GLULAM

Three sources of glulam were used for the tests described in this report. The first source was some 30 year old beams recovered from UBC bookstore, that was demolished. This material was used for getting preliminary information from pull out tests.

The next source was Surrey Laminators Ltd. in Surrey B.C. The glulam grade chosen was 24f-EX, Douglas Fir. This material was used for the beam test, racking tests and one preliminary knee joint test.

The final part was prepared by Structurlam Ltd. in Penticton B.C., and used for the remaining knee joint tests. The material grade was 24f-EX and glulam was made of Douglas Fir lumber.

The inclination of the hole in the glued-in re-bar joint results in compression perpendicular to grain so this material property was tested. Compression perpendicular to grain was tested for four specimens. The compressed area was 130 x 130 mm. See Figure 3.1. The height of the specimen was 376 mm. Results are summarized in Table 3.1.

Specimen #	Maximum stress compression perp. to grain MPa
1	5.2
2	5.7
3	6.7
4	6.3
Average	6.0

Table 3.1 Compression perpendicular to grain test data.

This value is similar to 5.9 MPa stated in CAN/CSA-089.

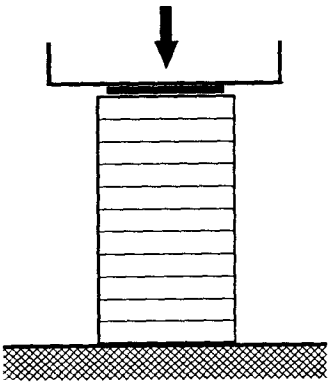

Figure 3.1 Compression perpendicular to grain specimen.

3.3 PARALLAM

Parallam 2.0E-SP PSL was provided by Truss joint MacMillan Ltd. Parallam was only used for a prewelded connection and tested in pull-out test. Because of a problem with glue leaks through the pores inside the cross-section, the use of this material was discontinued at this time. Thicker glue might be used for parallam to avoid the leaks. Because the data obtained from tests with parallam specimens was not reliable the results are not presented in this report.

3.4 STEEL RODS

Regular strength, deformed weldable reinforcing bars were used in the tests. Two bar diameters were tested : 10 mm and 20 mm. Reinforcing bars were chosen, because of their low price compared to threaded rods used by some other researchers for similar applications. Re-bars can be easily bent and cut to the desired length. Tension tests were performed for both re-bar diameters. Three specimens of each diameter were tested. Table 3.2 summarizes the results showing the average values. Figure 3.2 shows the typical load deformation relation for #10 re-bar.

Bar diameter - mm	10	20
Yield force - kN	45.2	144.2
Ultimate force - kN	67.5	202.2
Yield stress - MPa	452.1	481.5
Ultimate stress - MPa	675.0	674.1

Table 3.2 Re-bar tension tests results.

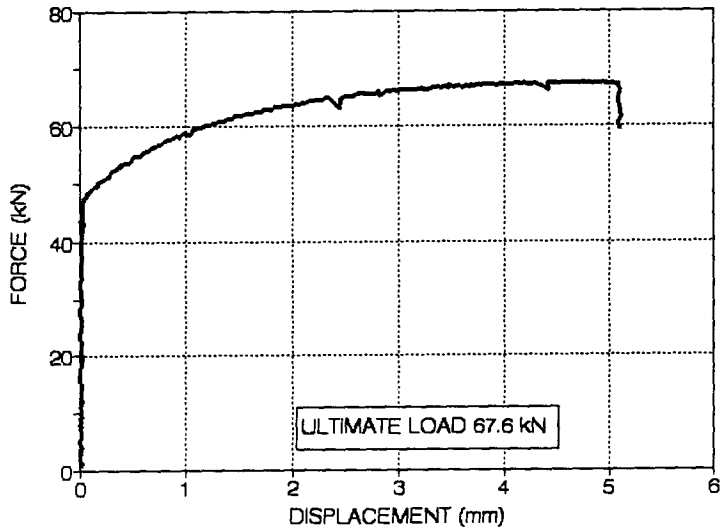

Figure 3.2 Force displacement relation for #10 re-bar tested in tension.

3.5 STEEL PLATES

All steel plates used for glued-in rod joints were type A-36, cut from flat bars. Specified minimum tensile strength was Fu = 400 MPa. The following flat bar dimensions were used for the different tests : 1/4" x 2" (6.4 x 50.8 mm) , 1/2" x 3" (12.7 x 76.2 mm) , 1/2" x 5" (12.7 x 127 mm) , 1/2" x 6" (12.7 x 152.4 mm).

3.6 BOLTS AND STUDS

Studs (See Figure 3.3), cut from threaded rods, were used in specimens for :

1. Pull-out tests.
2. Beam test.
3. Racking tests.

The diameter of the rod was 5/8" (15.9 mm). The rod was made of high strength steel (ultimate tensile stress - 830 Mpa), with thread type NF (National Fine).

The studs were replaced by the bolts in knee joints, because of the geometry of a knee joint. Connectors between the glulam steel plate and the outside strap had to be inserted from outside through the strap. The strap is a steel plate, which connects two glulam elements. The glulam steel plates are the internal parts of the connection fixed to glulam in the plant. The bolts were of No 7 grade with NF thread.

Figure 3.3 Glued-in re-bar connection used as a beam splice joint.

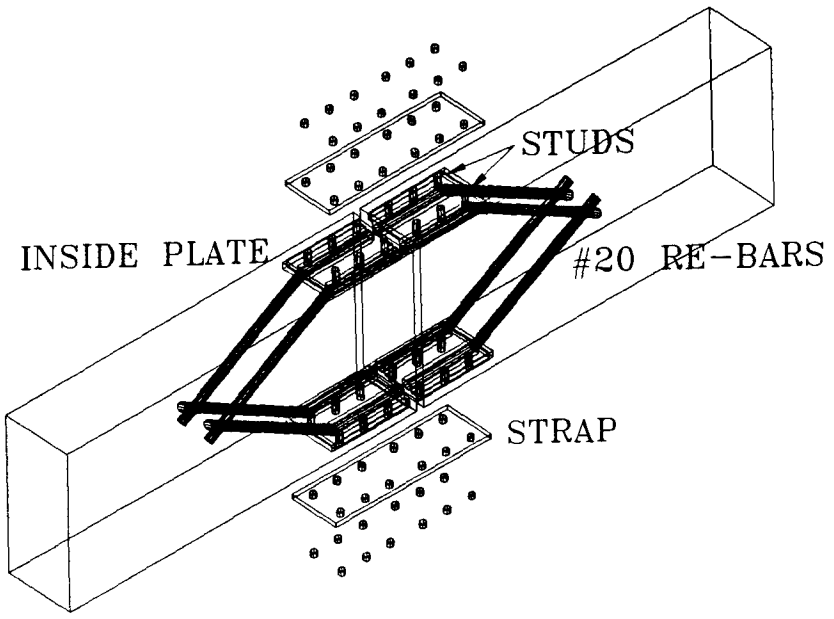

3.7 EPOXY

Only one type of epoxy - IFC-SP, was used for all the connections tested in this research program. This adhesive was manufactured by Industrial Formulators of Canada Ltd., Burnaby B.C. Raisin and hardener were shipped in separate bottles and mixed in proportion 42 to 100 by weight before application. The pot life was approximately 2 hours depending on the outside temperature. After gluing all specimens were left for 7 days before testing.

The glue was poured in to the holes before the re-bars were inserted. Because of the inclination of holes, there was no problem with air pockets inside the hole and no plugs were needed. Extra glue from the hole was used to ensure the proper contact between the glulam steel plate and the glulam surface, because of the presence of the compression perpendicular to grain. If needed additional glue was poured between the glulam steel plate and the glulam surface after the re-bars were inserted, to assure a tight fit.

The inclined holes eliminated shaking of the specimen to ensure the proper glue distribution, and plugs at the hole ends, needed when the holes are drilled parallel to grain.

CHAPTER 4

PULL-OUT TESTS

4.1 TESTS OBJECTIVES.

The first objective of the pull-out tests was to establish the embedment lengths of the re-bars required to ensure failure in the steel. The holes for the re-bars were drilled at different angles to grain. The first series of pull-out tests described in this thesis was performed to repeat experiments conducted by the mentioned researchers but using Canadian materials.

The concept of gluing bars at the angle was first used in Russia, see Turkowskij, 1990. The appearance of the Russian connection however is unacceptable from a Canadian architectural point of view. Further more, the exposed weld, and the fact that the welding is performed close to the glulam surface, burning the wood surface is undesirable.

The second objective was therefore to eliminate the welding close to glulam, possibly damaging the epoxy glue, and improve the appearance of the connection. This was achieved by developing the "pre-welded" joint, in which the welding is performed before the re-bars are glued, away from glulam, and on the underside of the steel plate, making the weld invisible.

The third objective of this series of tests was to develop a reliable method of manufacturing glued-in rod joints.

It was decided to exclude the glue type and the hole size from the test objectives.

4.2 EVOLUTION OF PULL-OUT TEST SPECIMEN

This section describes the evolution of the pull-out test specimen.

1. Preliminary joint.

The preliminary joint was similar to one used by Turkowskij, (1990). The re-bars were glued in and then welded to the slotted steel plate. The preliminary joint is presented on Photograph 4.1. Note that the appearance is not attractive

2. Pre-welded connection.

The re-bars are here pre-welded to the steel plate before glueing, as described earlier. Daps in the glulam are cut so the flat part of glulam and the steel plate are touching each other. Additional glue is added for better contact, between the steel plate and glulam. This joint has several advantages compared to the preliminary connection.

- increase of the bearing area.
- avoid heating of epoxy glue while welding, which would decrease the bond stress.
- improved appearance since weld is hidden and the wood is not burned by welding.

The only disadvantage of the pre-welded joint is more labor intensive since greater accuracy is needed for proper fitting.

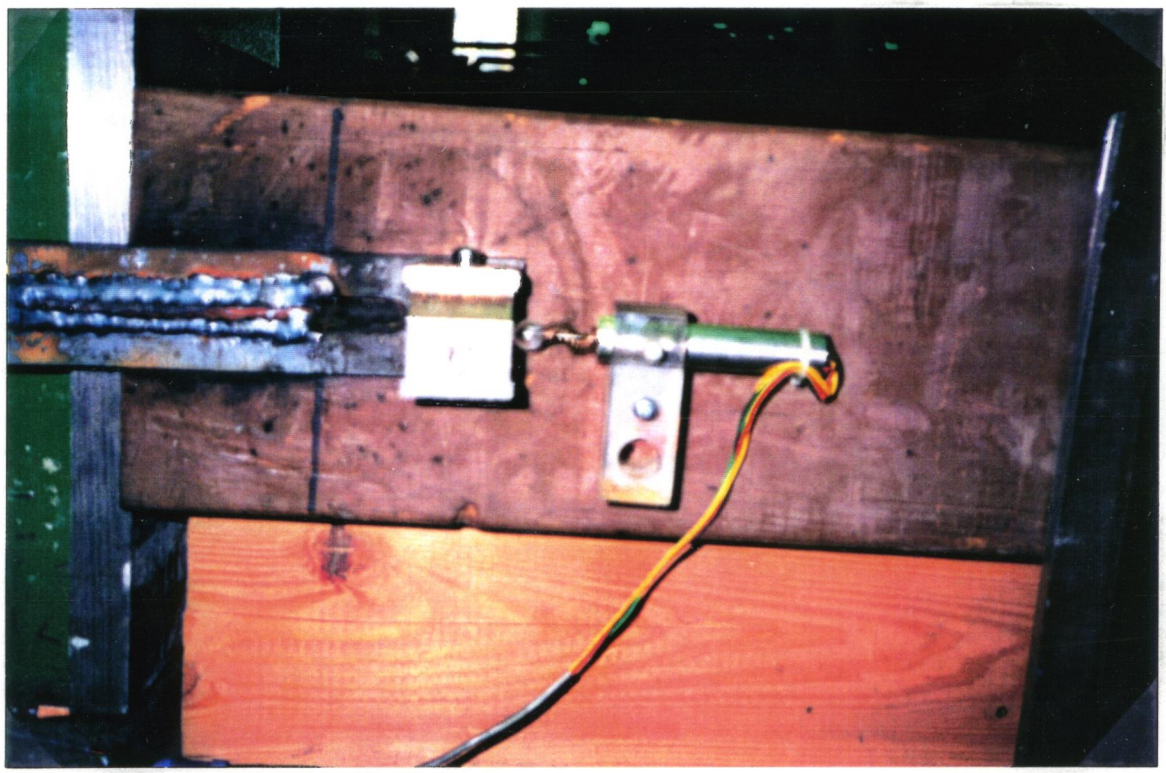

Photograph 4.1. Preliminary joint.

4.3 PARAMETERS.

During pull-out tests the effect of three parameters on the load displacement behavior was examined :

1. Embedment length of the reinforcing bar.

The aim was to find the embedment lengths of the re-bars, which will ensure a stronger bond between re-bar and glulam than the tensile resistance of the rod. This will result in tension failure of the re-bars, for all cases when the embedment length is longer than the boundary value.

2. Inclination of the hole.

Flatter angles result in smaller residual stresses in the bent section of the re-bar, but rods glued in at small angle to grain engage less of the glulam cross-section. This is similar to the behavior of the skin connectors. Larger angles, (up to 45 degrees), increase shear capacity of the cross-section and get hold of more glulam but result in higher residual stresses at the bent section of the re-bar.

3. Diameter of the reinforcing bar.

The first series of tests was done with #10 re-bars. The second series used #20 bars. The embedment lengths to ensure the re-bar tension failure were found for both diameters.

4.4 FABRICATION OF SPECIMENS

FABRICATION STEPS OF THE PRELIMINARY JOINT.

This section will describe the manufacturing steps of the preliminary joint, as done by Turkowskij, 1990.

1. Drilling of holes in glulam.

The hole diameter was 4 mm larger than diameter of re-bars. This was recommended by previous research - see Turkowsij, 1990, and Townsend, Buchanan, 1990. The drilling technique is presented on Photograph 4.2. The steel drilling guide was used to ensure the proper location and angle of the hole.

2. Cutting of re-bars to the desired length.

Length of re-bars was equal to the inside length of the hole plus 150 mm which was bent down.

3. Glueing of re-bars into the pre-drilled holes.

Epoxy was poured into the holes and re-bars were inserted. Due to the inclination of

the hole there were no problems with the air pockets.

4. Bending of re-bars

Re-bars were bent, without heating, to make the outside part parallel to the glulam surface.

5. Welding of the re-bars to the slotted steel plate.

The strap, was inserted on top of the re-bar and welded around the slot. The strap was a steel plate with slotted hole of the same length as a bent down re-bar. While manufacturing the specimens with #20 re-bars fabrication process was improved :

A. The re-bars were bent before glueing.

B. The slotted plate was replaced by the solid plate.

C. The re-bars were welded to the lower surface of the strap.

Figure 4.1 presents the manufacturing steps for the preliminary connection.

Figure 4.1 Manufacturing steps for the preliminary connection.

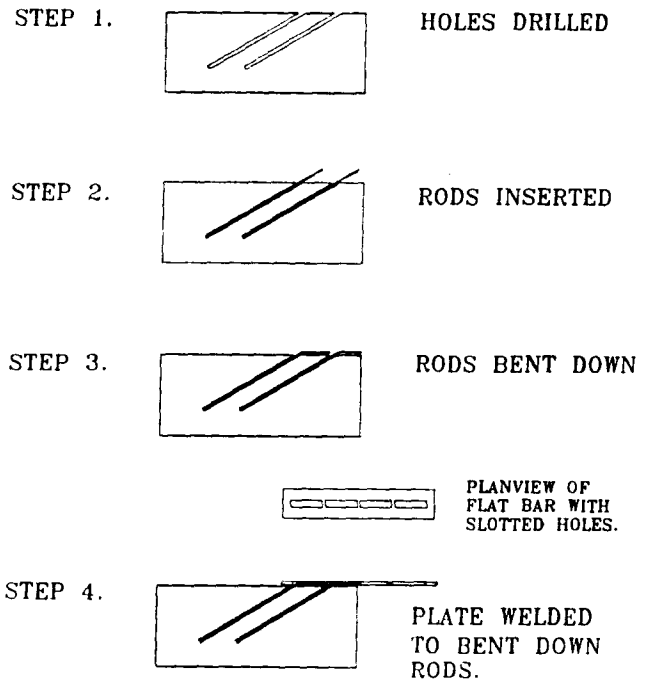

Photograph 4.2. The hole drilling technique.

FABRICATION STEPS FOR THE "PRE-WELDED" JOINT.

The following section will describe the manufacturing steps for the "pre-welded" joint.

1. Cutting out groves in glulaml

The pre-welded connection was designed to increase the bearing area available for compression perpendicular to grain, and to improve the appearance of the joint. The idea was to hide the connection inside glulam. The glulam steel plate was flush with the glulam surface. To achieve this daps for the bent re-bar sections and the plate had to be prepared. The shape of the openings is presented on Figure 4.2.

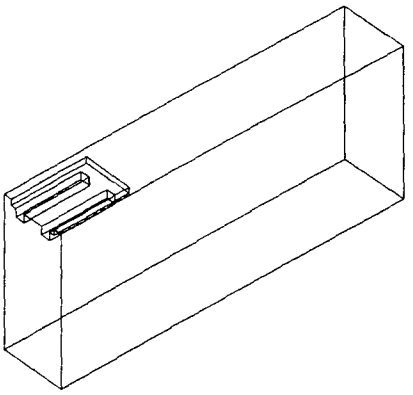

Figure 4.2 Prefabrication of the glulam for the pre-welded joint.

2. Drilling of holes in glulam.

The holes in glulam were drilled using the same technique as for the preliminary joints, after the grooves were cut.

3. Cutting and bending of re-bars.

The re-bars were cut and bent before gluing.

4. Tackwelding of the inserted re-bars to the steel plates.

The re-bars were inserted in the holes, steel plates placed on top of them, and then they were tackwelded. The purpose of this was to ensure the proper positioning of the re-bar in relation to the steel plate.

5. Welding of re-bar to the steel plate.

The re-bars and the steel plate were then removed from the hole and fully welded to the steel plate, away from the specimen, forming an assembly. The weld was positioned on the inside face of the plate.

6. Gluing of the re-bars in the holes.

The epoxy was mixed and poured in to the holes, and the assembly was inserted. The steel plate which was welded to the re-bar was resting against the glulam surface. Additional glue was poured between the steel plate and glulam surface to ensure the contact, and increase the bearing area. All steel surfaces, plates and re-bars, had been sand blasted before gluing. Failure between steel and the glue was not observed in any of the tests.

4.5 TEST PROGRAM

Pull-out tests were performed for the following test configurations :

1. Tests with #10 re-bars.

The effect of hole inclination, and re-bar embedment length were examined. The failure modes of specimens using #10 bars were observed.

2. Tests with #20 re-bars.

The effect of hole inclination, and re-bar embedment length were examined. The failure modes of specimens using #20 bars were observed.

3. Instrumented bar test.

The stress distribution along the embedded length of re-bar was examined.

4. Pre-welded connection.

The effect on the bearing stresses of the steel plate being pre-welded to re-bars and failure modes was examined. A manufacturing technique for the pre-welded joint was developed.

4.6 TEST SETUP AND TESTING METHOD.

All the tests described in this report were performed at the structures lab of the Department of Civil Engineering of U.B.C. In Vancouver. The test setup (See Photograph 4.3.), Used for the pull-out tests consists of :

1. Hydraulic jack and its support.
2. Horizontal support.
3. Vertical support.

The hydraulic jack was fixed by bolts to the steel frame which in turn was bolted to the concrete floor of the lab. The test specimen was placed against the horizontal support, which was also bolted to the floor. The vertical support was then placed on the two bolts sticking out from the floor and tightened against the specimen, to prevent the rotation of the specimen. The load cell was connected to the end of the hydraulic jack. A steel strap connected the specimen and the load cell, via pin. On the other end, the strap was fixed to the specimen via studs.

The force from the hydraulic cylinder, travelled from hydraulic jack through the steel plates to the re-bars. It was then transferred to the glulam by the glue bond between the re-bars and the wood. The load was increased at the constant rate, using a manual gage, until the failure of the specimen occurred.

Two sets of readings were recorded by the data acquisition system. One channel of data contained reading of the force from the load cell. The other was readings of the LVDT, which measured the relative displacement between the specimen and the steel strap. The body of the LVDT was fixed to the upper surface of glulam, while the moving part was resting on a magnetic base, which was sitting on the top of the strap.

Photograph 4.3. Pull-out tests setup.

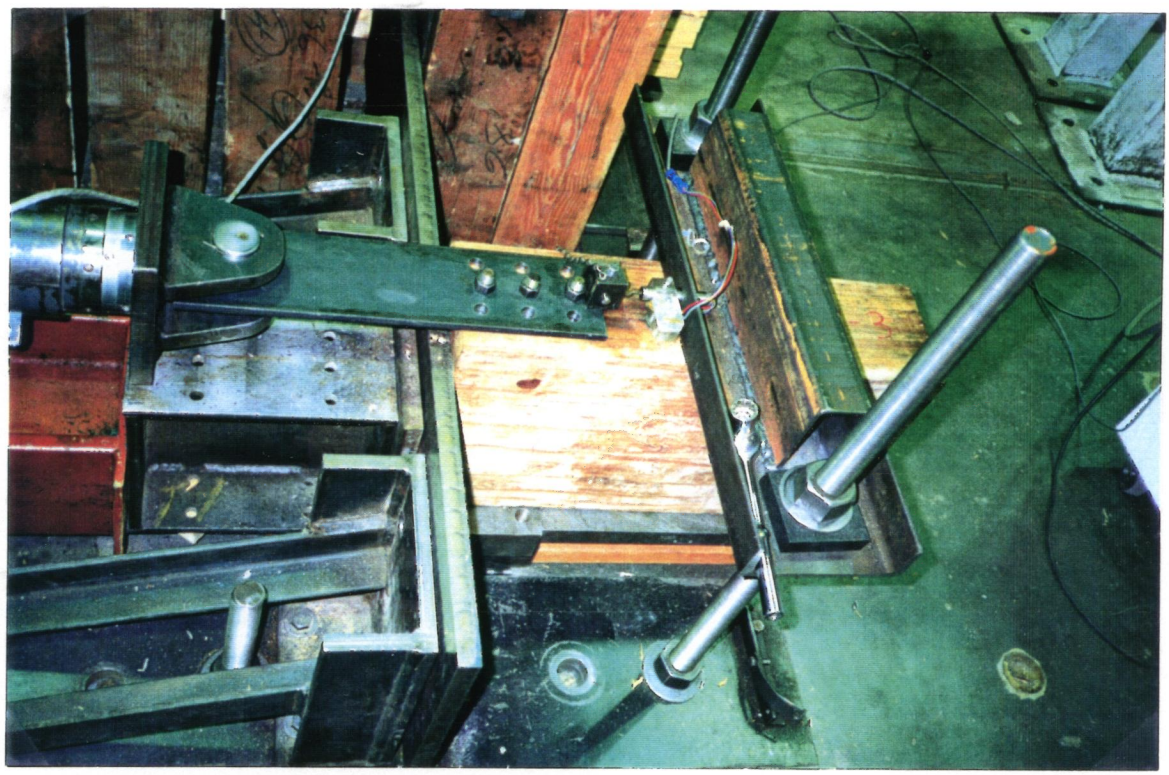

4.7 TESTS WITH THE PRELIMINARY CONNECTION.

Three types of experiments were preformed for the preliminary connection using single bars :

1. Tests with #10 re-bars.
2. Tests with #20 re-bars.
3. Test with the instrumented bar.

4.7.1 TESTS WITH #10 RE-BARS

The effects of two parameters were checked in this series of tests. The first one was the embedment length of the re-bar. The embedment length was measured along the re-bar from the glulam surface to the end of the rod. The re-bars were glued in on the entire length of the hole. Three embedment lengths were tested : 130, 300, and 380 mm.

The second parameter was inclination of hole relative to the direction of the grain. Three angles examined were : 15, 30, and 45 degrees.

The analysis of the tests results is presented according to the two failure modes, which are defined below.

1. Pull-out of the re-bar.

The bond between the glue and glulam fails and the bar is pulled out of the specimen. Failure between the steel and epoxy was not observed.

2. Tension failure in re-bar.

The failure takes place in the steel without affecting the wood. The re-bar yields and breaks in tension at the glulam surface, where it may have been weakened by the bending and by the welding.

PULL-OUT FAILURES.

Only specimens with the smallest embedment length of 130 mm failed by pull-out. Tests results are presented in Tables 4.1-A, 4.1-B, and 4.1-C, for 15, 30 and 45 deg respectively.

The following symbols are used in the Tables :

SPEC # - specimen number

Ld - embedment length

ALPHA - hole inclination to grain.

Fmax - maximum force applied during test

Dmax - displacement of the steel plate relative to glulam at maximum force.

STRESS - stress in re-bar at failure.

SPEC #	Ld (mm)	ALPHA (deg)	Fmax (kN)	Dmax (mm)	STRESS (MPa)
BL-8	130	15	59.7	2.5	573
BL-23	130	15	66.7	2.5	640
BL-24	130	15	67.8	2.4	651
AVERAGE			64.7	2.5	621

Table 4.1-A. Pull out tests results. #10 re-bars. ALPHA = 15 deg. Pull-out failures.

SPEC #	Ld (mm)	ALPHA (deg)	Fmax (kN)	Dmax (mm)	STRESS (MPa)
BL-1	130	30	69.7	9.1	606
BL-2	130	30	73.6	4.5	640
BL-13	130	30	69.0	4.5	600
AVERAGE			70.8	6.0	616

Table 4.1-B. Pull out tests results. #10 re-bars. ALPHA = 30 deg. Pull-out failures.

SPEC #	Ld (mm)	ALPHA (deg)	Fmax (kN)	Dmax (mm)	STRESS (MPa)
BL-5	130	45	68.3	11.1	483
BL-6	130	45	68.7	11.0	486
BL-22	130	45	73.3	9.7	518
AVERAGE			70.1	10.6	496

Table 4.1-C. Pull out tests results. #10 re-bars. ALPHA = 45 deg. Pull-out failures.

SUMMARY

1. The embedment length of 130 mm results in pull-out failures for all tested hole inclinations.

2. Essentially the same maximum forces were obtained for 30 and 45 degrees, while the values for 15 degrees were 7% lower.

3. The displacement of the plate at failure increases with increase of the hole inclination. Smallest displacements were observed for 15 deg angle and the largest for 45 deg.

4. The stresses at failure in the re-bars were above the yield stress - 400 MPa, for all specimens.

TENSION FAILURE IN RE-BARS.

All specimens with an embedment length of 300 and 380 mm failed as tension failure in the re-bar. The bars broke in tension just outside the hole, close to the glulam surface. The tests results are presented in Tables 4.2-A, 4.2-B, and 4.2-C.

The following symbols are used in the Tables :

SPEC # - specimen number

Ld - embedment length

ALPHA - hole inclination to grain.

Fmax - maximum force obtained during test

Dmax - displacement of the steel plate relative to glulam at maximum force.

STRESS - maximum stress in the re-bar

SPEC #	Ld (mm)	ALPHA (deg)	Fmax (kN)	Dmax (mm)	STRESS (Mpa)
BL-9	300	15	70.6	7.4	678
BL-17	300	15	84.1	6.4	807
BL-25	300	15	74.9	8.6	719
Average			76.5	7.5	734
BL-16	380	15	84.1	6.7	807
BL-19	380	15	78.3	7.7	752
BL-26	380	15	76.2	7.4	731
Average			79.5	7.3	768
AVERAGE	**FOR**	**ALPHA=15**	**78.0**	**7.4**	**748**

Table 4.2-A. Pull out tests results. #10 re-bars. ALPHA = 15 deg. Re-bar tension failures.

SPEC #	Ld (mm)	ALPHA (deg)	Fmax (kN)	Dmax (mm)	STRESS (Mpa)
BL-3	300	30	86.2	6.3	750
BL-4	300	30	76.4	8.3	665
BL-12	300	30	91.1	14.6	793
Average			84.5	9.3	735
BL-14	380	30	82.2	9.0	715
BL-11	380	30	79.7	14.8	693
BL-10	380	30	72.1	13.1	627
Average			78.0	12.3	679
AVERAGE	**FOR**	**ALPHA=30**	**81.3**	**11.0**	**707**

Table 4.2-B. Pull out tests results. #10 re-bars. ALPHA = 30 deg. Re-bar tension failures.

SPEC #	Ld (mm)	ALPHA (deg)	Fmax (kN)	Dmax (mm)	STRESS (Mpa)
BL-15	300	45	79.3	6.2	561
BL-21	300	45	77.3	9.7	547
BL-27	300	45	78.9	7.3	558
Average			78.5	7.7	555
BL-7	380	45	78.1	12.3	552
BL-18	380	45	75.9	16.3	537
BL-20	380	45	76.2	14.8	539
Average			76.7	14.5	542
AVERAGE	**FOR**	**ALPHA=45**	**77.6**	**11.1**	**548**

Table 4.2-C. Pull out tests results. #10 re-bars. ALPHA = 45 deg. Re-bar tension failures.

SUMMARY

1. Embedment lengths of 300 and 380 mm produce bond between re-bar and glulam stronger than tensile resistance of the rod. This causes re-bar tension failure.

2. The highest values of the force were obtained for angle alpha=30 degrees. Forces for other angles were close to each other and 5% less than the average of the specimens with 30 degree angle.

3. Displacement of the plate was the same for 30 and 45 degree angles. Displacement at failure for specimens with 15 degree angle was 30% smaller.

FORCE DISPLACEMENT RELATION FOR RE-BAR TENSION FAILURES

The following graph presents the relation between the force and displacement for specimen BL-10, which is typical for failures of re-bars. The embedment length was 380 mm. The angle of hole inclination was 30 degrees.

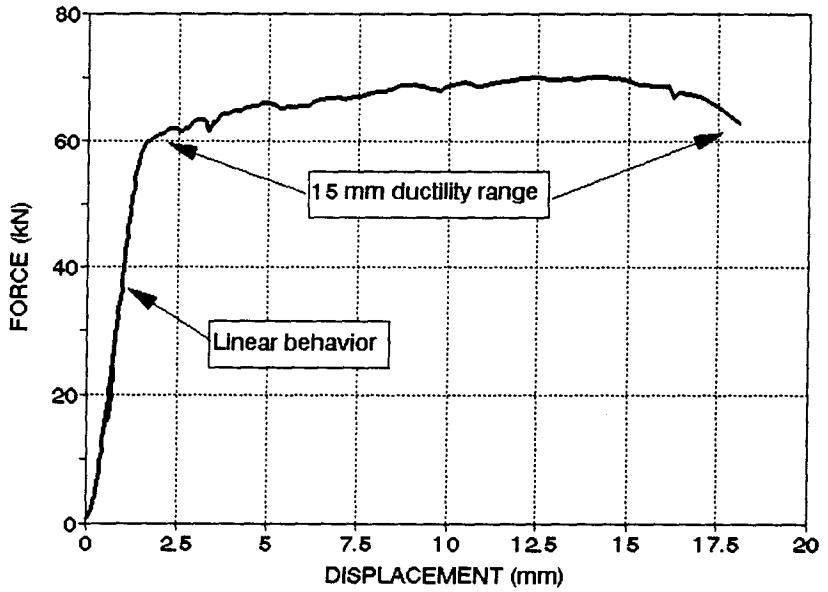

Figure 4.4 Force displacement relation for specimen BL-10, typical for re-bar tension failures.

The relation between force and displacement can be divided into two areas. The first one for forces up to 60 kN which is a linear relationship. For the forces higher than 60 kN, (stress in re-bar - 520 MPa), the re-bar starts to yield, and displacement is growing almost without the increase of force. The re-bar breaks after 15 mm elongation which is desirable for ductile connections. However the maximum force was 71 kN at 12.5 mm, causing a stress of 617.

SUMMARY AFTER TESTING #10 RE-BARS.

1. The tension failure occurs for the re-bars having an embedment length more than 300 mm.
2. 30 degree inclination results in the slightly higher force at failure.
3. Force displacement diagrams show a combination of linear behavior and a long ductility range.

4.7.2 TESTS WITH #20 RE-BARS

The main purpose of repeating the pull-out tests using #20 bars was to establish the embedment length needed to obtain tension failure in the re-bars for the larger bar diameter. To establish the embedment length needed to obtain the tension failure of re-bar more exact than for the #10 bars, five embedment lengths were tested : 130, 200, 260, 300, and 380 mm. As for previous tests three different inclinations were tested : 15, 30, and 45 degrees.

The analysis of the tests results is also presented according to the failure modes. Three failure modes were observed.

1. Compression perpendicular to grain failure.

The portion of re-bar close to the glulam surface crushes in the wood. The reason is that a bearing area is too small.

2. Pull-out of the re-bar.

The bond between the glue and glulam fails and the bar is pulled out of the specimen.

3. Tension failure in re-bar.

The failure takes place in the steel without affecting the wood. The re-bar yields and breaks in tension close to the glulam surface, weakened by the bending and by the welding

COMPRESSION PERPENDICULAR TO GRAIN FAILURE.

Compression perpendicular to grain failure occurred in the first three specimens, because not enough attention had been given to this failure mode. For all the remaining tests with #20 re-bars, the bearing area was increased, by inserting the steel plates between the strap and the glulam surface.

The following table presents tests results of the specimens, which failed by compression perpendicular to grain.

SPEC #	Ld (mm)	ALPHA (deg)	Fmax (kN)	Dmax (mm)	STRESS (MPa)
SP-1	380	45	222.0	6.4	532
SP-2	200	30	114.9	13.7	333
SP-5	260	45	134.7	5.7	317

Table 4.3 Pull out tests results. #20 re-bars. ALPHA = 30, 45 deg. Compression perpendicular to grain failures.

SUMMARY

1. A different type of failure was observed. For the higher forces compression perpendicular to grain initiates the first failure, when insufficient bearing area is provided.

2. This shows the importance of checking compression perpendicular to grain forces.

PULL-OUT FAILURE OFF THE RE-BAR.

Three specimens failed by pull-out failure of the re-bar. The following table presents the tests results.

SPEC #	Ld (mm)	ALPHA (deg)	Fmax (kN)	Dmax (mm)	STRESS (MPa)
SP-7	200	45	117.9	23.8	278
SP-10	260	15	185.3	15.6	593
SP-12	130	45	75.4	3.6	177

Table 4.4 Pull out tests results. #20 re-bars. ALPHA = 15, 45 deg. Bar pull-out failures.

SUMMARY

1. Embedment length needed to cause re-bar tension failure is bigger than 260 mm for 45 and 15 degree angles of hole inclination.

2. The force required to pull out the re-bar, increases with the increase of embedment length.

TENSION FAILURE OF RE-BAR

Tension failure of the re-bar occurred for #20 re-bars only after additional steel plates were inserted between the strap and the glulam surface, this increased the bearing area. Six specimens failed by re-bar tension failure. Tests results are presented in Tables 4.3-A, and 4.3-B.

SPEC #	Ld (mm)	ALPHA (deg)	Fmax (kN)	Dmax (mm)	STRESS (Mpa)
SP-9	260	30	179.8	19.0	521
SP-11	260	30	173.4	17.8	503
SP-4	300	30	164.8	16.5	478
SP-8	380	30	164.4	22.2	477
Average			170.6	18.9	495

Table 4.5-A. Pull out tests results. #20 re-bars. ALPHA = 30 deg. Bar tension failures.

SPEC #	Ld (mm)	ALPHA (deg)	Fmax (kN)	Dmax (mm)	STRESS (Mpa)
SP-3	380	15	190.9	11.0	608
SP-6	300	45	137.1	20.9	324

Table 4.5-B. Pull out tests results. #20 re-bars. ALPHA = 15,45 deg. Bar tension failures.

SUMMARY

1. The tests showed with reasonable degree of confidence that the embedment length to create the tension failure in the re-bar was 260 mm for 30 degree angle. (4 tests).
2. Embedment lengths for other lengths and angles are less certain.
3. The more the bar is bent the higher are the residual stresses, which reduce the tensile strength of the re-bar. The highest force was recorded for 15 degree angle and the lowest for the 45 degree angle. The presence of welding in this area of the re-bar also decreases the tensile strength of the bar.
4. The longest displacement at failure was observed for the 45 degree angle and the shortest for 15 degree angle. The reason for that is that the steeper angles create higher compression perpendicular to grain stresses and hence longer displacements.

FORCE DISPLACEMENT RELATION FOR TENSION FAILURE IN THE RE-BARS.

The following graph presents the force displacement relation for Specimen SP-9, typical for the tension failure of the re-bars. The embedment length was 300 mm. The inclination was 30 degrees.

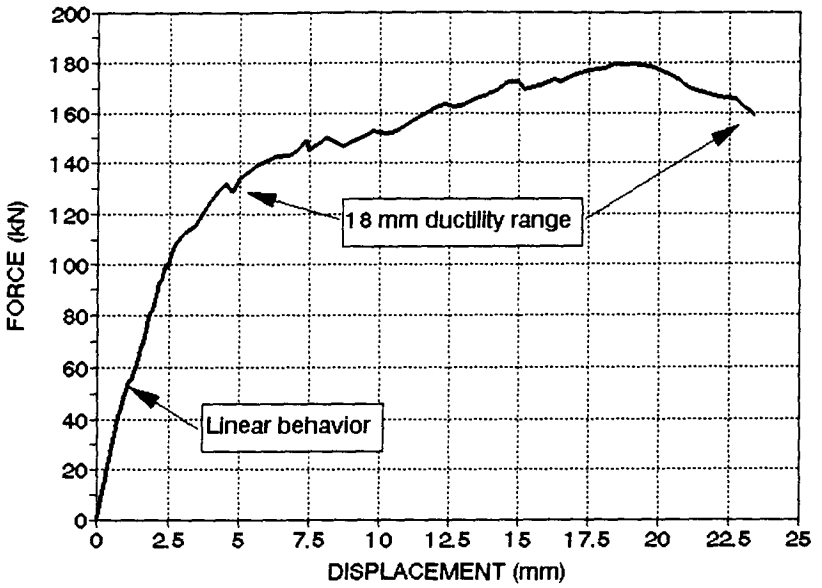

Figure 4.5 Force displacement relation for specimen SP-9.

The relation between force and displacement can be divided in to two areas. The first one up to the force of 120 kN is a linear relation. Then a non linear part consists of yielding of the rod and strain hardening, similar to the straight tension tests. (No bent in re-bar)

SUMMARY FROM TESTING OF #20 RE-BARS.

1. When the embedment length is more than 260 mm for 30 degree angle of hole inclination, the failure occurs in the re-bars.

2. The more the rod is bent, the less is the force needed to break it in tension. This is caused by the combination of welding stresses, cold bending, and compression perpendicular to grain component.

3. The force displacement diagrams show the following behavior : linear relation, followed by yielding, strain hardening, and rupture.

4.7.3 TEST WITH AN INSTRUMENTED BAR

After testing the #10 re-bars, it was observed that the re-bar will yield if the embedment length is at least 300 mm. The test however did not show the minimum embedment length needed to create the tension failure in the re-bar.

Another way of determining the effective length of the re-bar, would be to find the stress distribution along the embedded length. That was the objective of this test.

The instrumented bar test was performed with an embedment length of 380 mm, and an inclination of 30 degrees. A reinforcing bar was equipped with strain gages. Flat surfaces were machined, on one side of the bar, used as bases for the strain gages. Six strain gages were attached to the bar using a special glue. The first was placed at 45 mm from the glulam surface, others at 55 mm, 70 mm, 90 mm, 130 mm, and 210 mm. For the location of strain gages see Photograph 4.4, and Figure 4.8.

Figure 4.7 represents forces calculated from the readings of the strain gages at the different locations showed on X-axis. The applied force can be read on Y-axis.

Six load levels were used. They are : 4.2 kN, 8.5 kN, 12.7 kN, 16.8 kN, 19.8 kN, and 25.8 kN.

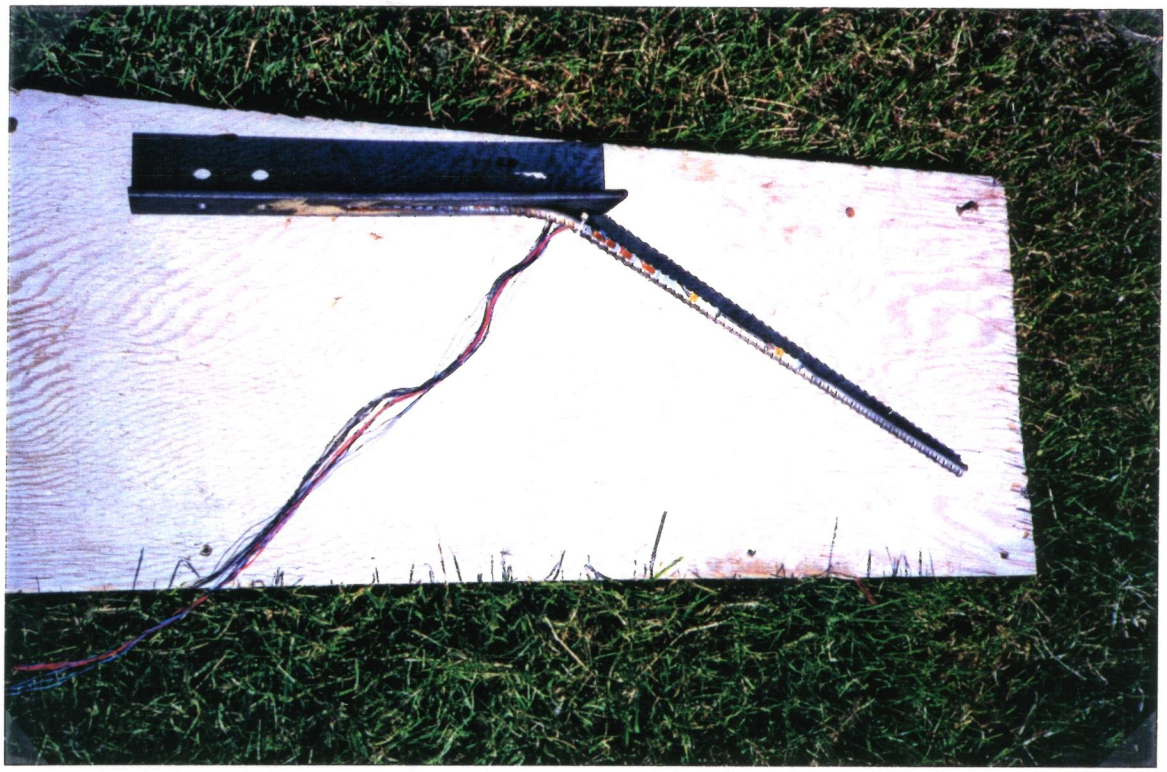

Photograph 4.4. Instrumented #10 re-bar.

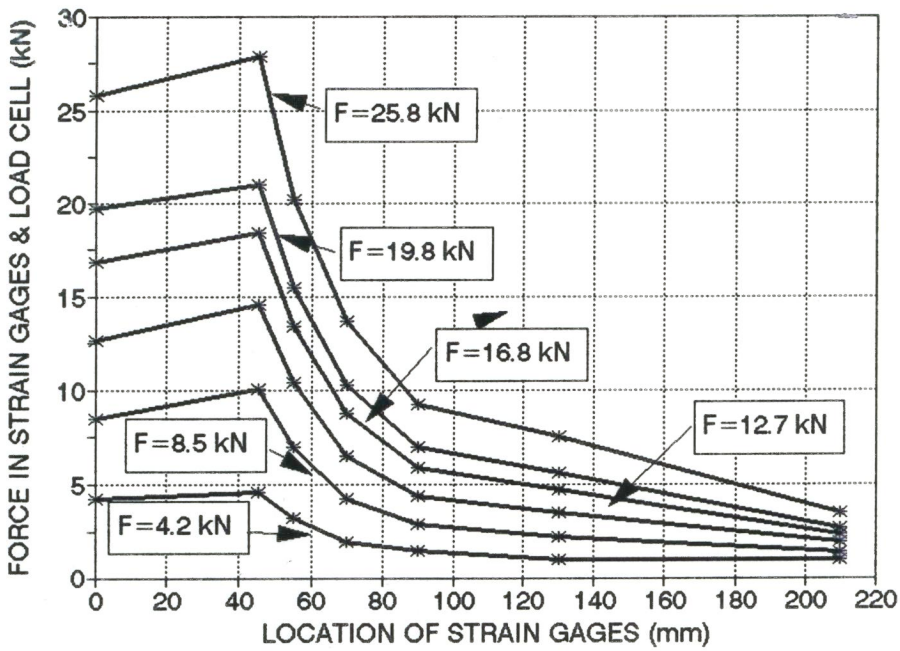

Figure 4.7 Force distribution along the re-bar for increasing loads.

The initial increase of the force is caused by the fact that the readings were taken only

on one side of the re-bar. The shape of the lines on the graph indicates rapid decrease of force up to strain gage 4 situated 90 mm inside glulam. See Figure 4.7.

At this point 70 of the force is already transferred to glulam. From here the decrease of the force is less. The last strain gage was situated 210 mm inside glulam. Its reading indicated that at this point 93 % of the force was transferred to glulam. Assuming the same rate of decrease , the force was fully transferred to glulam by the re-bar length of 250 mm.

Figure 4.8 presents the distribution of the stress along the re-bar loaded with a horizontal force of 26 kN.

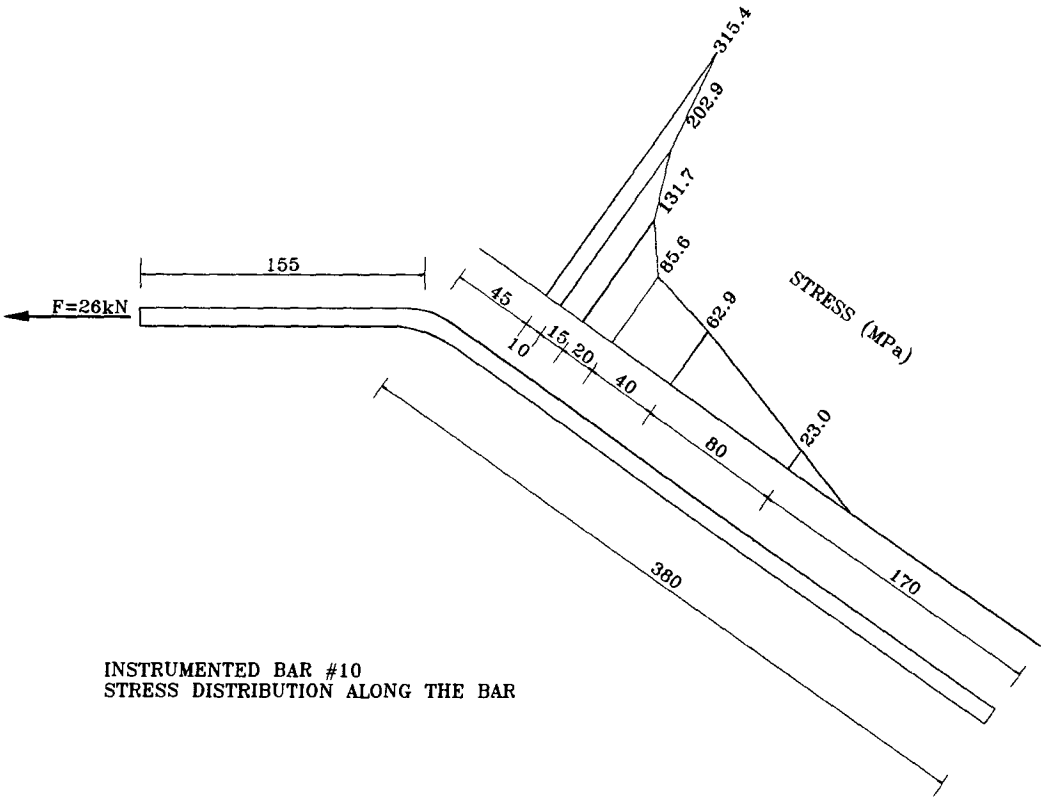

Figure 4.8 Stress distribution along the re-bar.

CONCLUSIONS

1. The tensile force in the glued-in re-bar is transferred to the glulam mostly by the section of the bar closest to the glulam surface. (70 % of the force is transferred by the first 90 mm of re-bar length.)

2. The transfer of the force is less along the next length - 120 mm of the re-bar. (23 % is

transferred by this section of re-bar)

3. Approximately 250 mm of # 10 re-bar length is needed to transfer 100 % of the tensile force to the glulam, under the load of 26 kN, which is 30% of ultimate.

CONCLUSIONS FROM TESTS WITH "PRELIMINARY CONNECTION"

1. Safe embedment lengths to insure tension failure in the re-bar were established :

   250 mm for #10 re-bar

   300 mm for #20 re-bar

2. The inclination was chosen as 30 degrees.
3. Sufficient bearing area for compression perpendicular to grain has to be provided.
4. Appearance of the connection must be improved, in order to have an acceptable product.

4.8 PRE-WELDED CONNECTION

4.8.1 PRE-WELDED CONNECTION USING GLULAM

After the tests with the preliminary connection, the joint was redesigned, and called the "prewelded connection". For the description of the development of the joint see section 4.3. Four specimens with pre-welded connection were prepared : two with a single #20 re-bar, and two with double #20 re-bars. (side by side). All four specimens failed by tension failure in the re-bar. See photograph 4.5.

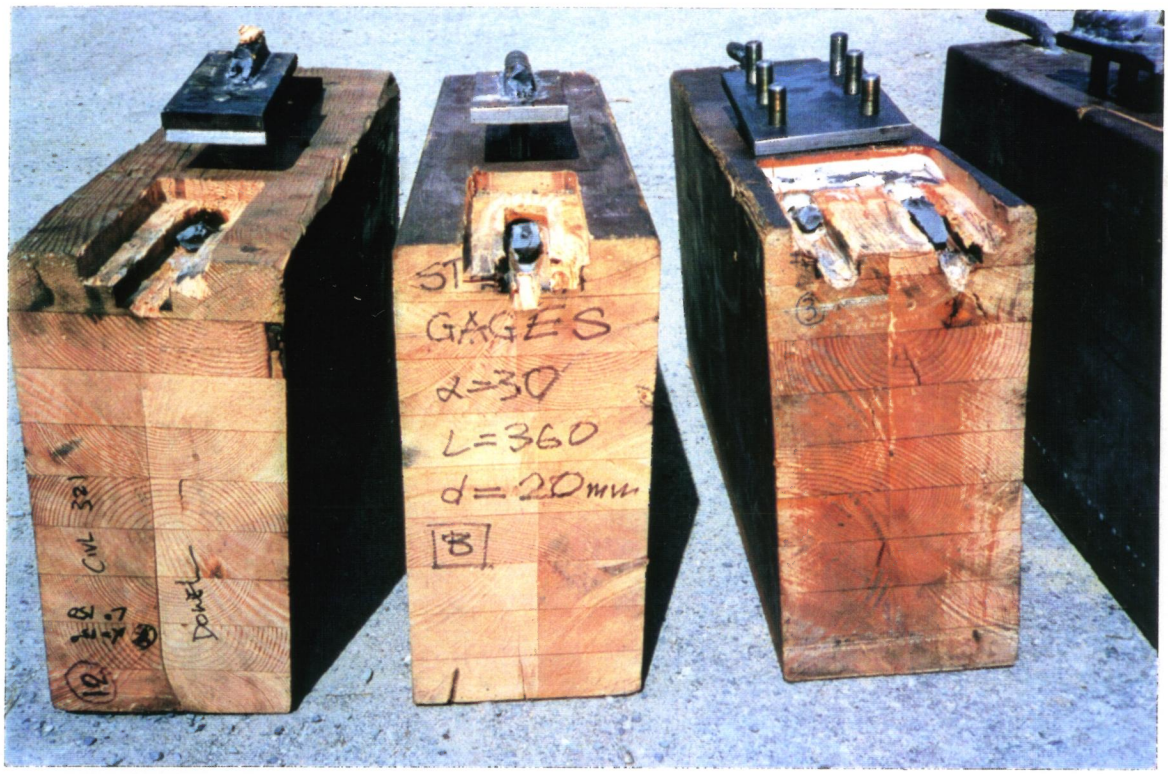

Photograph 4.5 Pre-welded joints after failure.

The following table presents tests results.

SPEC #	Ld (mm)	ALPHA (deg)	Fmax (kN)	Dmax (mm)	STRESS (Mpa)
CON-1	380	30	214.8	12.5	595
CON-4	380	30	158.4	8.3	438
Average			188.6	10.4	517

Table 4.6-A. Pull out tests results. Pre-welded joints. Single #20 bar.

SPEC #	Ld (mm)	ALPHA (deg)	Fmax (kN)	Dmax (mm)	STRESS (Mpa)
CON-2	2 x 380	30	334.4	18.8	463
CON-3	2 x 380	30	354.9	10.7	492
Average			344.7	14.8	478

Table 4.6-B. Pull out tests results. Pre-welded joints. Double #20 bar.

SUMMARY

1. Tension failure in the re-bars was observed for both single and double rod joints.
2. 26% difference in ultimate force values was recorded for the single bar specimens. The reason is the variability of steel material used for reinforcing rods, and possible welding damage. No sign of wood failure was noticed, in any of the specimens. For double bar specimens the difference between the ultimate forces was only 6%.
3. The double bar joints failed at 90% of twice the force of single specimens.

FORCE DISPLACEMENT RELATIONS

The following two graphs present the force displacement relations for single and double bar joints. See Figures 4.7 and 4.8. The force displacement relations showed two types of behavior : linear and nonlinear. For the smaller forces the displacement relation remained linear. After the re-bar started to yield the displacement was growing faster than the force and a yielding plateau was observed.

For double bar specimen linear behaviour and yield plateau can be easily separated. See Figure 4.8. Single bar specimen relation is less clear and shows 30% shorter ductility range than that of the double joint.

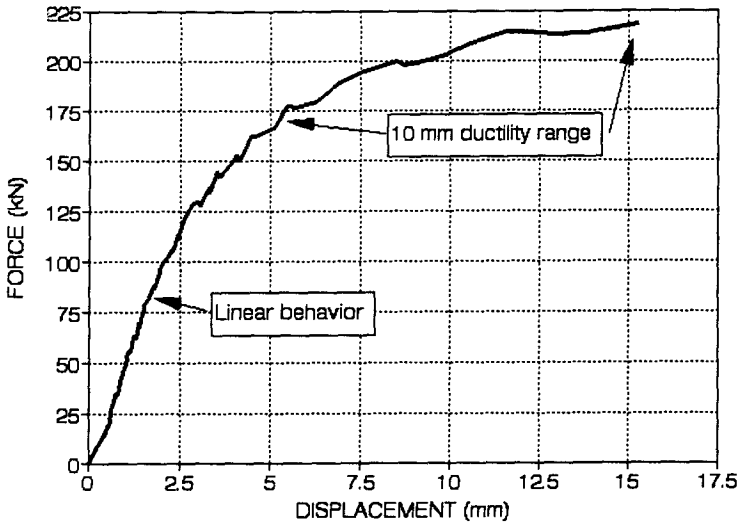

Figure 4.7 Force displacement relation for specimen CON-1.

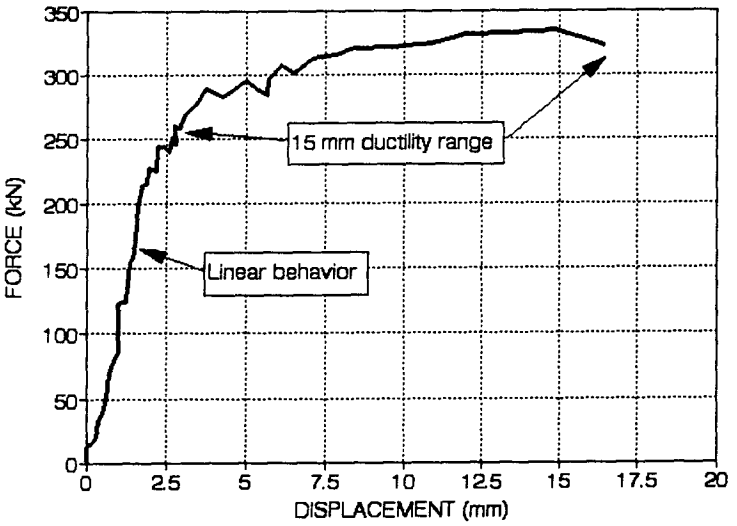

Figure 4.8 Force displacement relation for specimen CON-2.

CONCLUSIONS FROM TESTING PRE-WELDED GLULAM JOINTS

1. In the prewelded connections, the compression perpendicular to grain stresses had been designed not to exceed the bearing capacity. They were as follows :

5.9 Mpa for single bar specimens.

5.3 MPa for double bar specimens.

As a consequence no compression perpendicular to grain failures were observed.

2. Tension failures in the re-bars were observed for double re-bar specimens. The two bars failed simultaneously.

3. Manufacturing techniques for the pre-welded connections were developed.

4.9 CONCLUSIONS FROM PULL-OUT TESTS.

1. The pull-out tests provided information that enables us to design structural timber connections which will fail by tension failure in steel without affecting the wood.

2. Safe embedment lengths to get re-bar tension failure are as follows :

- 250 mm for #10 re-bar
- 300 mm for #20 re-bar

3. Specimens with double bars have the same failure mode - tension failure of the re-bar, as single bar joints.

4. 30 degree hole inclination to grain results in optimum force values and enhances the shear capacity of the cross-section.

5. A manufacturing technique for pre-welded joints was developed for single and double bars. The joints can be prefabricated in the glulam plant and erected similar to steel structure by using steel straps and bolts.

6. The force displacements relations of specimens which failed by tension failure in the re-bar, are similar to normal steel tension tests.

7. The glue bond failures occur at stresses above yield and close to ultimate tensile resistance of the re-bars.

CHAPTER 5

BEAM TEST

5.1 TEST OBJECTIVES

The subsequent step in the development of the pre-welded glued-in rod connection was manufacturing and testing of a beam splice connection, with double bars top and bottom. See Figure 5.1.

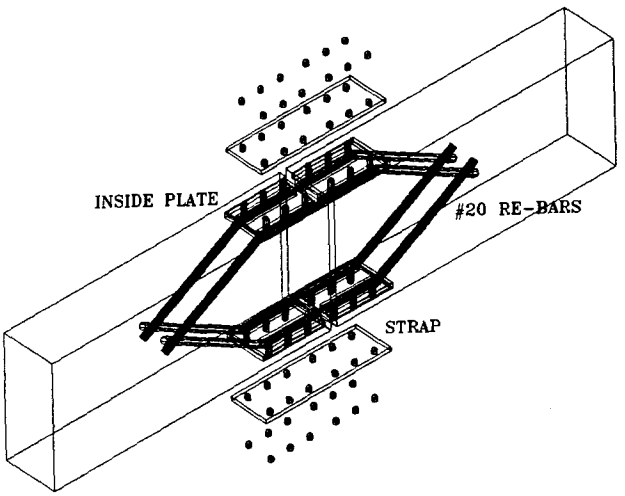

Figure 5.1 Beam splice connection using glued-in rods.

TEST OBJECTIVES

1. Develop a manufacturing method for a beam splice connection.
2. Check the behaviour of a "real" connection - joining two glulam elements.
3. Compare the maximum tensile force in the re-bars, at tension failure of the re-bars, with pull out test results.

5.2 BEAM SPLICE CONNECTION

A splice connection using double #20 re-bars, top and bottom, was placed in the middle of the span of a 3.6 m long glulam beam. The cross-section of the beam was 175 x 380 mm. The embedment length of the re-bars was increased from 380 mm (pull out tests) to 470 mm. This was done to develop a manufacturing technique for gluing longer re-bars. Longer re-bars increase the shear capacity of the cross-section, which may be useful for other applications of glued-in rod joints. 30 degree hole inclination was used. Holes were inclined out of plane, so the bars could cross in the middle of the cross-section, without piercing each other.

5.3 TEST SETUP AND TESTING METHOD

The beam was loaded in bending by two point loads (0.6 m apart) in the middle of the span.

Figure 5.2 Beam test setup and instrumentation.

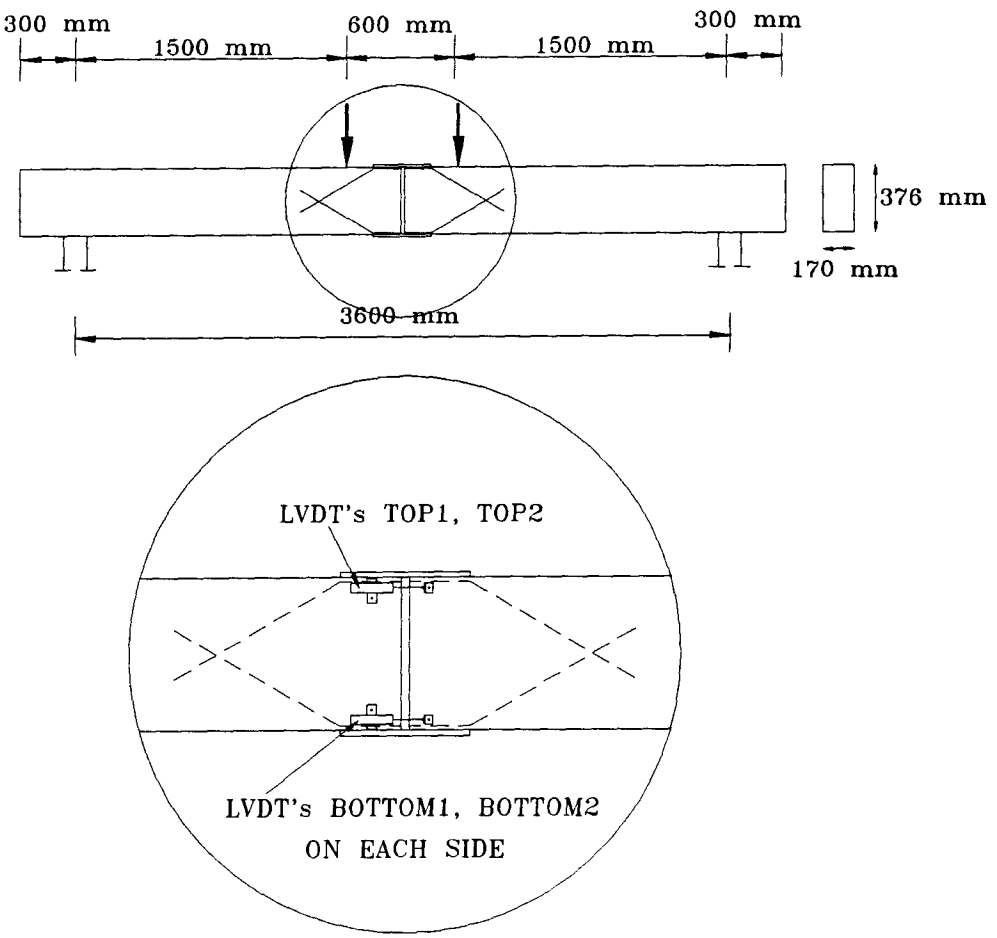

The following measurements were recorded :

1. Loading force from the load cell.
2. Mid span deflection.
3. The movement of the gap between the two glulam pieces by 4 LVDT's placed at the corners of the cross-section.

Instrumentation of the specimen is presented on Photograph 5.1, and Figure 5.2.

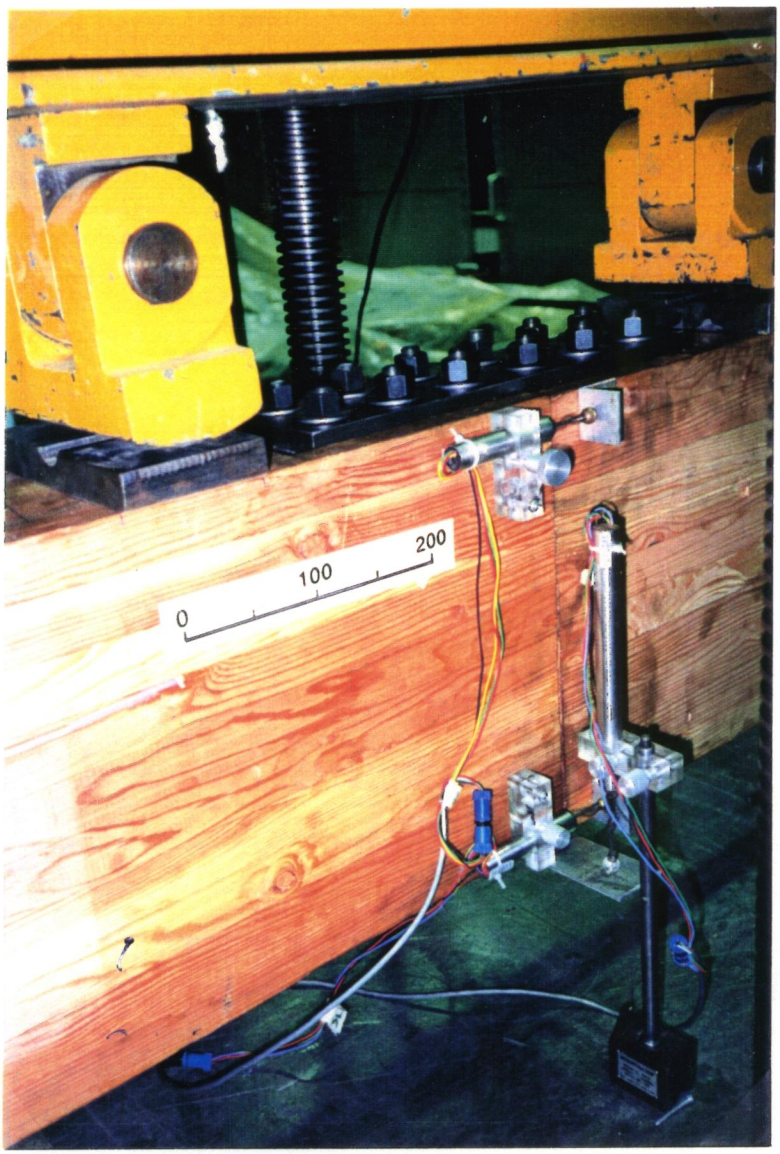

Photograph 5.1 Instrumentation of the beam test specimen.

A load controlled load application was used. The beam was loaded in five load increments with maximum forces of : 50, 75, 100, 125, and 122 - failure. After each loading specimen was unloaded.

5.4 BENDING MOMENT - MID SPAN DEFLECTION ANALYSIS

Relation between the bending moment in the middle of the span and mid span deflection, for all five loadings is presented on Figure 5.3.

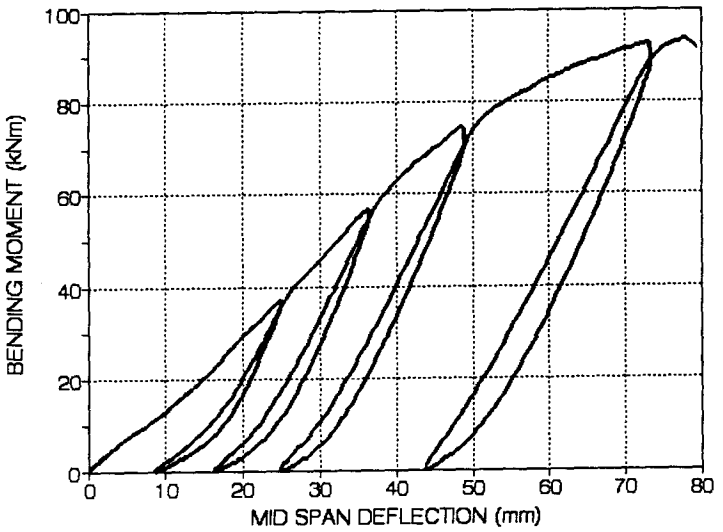

Figure 5.3 Mid span deflection and bending moment relation for all loadings of the beam test specimen.

Large permanent deflections were noticed after each loading cycle. Before the last loading permanent deformation reached 44 mm.

Maximum bending moment value was 92 kNm which was 95% of the glulam resistance, calculated assuming maximum bending stress for 24f-EX D-Fir glulam - 30.6 MPa.

The specimen failed by tension failure in the re-bars, at the bottom part of the joint. See Photograph 5.2. The maximum force in the re-bars was 237 kN, which was 70 % of the average force for the double # 20 re-bar pull-out specimen. The maximum stress in the re-bars was 344 Mpa.

Photograph 5.2 Re-bar tension failure in the beam specimen.

5.5 GAP MOVEMENT ANALYSIS

Gap movement analysis is based on the readings of four LVDT's measuring the opening and closing of the gap between two glulam pieces. Figure 5.4 presents the gap movement during loading #4, where the stress in the re-bars reached 344 Mpa.

The permanent bottom gap opening after this loading reached 6 mm. On the top side of the joint, permanent gap closing was 1 mm.

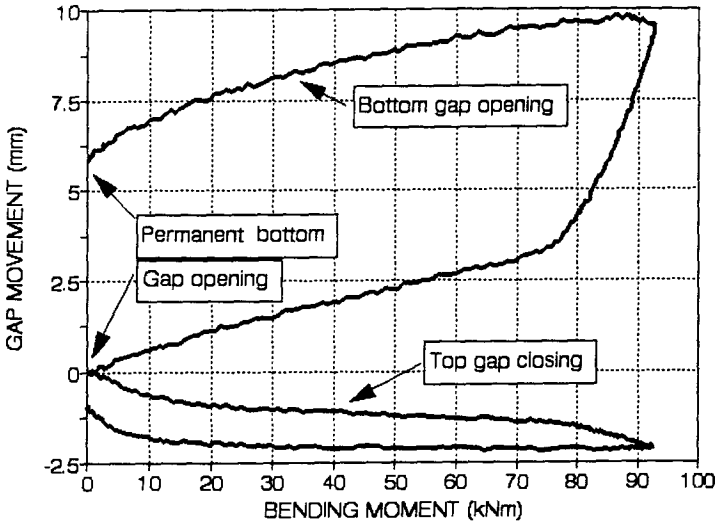

Figure 5.4 Gap movement and bending moment relation. Beam test. Loading #4.

5.6 CONCLUSIONS

1. The beam splice joint using glued-in rods failed by tension failure in the re-bars, what indicates, that the joint connecting two glulam elements can fail by the steel failure.

2. Force in the re-bars during failure was lower than the average from the pull-out tests.

- beam test F = 237 kN, stress in re-bars 344 MPa

- pull out tests F = 345 kN, stress in re-bars 478 MPa

The reason for the difference in the maximum force values may be different bearing conditions. During pull-out tests the specimens rested against the rigid steel plate, while during the beam tests two glulam parts rested on each other.

3. Very large deflections were noticed during the beam test. A solid beam of the same cross section and span would deflect - 12.5 mm. The glued-in rod joint deflected 76 mm. There were several reasons :

A. Oversize holes for the studs. (2 mm oversize)

B. Compression perpendicular to grain failure at the bottom of the joint.

4. The inside steel plate area should be designed to resist compression perpendicular to grain.

5. Beam splice joint was very labor intensive, relative to the information obtained, because

two joints have to be manufactured.

6. The test setup was not effective since load could not be reversed.

7. It was decided to change the test setup. New tests should be able to load the glued-in rod joints under cyclic loading - tension and compression, in order to provide better information for the earthquake behaviour of the joints.

CHAPTER 6

RACKING TESTS

6.1 TEST OBJECTIVES

The racking test was designed to be a more efficient test method than a beam test, as discussed in the previous chapter.

TEST OBJECTIVES

1. Design a glued-in rod column foundation joint.
2. Develop a manufacturing method of making a glued-in rod joint, connecting a glulam column to a steel foundation plate.
3. Check the behaviour of glued-in rod joints under cyclic loading. Similar to a column loaded with wind or earthquake loads.
4. Check the possibility of tension failure in re-bars, for joints equipped with 2, 3, and 4 re-bars.
5. Evaluate the change of capacity of a joint with the increase of bearing area.
6. Check the moment capacity of multi bar glued-in rod joints and compare the ultimate forces with pull-out and beam tests.
7. Examine vertical and horizontal displacements of the joint area when subjected to cyclic loading.
8. Find the moment-rotation behaviour.

6.2 RACKING TEST SETUP

Racking test setup (See Photograph 6.1) consists of two parts :

1. A loading jack with a load cell bolted to a steel frame, fixed to the concrete floor by bolts.
2. Foundation plate, fixed to the floor by bolts.

A stiffened bracket was manufactured, and attached to each side of a test specimen. One leg of the bracket was attached to the foundation plate. The other was attached to the

glulam via the glued-in re-bar. See Figure 6.1.

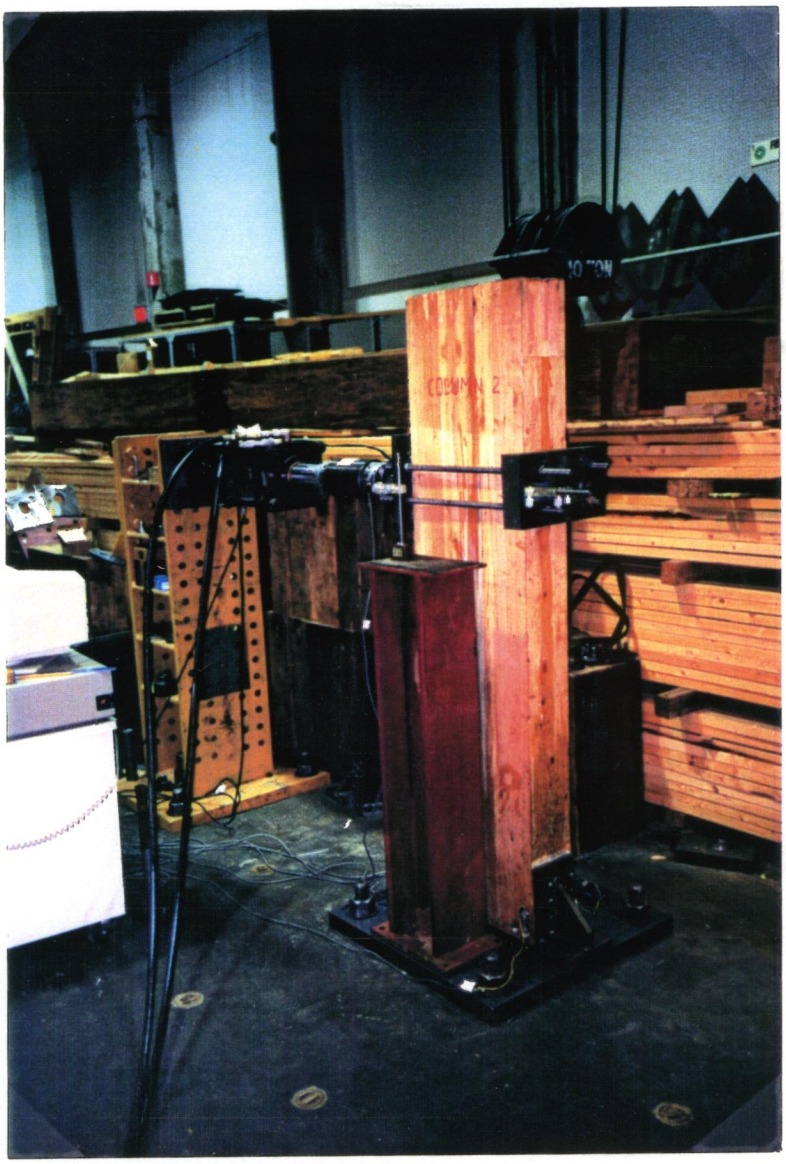

Photograph 6.1 Racking tests setup.

6.3 TEST READINGS AND INSTRUMENTATION OF THE SPECIMEN

The following measurements were recorded during racking tests :

1. The loading force from the load cell.
2. The horizontal displacement of the column at the height of the force.
3. The vertical displacement, at the glulam face, was measured by four LVDT's situated at the corners of the glulam cross-section.

4. The horizontal displacements of the outside connector was measured by two horizontal LVDT's.

From the above measurements the movement of the lower end of glulam face can be determined. See Figure 6.1.

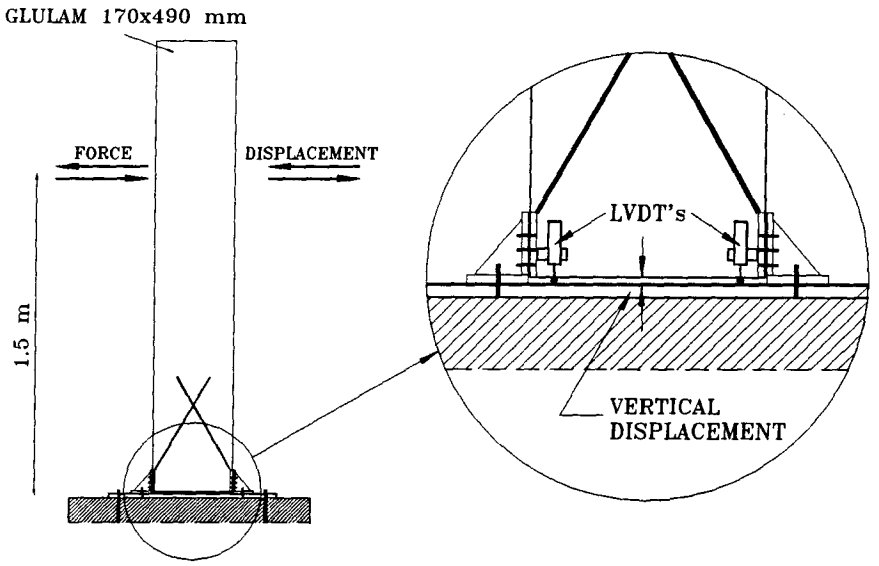

Figure 6.1 Instrumentation of the racking tests setup.

6.4 EVOLUTION OF THE RACKING TEST SPECIMEN

Each racking test specimen was equipped with two glued-in rod joints of the same size.

Specimen 1, which was the undamaged part of the beam test, had a joint with two #20 re-bars.

Specimen 2 had three #20 bars - See Figure 6.2

Specimen 3 had four #20 re-bars - See Figure 6.3

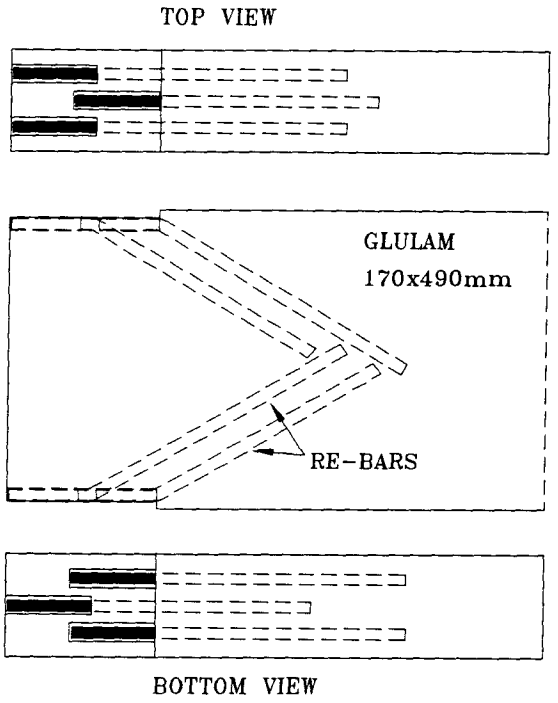

Figure 6.2 Specimen 2.

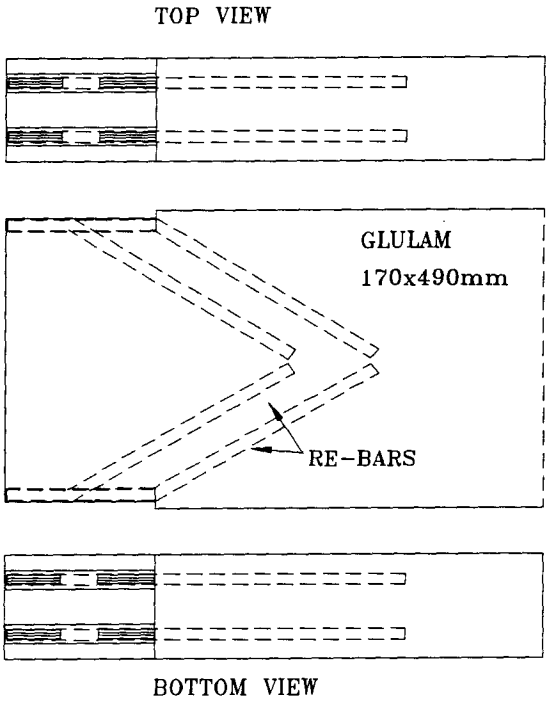

Figure 6.3 Specimen 3.

Specimen 4 had four #20 re-bars similar to Specimen 3 but the distance between the rods parallel to grain, was increased and so was the length of the inside plate. The length

of the steel plate was increased from 250 mm to 400 mm. This was necessary because of the high compression perpendicular to grain stresses developing in the joint. See Photograph 6.2

Photograph 6.2 Specimen 4 during manufacturi.g.

6.5 LOADING

The same loading pattern was used for all racking tests. The specimens were loaded by a horizontal force 1.5 m above the foundation plate. The force was applied in two directions. The first load cycle was 10 kN in both directions. The next loadings were applied

with increment equal to 10 kN. The load control pattern was used.

The specimens were loaded with four full load cycles at each load level. After each load level, the specimen was unloaded and the data was saved.

Figure 6.4 presents the relation between loading force and time.

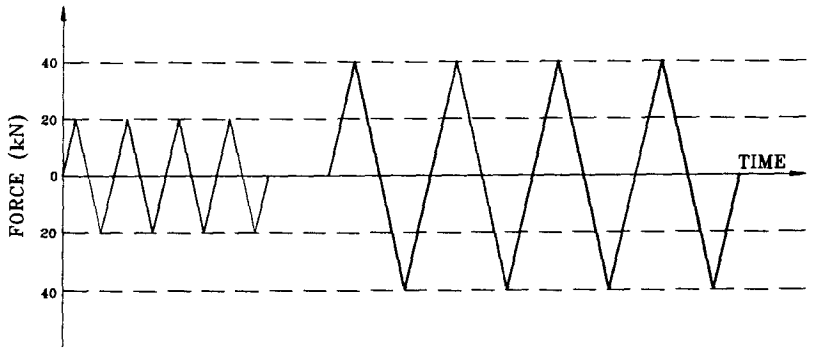

Figure 6.4 Loading force and time relation during racking tests.

6.6 MOMENT DISPLACEMENT DIAGRAMS

The relations between the bending moment and the displacement illustrate the overall behaviour of the joint. The following sections present this relation in graphical form for selected loadings. The general character of the graph is discussed. The analysis of maximum bending moments and displacement at failure is presented. The diagrams present the average of four cycles at the stated load levels.

6.6.1 SPECIMEN 1. (2-#20 re-bars)

A linear relation between the bending moment and the displacement was present only during the first load level. (Maximum bending moment 15 kNm) Then the loops were progressively pinched up to the final load, where there was almost no moment resistance but a displacement of 40 mm. See Figure 6.5. Specimen 1 failed by tension failure in the re-bars, at a bending moment of 92 kNm and a vertical displacement of 62 mm. See Photograph 6.3.

The maximum force in the re-bars was 237 kN, which resulted in a stress of 395 MPa.

The ultimate value was similar to the one obtained during the beam test.

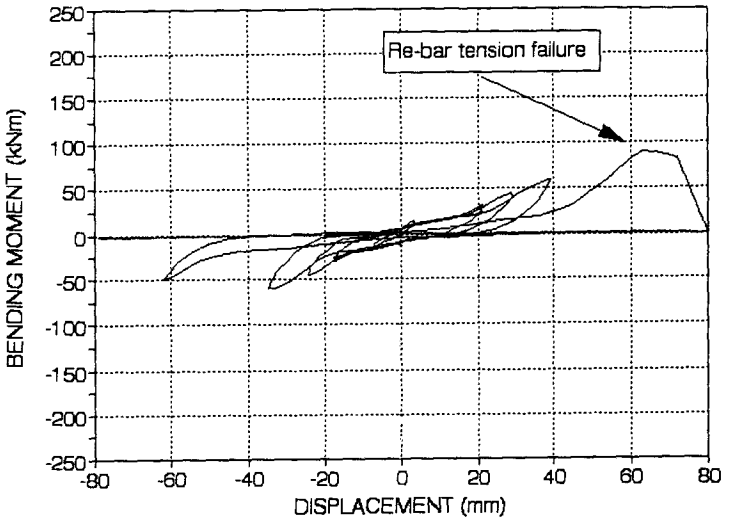

Figure 6.5 Bending moment and displacement relation for Specimen 1.

RESULTS:

1. Specimen 1 showed a very weak behaviour under cyclic load. The reason might be that this joint was loaded previously during the beam test.
2. The final failure mode was tension failure in the re-bars. The two re-bars failed in tension at the same load.

6.6.2 SPECIMEN 2. (3-#20 re-bars)

Specimen 2 maintained a linear relation between bending moment and displacement up to a moment of 125 kNm. See Figure 6.6. Then up to 175 kNm a slightly pinched behaviour was observed.

The first failure occurred at 200 kNm, when the single bottom bar failed. The moment dropped to 150 kNm, but subsequently increased to 225 kNm, at which point, the next two re-bars failed. The load was then reversed. On the other side of the joint one re-bar broke at 175 kNm, and the moment held steadily at 150 kNm, up to the end of stroke in the actuator, due to yielding of re-bars.

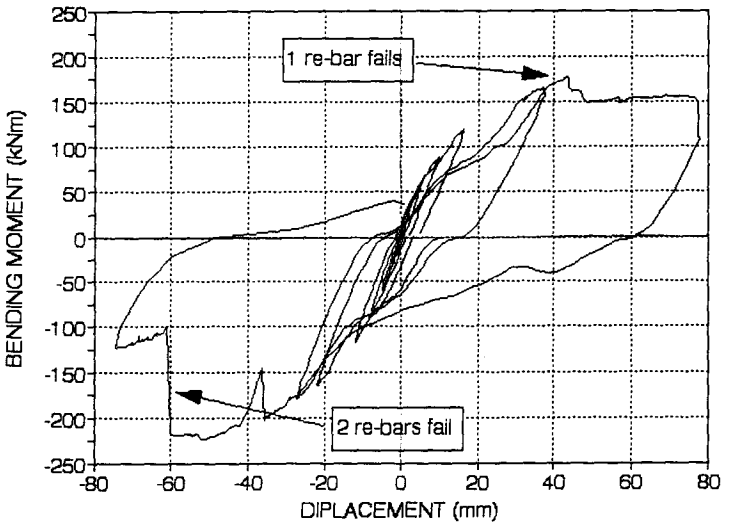

Figure 6.6 Bending moment and displacement relation for Specimen 2.

RESULTS:

1. Specimen 2 showed linear behaviour up to the moment of 125 kNm, which was a big improvement relative to Specimen 1.

2. The failure mode was tension failure in the re-bars, on both sides of the joint. The single re-bar, failed first, followed by the simultaneous failure in the two bars in the second row. (Close to the foundation plate)

3. When the glued in rod joint consists of two rows of re-bars, the row closest to the end of the specimen fails first.

6.6.3 SPECIMEN 3. (4-#20 re-bars)

Specimen 3, despite having one bar more in the joint (4 #20 re-bars) behaved linearly up to the same load level as Specimen 2.(M=125 kNm) See Figure 6.7. The pinching of the loops was more pronounce when the moment reached 150 kNm. During the next loading the two outside bars failed at 150 kNm.

After the load reversal, the specimen failed abruptly by tension failure in all four re-bars. See Photograph 6.4. The maximum bending moment was 200 kNm.

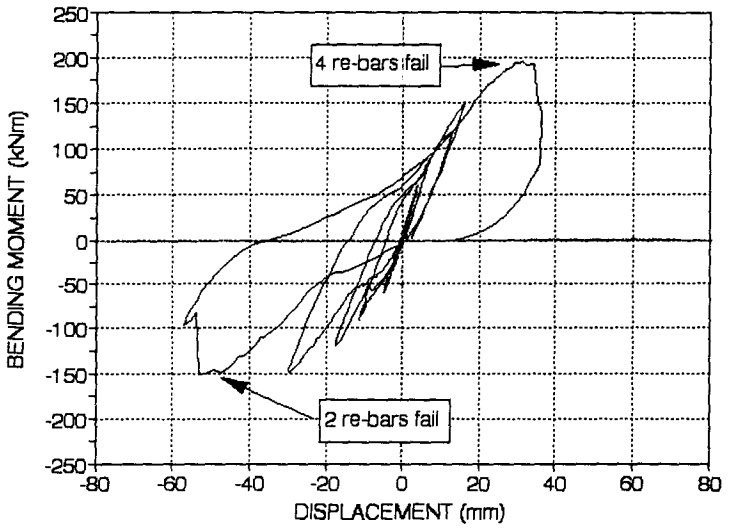

Figure 6.7 Bending moment and displacement relation for Specimen 3.

RESULTS:

1. Specimen 3, despite of the increase of re-bar area failed under similar load as Specimen 2. The reason might be, that the bearing area was to small for 4 bar joint, and wood crushing therefore governed the moment capacity.

2. Four re-bars in two rows failed at the same instant.

6.6.4 SPECIMEN 4 (4-#20 re-bars, plate length increased to 400 mm)

With the increase of bearing area, the moment displacement relation of Specimen 4 become different from previous specimens. See Figure 6.8. Linear character of the graph terminated at the bending moment of 50 kNm. Then the loops are more and more pinched. The same trend continues up to the bending moment of 245 kNm.

Specimen 4 failed by shear failure in the studs during the next loading at the bending moment value of 200 kNm. Then the load was reversed and the bending moment reached 245 kNm without failure, at which point the stroke limit was reached in the actuator.

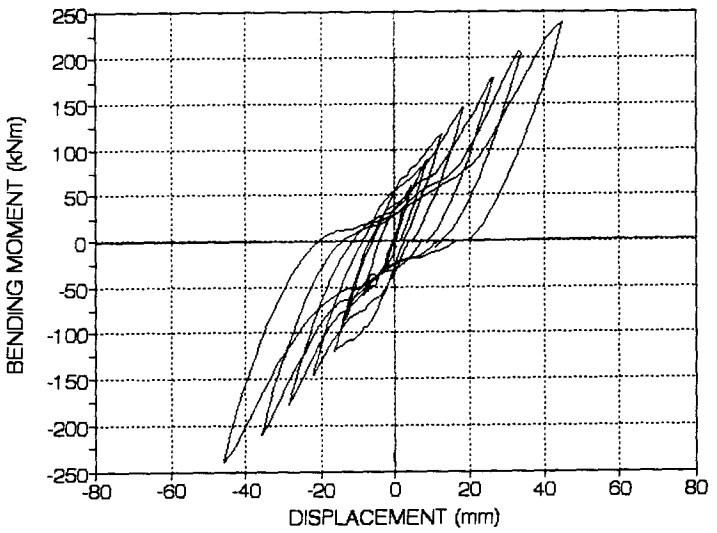

Figure 6.8 Bending moment and displacement relation for Specimen 4.

RESULTS:

1. With the increase of bearing area, moment capacity of the joint increased, because of lower compression perpendicular to grain stresses.

2. The character of the moment displacement relation changed showing bigger area inside the loops, which indicates more energy absorption.

3. It is evident from Figure 6.8 depicting the behaviour of Specimen 4 that the increased bearing area resulted in a joint with an acceptable behaviour. The loops are regular and less pinched, which is desired for the earthquake resistant structures. This was the objective of the development.

Photograph 6.3 Specimen 1 after failure. (above)

Photograph 6.4 Specimen 3 after failure. (below)

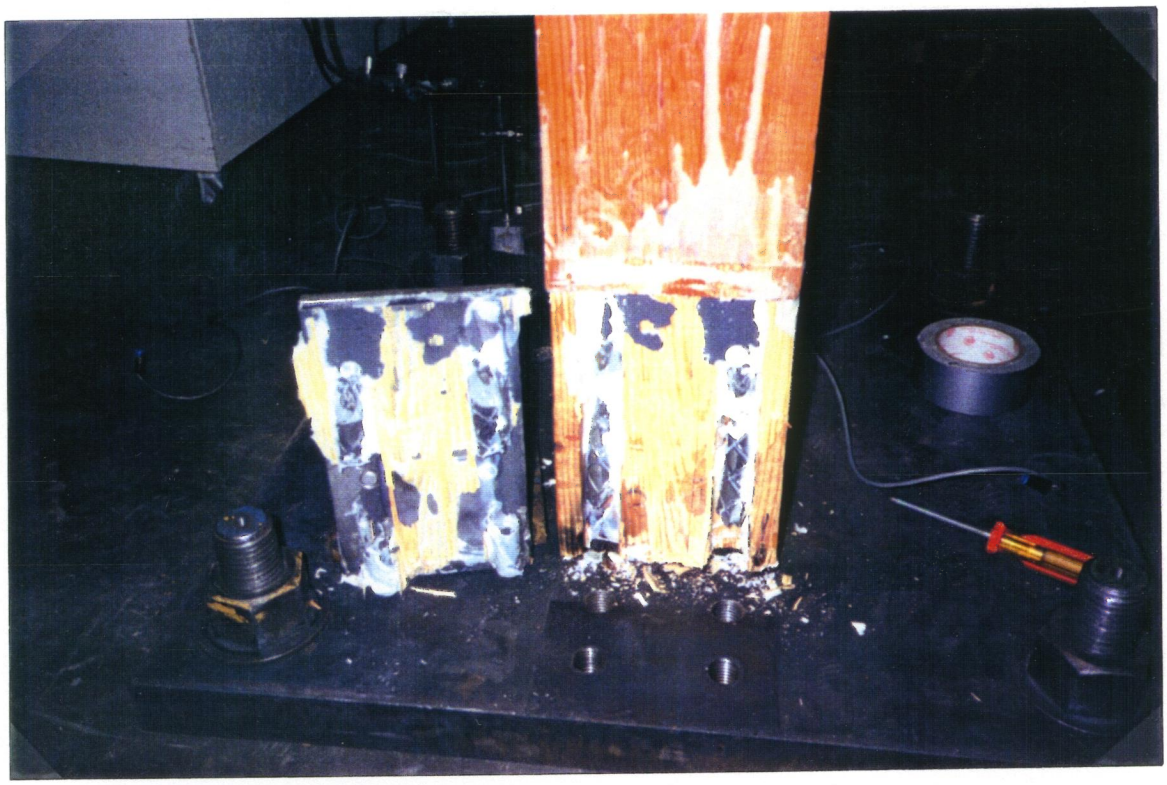

6.7 ULTIMATE MOMENTS, AND FORCES IN THE RE-BARS OBTAINED FROM TESTS AND A SIMPLIFIED MODEL.

The following graph presents forces in the racking test specimen.

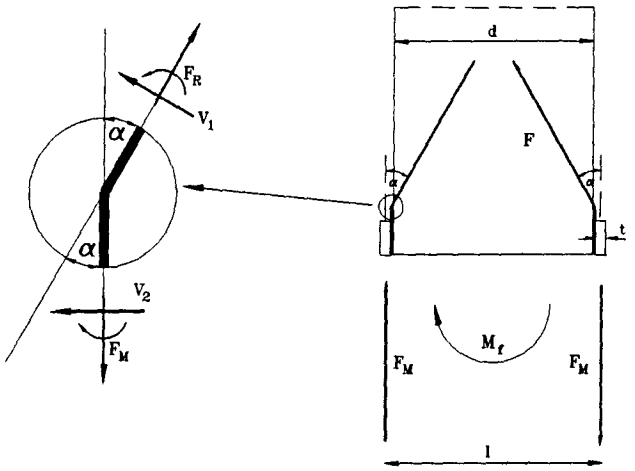

Figure 6.9 Forces in racking test specimen.

The calculation of ultimate bending moments assuming tension failure in the re-bars. Assumed maximum yield stress in re-bars is : Fv = 400 MPa, alpha = 30 degrees. Shear force V2 is assumed small in comparison to Fm, and it was neglected, for the calculation of Fr.

$$Frd = Fv \times Areb$$

$$Fmd = Fr / \cos(30)$$

$$Mrd = Fm \times l$$

where :

Frd - force in re-bars (model)

Fmd - force in the steel plate (model)

Mrd - bending moment at the base (model)

The following tables present design and test values obtained from analysis - Table 6.1 and recorded during testing - Table 6.2

Specimen	Frd (kN)	Fmd (kN)	Mrd (kNm)
1	240	276	93
2	360	414	184
3	480	478	214
4	480	478	214

Table 6.1 Design yield forces and bending moments in racking test specimens.

Specimen	Frt (kN)	Fmt (kN)	Mrt (kNm)	stress (MPa)	Frt/Frd
1	233	268	90	388	0.97
2	341	392	175	378	0.94
3	390	448	200	325	0.81
4	478	549	245	398	1.00

Table 6.2 Test results of ultimate forces and bending moments in racking test specimens.

where :

Frt - force in the re-bars (test)

Fmt - force in the steel plate (test)

Mrt - bending moment at base (test)

RESULTS:

1. Comparison of the design and the measured internal forces shows the effectiveness of glued in rod joints tested during racking tests. The most effective was Specimen 4. Specimen 2 was close, but the design of Specimen 3 was not balanced. This indicates the earlier drawn conclusion that not enough bearing area was provided in the joint of Specimen 3.

2. When glued in rod joints are properly designed, a ratio of stress obtained during tests at failure to steel yielding stress is around 1.0

6.8 ANALYSIS OF BEARING STRESSES OBTAINED FROM ANALYSIS AND MEASURED DURING TESTS.

The following table presents the maximum bearing force, assuming fc = 5.9 MPa constant on the whole area. Fct is the maximum bearing force obtained during testing.

Specimen	Ab (mm ^ 2)	Fc (kN)	Fct (kN)	Fbt/Fb %
1	30500	180	155	86
2	38000	224	227	101
3	38000	224	260	116
4	60800	359	318	89

Table 6.3 Maximum bearing forces from tests and analysis.

RESULTS:

1. The bearing stresses analysis indicates, that the design of Specimen 1 and 4 was balanced. Specimens 2 and 3 were over stressed.

6.9 ANALYSIS OF BOTTOM END MOVEMENTS UNDER LOAD

The movements of the bottom end of the specimen were monitored by four vertical and two horizontal LVDT's. The readings of these instruments were used to compare the behaviour of the two sides of the joint. They were also used to find the components of the overall displacement at the height of the force.

The vertical LVDT's provided data used to establish joints rotation. The horizontal LVDT's readings were used to obtain the sliding shear deformation. For the location of LVDT's see Photograph 6.5

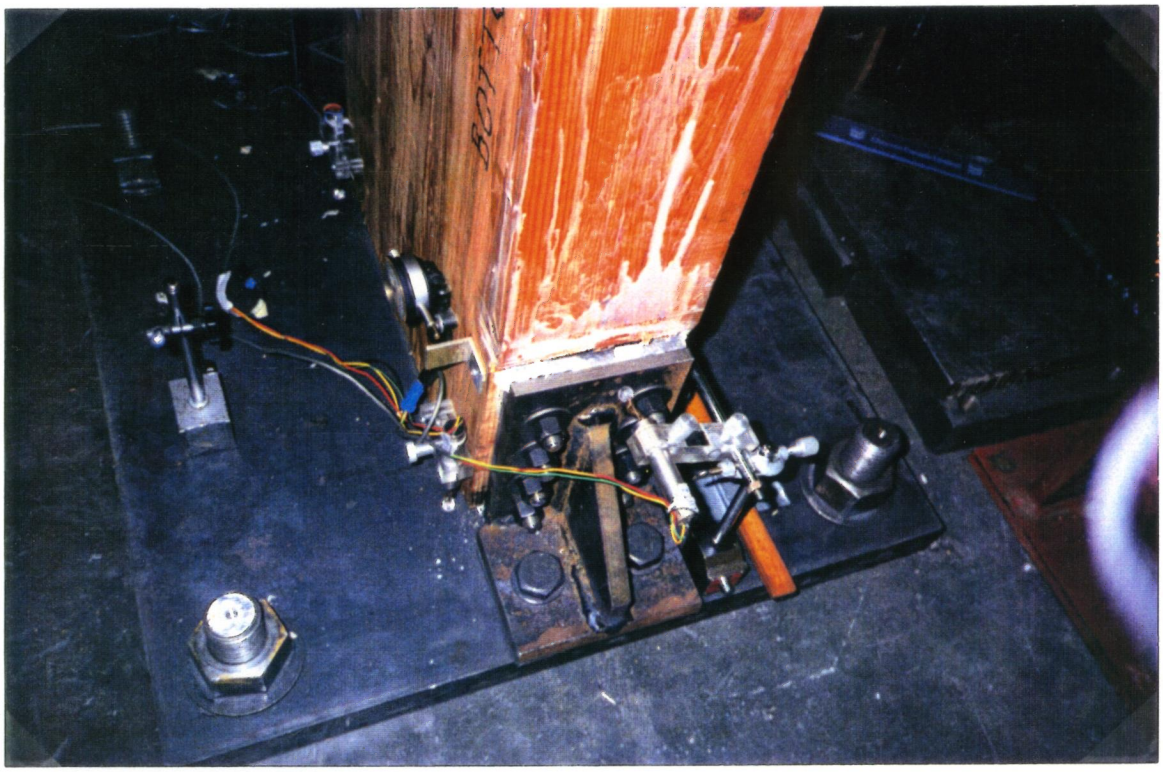

Photograph 6.5 Location of LVDT's during racking tests.

6.9.1 VERTICAL MOVEMENTS

During the analysis of the vertical movements of Specimens 2 and 3, different behaviours of two sides of the joint were observed. See Figure 6.10, which illustrates the behaviour of Specimen 3.

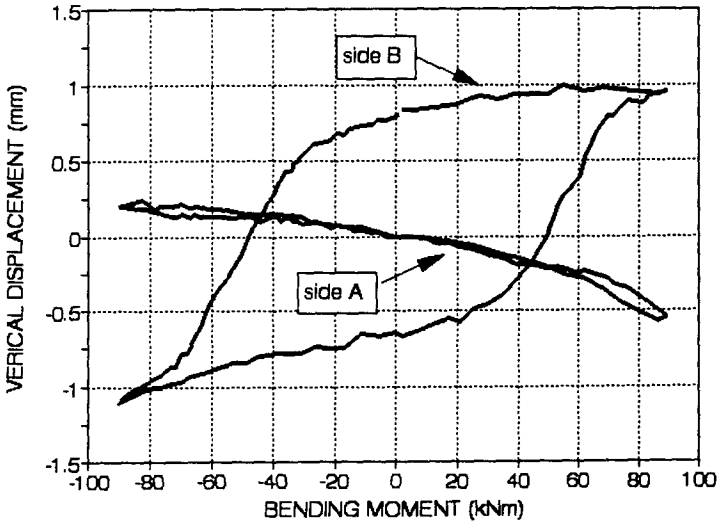

Figure 6.10 Vertical displacement of the joint area versus bending moment for Specimen 3.

During the first half of the load cycle, side A of the connection, is under compression and side B under tension. See Figure 6.11. The re-bar is bent outside under compression and deformed inside, crushing the wood on the tensile side. This should not happed in properly designed joint. When the loads are reversed, the re-bar which was bent outside is being straightened by the tensile load.

On the other side of the joint, the crushed-in re-bar is moved even more inside the wood under compression. Therefore side A shows the linear steel type behaviour, while on side B, because of the constant crushing under both directions of load, the non linear behaviour is noticed.

This explains why on side A lines are closer to each other during loading. On side B the loops are more apart because of the combined steel and wood crushing behaviour. When the bearing area was increased for Specimen 4 both sides represented "steel type" behaviour.

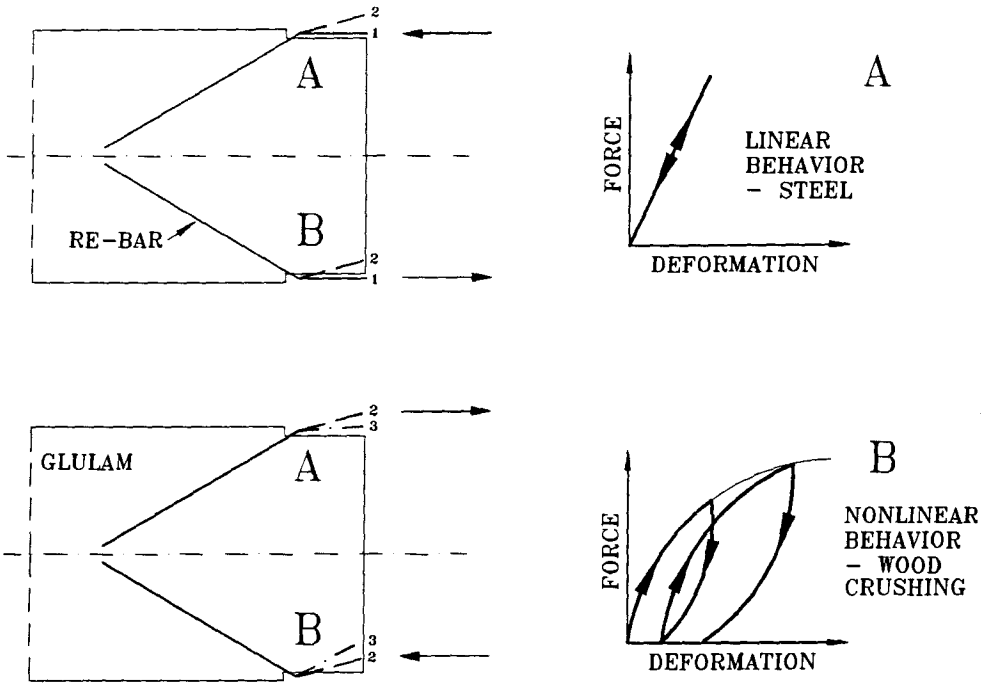

Figure 6.11 Movements of the steel plates during loading.

6.9.2 HORIZONTAL MOVEMENTS

The same phenomenon of different behaviour of two sides was noticed while analyzing readings of horizontal LVDT's. See Figure 6.12, presenting the data obtained during Specimen 3 experiments.

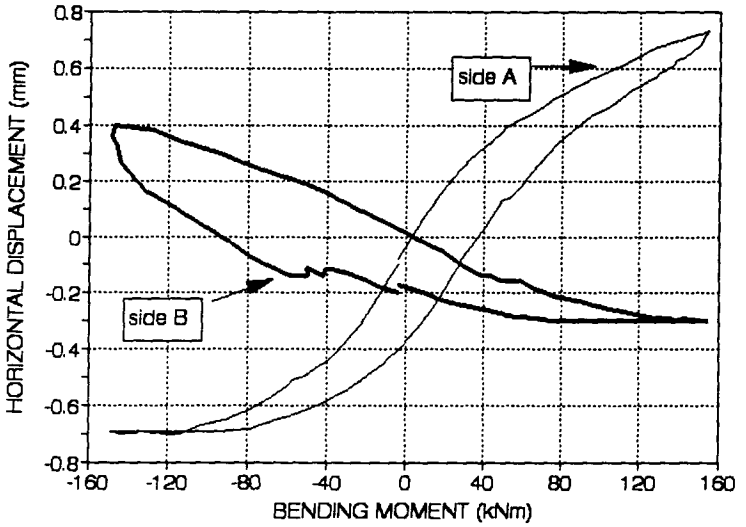

Figure 6.12 Horizontal movements of the joint area, Specimen 3.

6.10 DISPLACEMENT COMPONENTS

The displacements components were established in order to separate the components of the overall deformation at the height of the force. The percentage of glulam deformations and hinge rotation as well as sliding shear deformation is presented for the racking test specimens in graphical form in Figure 6.13.

The total horizontal displacement $d_{total} = d_{flex} + d_{rt} + d_{slsh}$

was due to the elastic and in-elastic deformations of the components namely :

* bending and shear deformation of glulam - d_{flex}

** hinge rotation - d_{rt}

*** sliding shear deformation - d_{slsh}

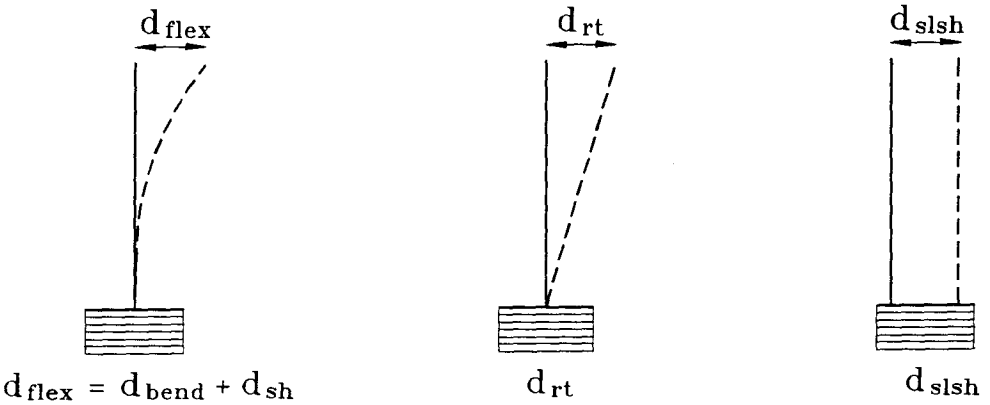

Figure 6.13 Displacement components of the racking test specimens.

All the displacement were estimated using simple models.

d_{flex} - was calculated according to the static rules, as a cantilever beam. (calculated)

d_{rt} - was calculated using the readings of the vertical LVDT's, as a rigid body. (measured)

d_{slsh} - was calculated using the readings of the horizontal LVDT's, as a translation. (measured)

6.10.1 The flexure deformation

The flexure deformation has two components : bending and shear.

$$d_{flex} = d_{bend} + d_{sh}$$

The flexural component can be calculated from the formula:

$$d_{bend} = \frac{P \times h^3}{3 \times E \times I}$$

where : P - horizontal force

h - distance from the force to the joint.

I - moment of inertia of the cross-section about the major axis (mm ^ 4)

E - modulus of elasticity of timber (MPa)

The shear component of the deformation can be estimated by

$$d_{sh} = \frac{k \times P \times h}{A \times G}$$

where : k - shear distribution factor - 1.5

G - shear modulus (assumed E/15 - 867 MPa)

A - cross-section area of the specimen (mm ^ 2)

6.10.2 Deformations due to hinge rotation.

Vertical LVDT's were placed at the corners of the joint region to measure the vertical displacements d1 and d2. See Figure 6.14

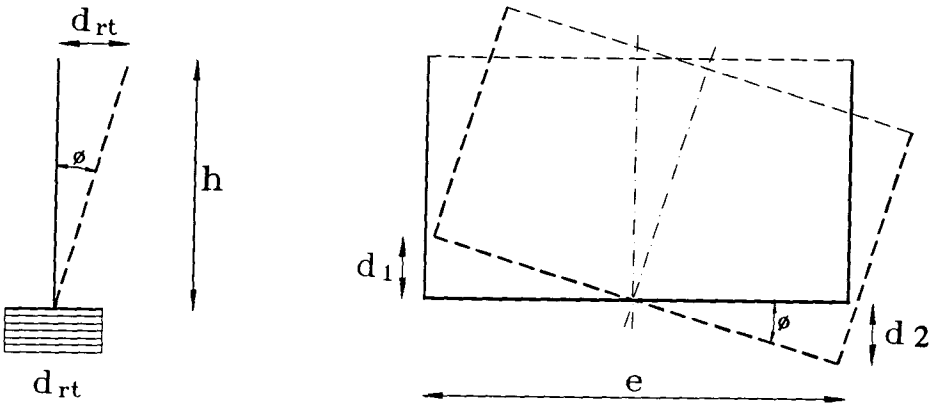

Figure 6.14 Deformations due to hinge rotation.

Deformation due to hinge rotation can be calculated from the following formula :

$$d_{rt} = h \times \tan\phi$$

where :

$$\phi = \frac{d_1 + d_2}{e}(deg)$$

where : d1, d2 - readings from vertical LVDT's (mm)

e - distance between LVDT's (mm)

6.10.3 Deformations due to sliding shear.

The horizontal deformation of the specimen relative to the foundation plate was measured using LVDT's placed horizontally at two sides of the joint. Deformation due to the sliding shear was taken as the average of two LVDT readings. The horizontal LVDt's were placed during the last two experiments: Specimen 3 and Specimen 4.

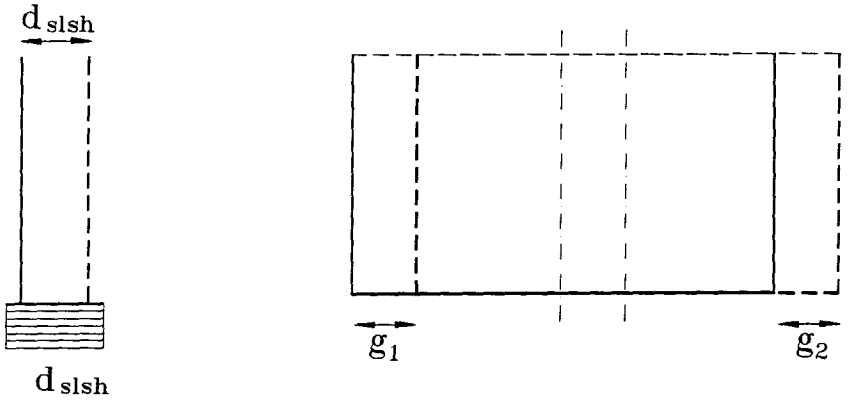

Figure 6.15 Deformations due to sliding shear.

$$d_{slsh} = \frac{g_1 + g_2}{2}$$

Where : g1, g2 - readings from horizontal LVDT's (mm)

6.10.4 Total deformations

All the components mentioned above can be now summed up to find the overall horizontal displacement.

$$d_{total} = d_{flex} + d_{rt} + d_{slsh}$$

The following graphs present both calculated and measured displacement for all four racking test specimens.

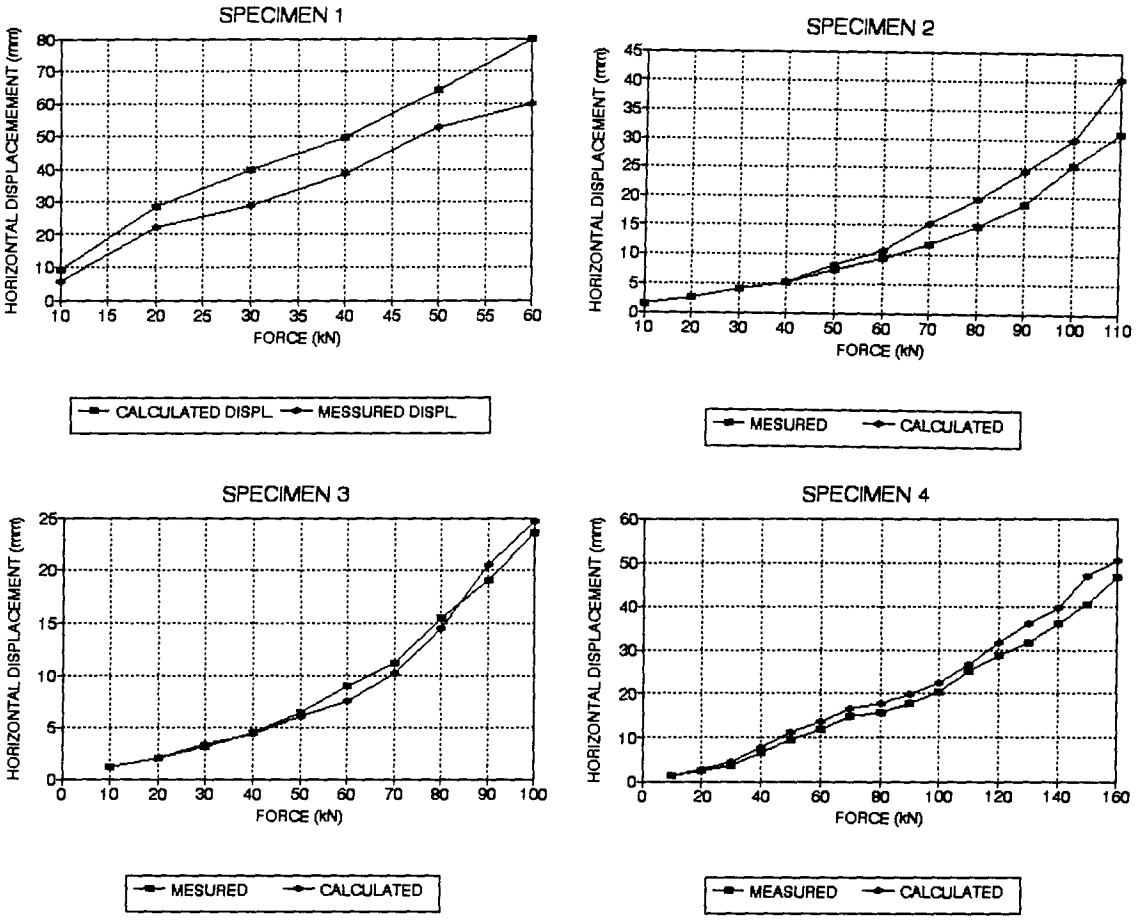

Figure 6.16 Calculated and measured displacement of racking tests specimens.

The deflection shown on Figure 6.16 as "calculated" is the summation of the calculated static deflection and measured : rigid body rotation and sliding shear.

The next four graphs present how these components were changing with the increasing loads, for all racking test specimens.

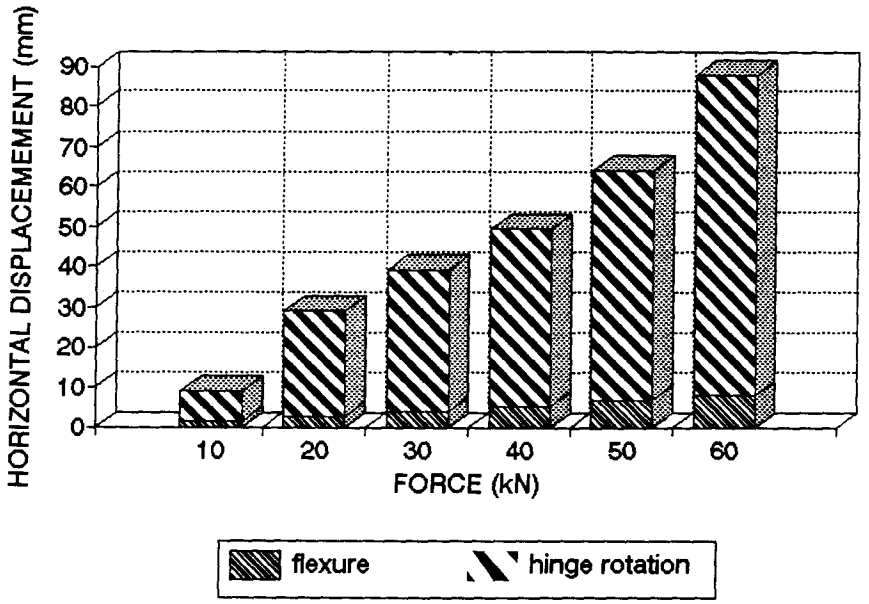

Figure 6.17 Horizontal displacement components - Specimen 1.

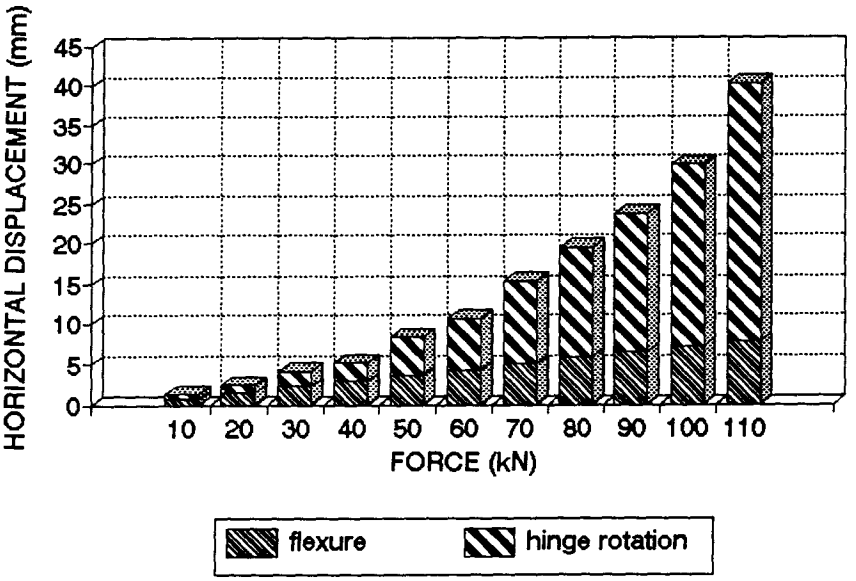

Figure 6.18 Horizontal displacement components - Specimen 2.

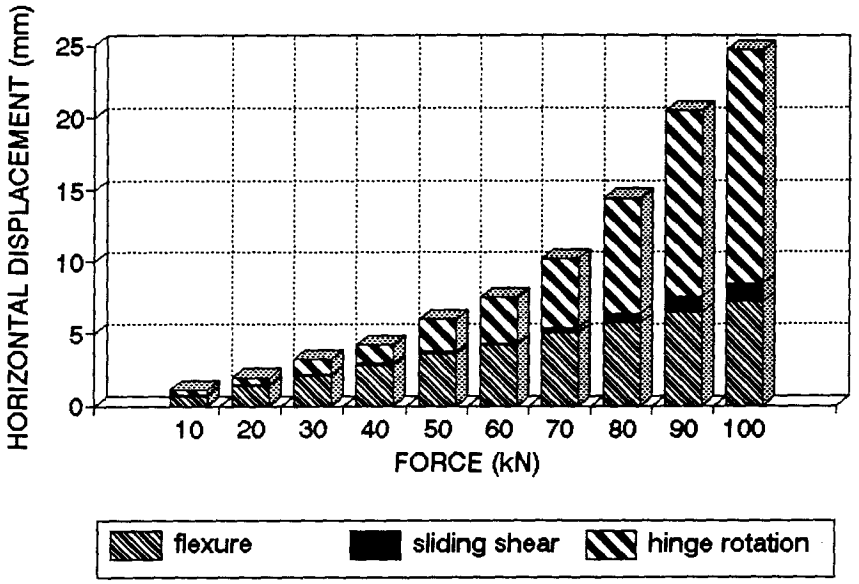

Figure 6.19 Horizontal displacement components - Specimen 3.

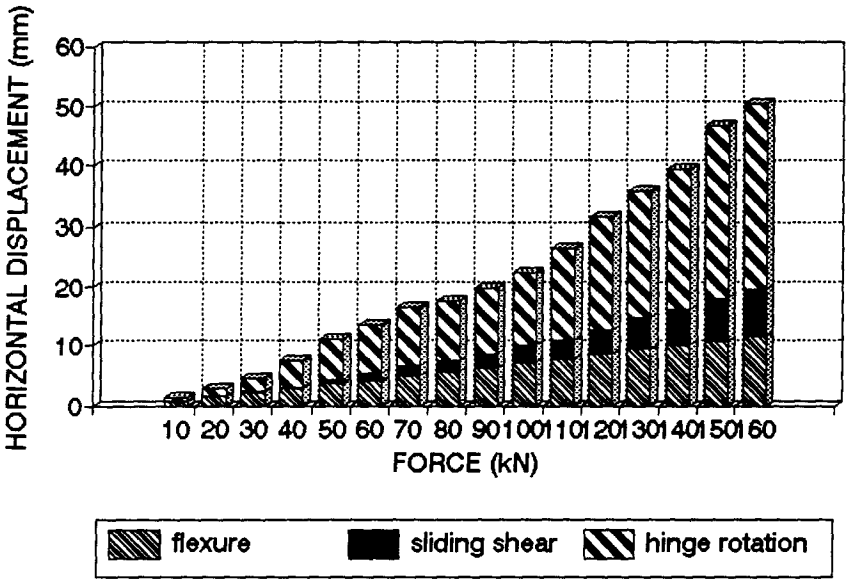

Figure 6.20 Horizontal displacement components - Specimen 4.

SUMMARY

1. The largest component comes from the rigid body rotations, which is about 70% of the overall displacement.
2. The second largest was glulam deflection around 30%.
3. Sliding shear component was less than 10%. The source of sliding shear component might be the slipping of bolts in the concrete floor.

6.11 CONCLUSIONS FROM RACKING TESTS

1. Proper bearing area has to be provided to obtain the full capacity of the glued-in rod joint.
2. Properly designed joint fails under a bending moment equal to Mr obtained from analysis, when the ultimate stress in re-bars is assumed Fv = 400 MPa.
3. Detailed analysis of the joint area showed that when the bearing area is too small, the two sides of the joint behave differently under load. This phenomenon is not significant in the design process.
4. Tension failure in the re-bars is present in multi bar joints. Maximum steel area that failed at the same instant was 1200 mm ^ 2 - 4-#20 re-bars.
5. Analysis of the deformation components showed that 70% of the deformation of the glued in rod joint comes from joint rotation. The joint rotation may come from movements of studs in oversized holes, steel plates deformations, and small re-bar movements.

CHAPTER 7

KNEE JOINT TESTS

7.1 TEST OBJECTIVES

The last type of tests described in this report is the knee joint test. Four full scale specimens, of the same geometry as designed in Appendix A, were tested under cyclic loading.

TEST OBJECTIVES:

1. Develop a technique for making a glued in rod knee joint.
2. Design a joint that fails by tension failure in re-bars on the exterior and interior of the knee joint connection.
3. Compare the ultimate bending moments (positive and negative) from testing with those from analysis.
4. Determine the rotational stiffness of the knee joint.
5. Establish the behavior of welded and bolted glued in knee joint.
6. Investigate the behaviour of glued in rod joints under reversed loading, assuming negative moment (wind, earthquake) around 20% of positive moment. (gravity load)

7.2 SPECIMENS - types of joints, and manufacturing steps

Five specimens were tested during the knee joint test experiments, which are described in this thesis. Specimen 1 was a preliminary one, to develop the manufacturing technique and to check the likelihood of tension failure occurring in the re-bars. It was built from material leftover from the racking tests.

The glulam for specimens 2,3,4, and 5 was prepared specially for the purpose of knee joint tests. The geometry of the knee joint was the same as one designed in chapter 3, where the preliminary frame analysis was presented.

The full size specimens consisted of the upper half of the column, and the lower half of the rafter connected by the glued in rod joint. The exterior connection had four # 20

re-bars on each end, while the interior was equipped with two # 20 re-bars glued into each part of glulam.

In Specimen 2 the interior steel plates and exterior strap were connected by welding.

Specimens 3,4 and 5 were of the same geometry but bolts were used for connecting the two parts.

MANUFACTURE OF THE CONNECTION

The glulam for the knee joint tests was made in Penticton by Structurlam Ltd. The initial step, to prepare the glued in rod joint, was to cut out the required gaps in the glulam and drill holes for the reinforcing bars. The geometry of the openings is presented on Figure 7.2.

The next step was to make the steel parts of the joint. The plates and straps were cut, the holes for the bolts (Specimen #3 to #5) drilled and taped. The straps had the same cross section as the inside plates, and were fixed to each other by welding. See Figure 7.1.

The reinforcing bars were cut to the desired lengths and bent to fit inside the holes so the flat part of the re-bar was touching the plates. The re-bars were then inserted in the holes and tackwelded to the plates, into the correct position. The assembly was then pulled out and the final welding was performed away from glulam. This was done to avoid burning of the glulam, and prevent damage to epoxy glue.

After the welding the assembly was glued to glulam by epoxy glue. One side, exterior or interior was glued at a time. After one day the specimen was flipped around and the steel plates were glued on the other side. The curing time used before testing was seven days.

After the glue had cured, the column and the rafter were fixed together by straps, which were bolted or welded to the plates. On the interior part of the connection, the strap was reinforced by two steel plates forming stiffeners. See Photograph 7.2

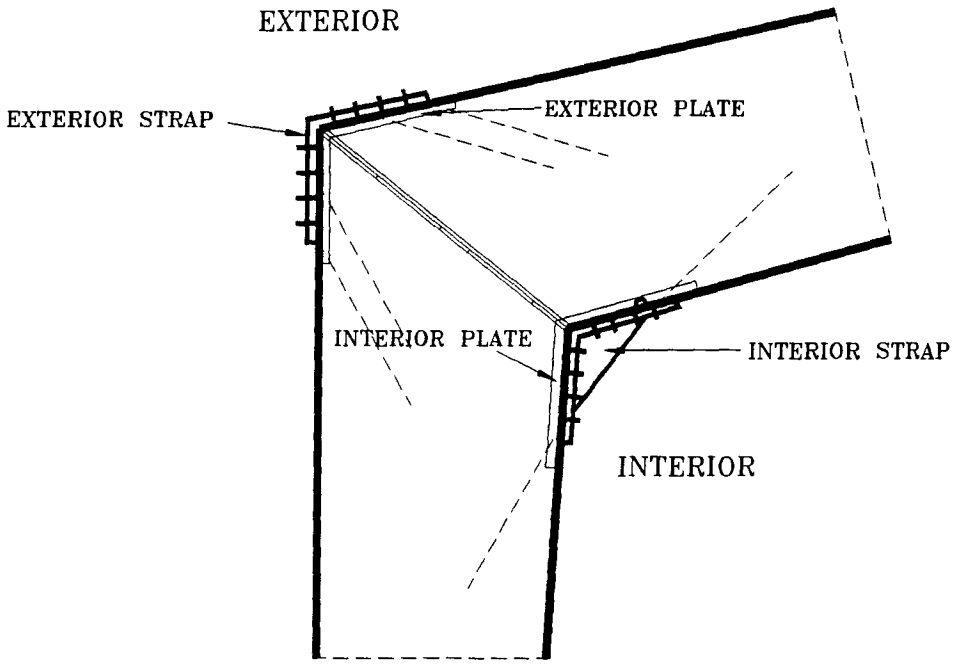

Figure 7.1 Knee joint using glued-in re-bars.

Figure 7.2 Manufacturing steps of the knee joint.

PREPARATION OF TIMBER

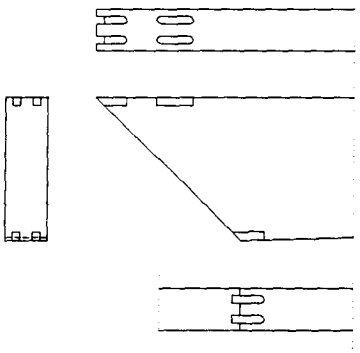

STEP 1
GROOVES FOR THE EMBEDDED REBARS ARE ROUTED TO A DEPTH OF 35mm FROM THE SURFACE

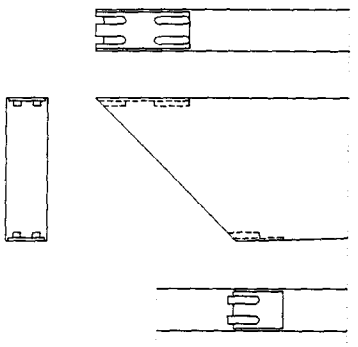

STEP 2
THE AREA TO BE COVERED BY THE STEEL PLATES IS ROUTED TO A DEPTH OF 12.7mm TO ACHIEVE A FLUSH OUTER SURFACE

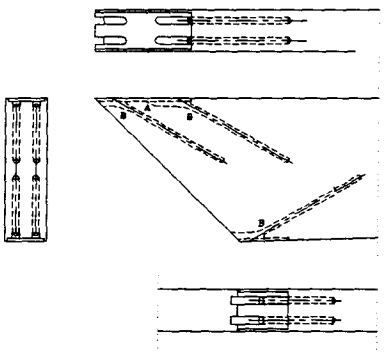

STEP 3
25.4mm HOLES OF LENGTH 460mm ARE THEN DRILLED AT 30 DEGREES PARALLEL TO GRAIN FOR THE REBARS AND POINT A & B ARE CHISELED FOR EASE OF REBAR INSERTION

PREPARATION OF STEEL PARTS

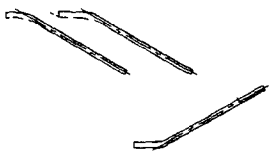

STEP 1
RE-BARS ARE CUT AND BENT

STEP 2
INSIDE PLATES ARE CUT FROM FLAT BAR - 12x152 mm. HOLES ARE DRILLED AND TAPED

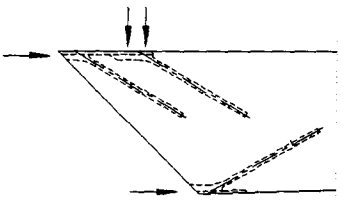

STEP 3
RE-BARS ARE INSERTED IN THE HOLES
INSIDE PLATE IS PLACED ON TOP AND TACKWELDED TO THE RE-BARS

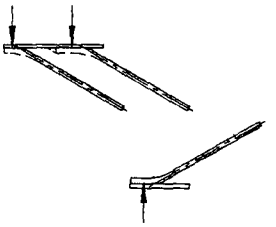

STEP 4
STEEL INSERTS ARE REMOVED FROM GLULAM.
WELDING OF RE-BARS TO STEEL PLATES (AWAY FROM GLULAM)

GLUEING

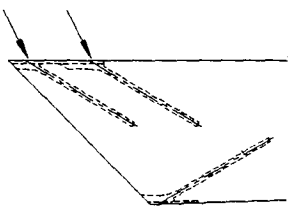

STEP 1
EPOXY IS MIXED AND POURED INSIDE THE HOLES

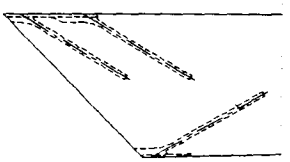

STEP 2
STEEL ASSEMBLIES ARE INSERTED INTO THE HOLES

7.3 TEST SETUP

The test setup for the knee joint tests consists of three major parts :

1. Actuator with transverse support.
2. Longitudinal support.
3. Brace preventing vertical deformations.

The specimec was connected to the jack, which was anchored to the concrete floor, and support via 50 mm diameter steel pins. See Figure 7.2. These pins were resting on 20 mm thick steel plates fixed top and bottom on one side to the actuator and on the other side to the longitudinal support.

The force was then transferred to the wood by steel plates attached by glulam rivets. Two steel plates were nailed at either sides of the specimen. The setup is presented on Figure 7.3 and Photograph 7.1.

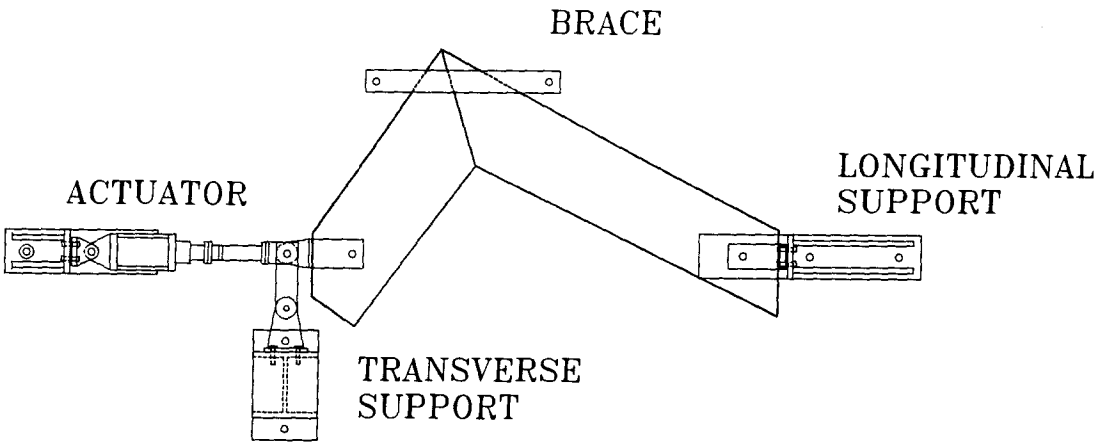

Figure 7.3 Knee joint test setup.

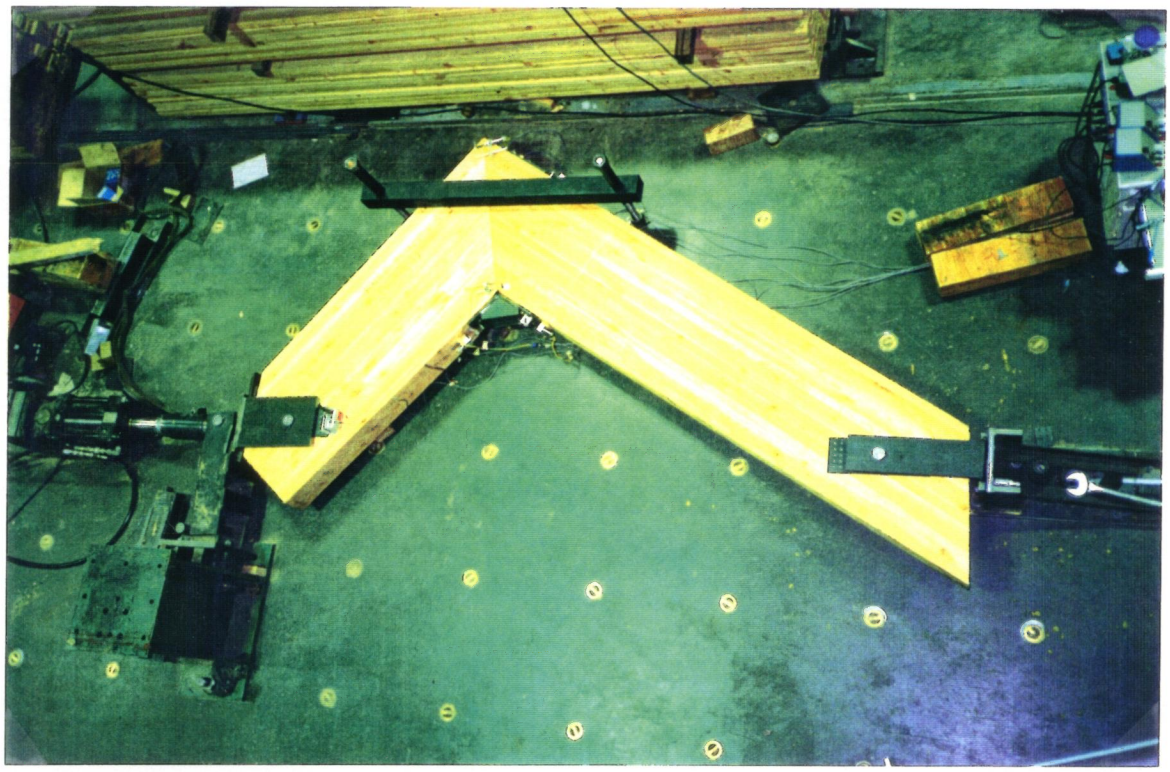

Photograph 7.1 Knee joint test setup.

7.4 INSTRUMENTATION OF THE SPECIMEN

The data acquisition system was used to read 8 channels of data. The loading force was read from the load cell. The change of the distance between the pins was recorded by a electronic displacement gage.

The opening and closing of the gap between the glulam members was monitored by two LVDT's , one situated on the exterior and one on the interior part of the joint.

The movement of the steel plates, relative to the glulam, was recorded by 4 LVDT's. Instrumentation of the internal part of the specimen is presented on Photograph 7.2.

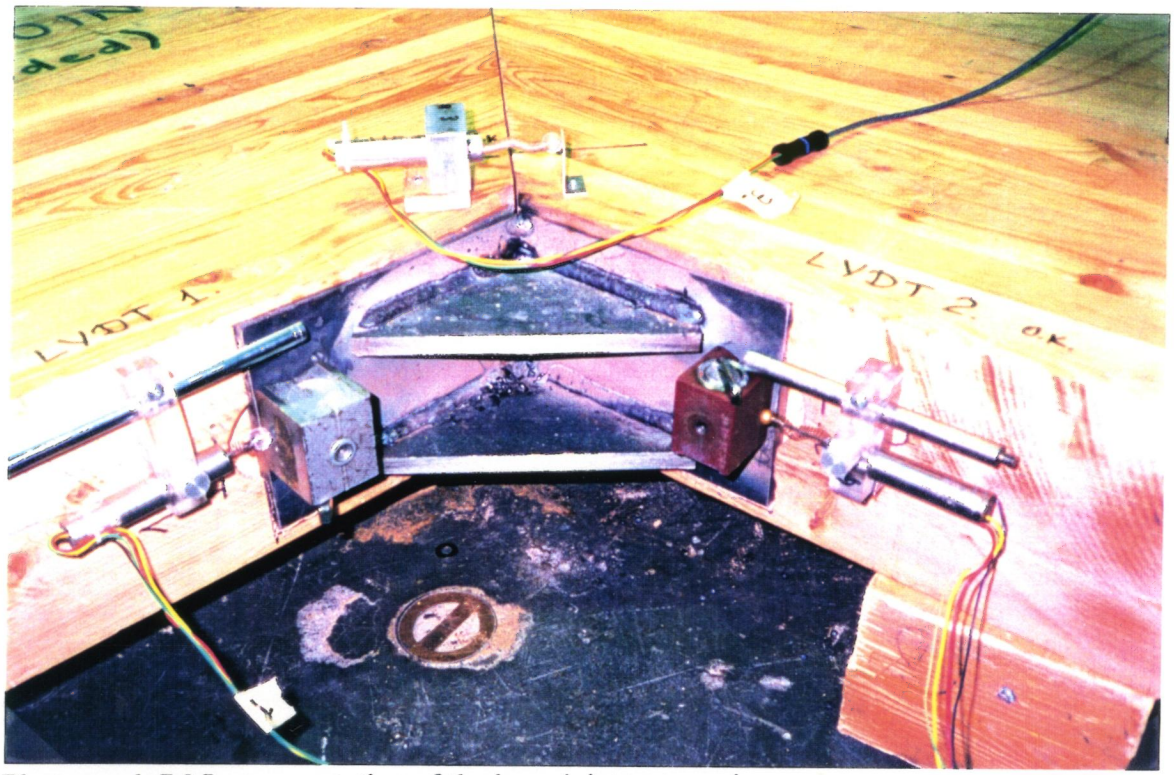

Photograph 7.2 Instrumentation of the knee joint test specimen.

7.5 TESTING PROCEDURE

All specimens were tested under cyclic loading. Four cycles of each load step were applied. Load steps of 10 kN were used for Specimen 1, and 20 kN for other specimens. The specimen was unloaded, and the data was saved on disks, before the next load step was applied.

The specimens were loaded with the bigger force under compression then under tension. The tensile force was about 20% of the compressive loading, because of the conditions in the design, performed in Chapter 2. See Figure 7.4. The first failure was designed to be the tension failure of the exterior re-bars, when the specimen was loaded in compression.

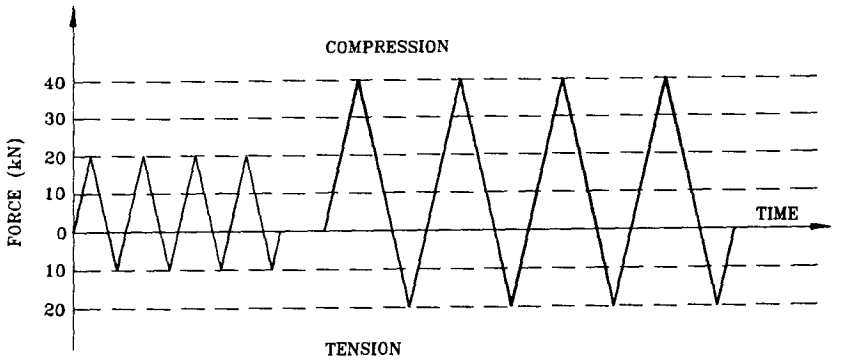

Figure 7.4 Loading history during knee joint tests.

7.6 ANALYSIS OF TEST DATA

The observations from the tests would be presented for all the joints in the following order.

1. Overall behaviour of the joints - displacement between pins, bending moments.
2. Rotation of the joint.
3. Movements in the steel plates.
4. Conclusions.

7.6.1 OVERALL BEHAVIOR OF JOINTS

7.6.1.1 SPECIMEN 1

Specimen 1 was a preliminary knee joint built from glulam left over from the racking tests. The glulam cross-section was 175 x 495 mm. The joint was equipped with four #20 re-bars on the exterior and two #20 re-bars on the interior part of the connection. The interior and exterior straps were connected by bolts, to the column and the rafter. (bolt diameter = 16 mm).

The following analysis is based on the relationship between bending moment at the joint and the change of the displacement between the pins. Specimen 1 was loaded with 16 different load increments, each having four cycles of tension and compression. The average of four cycles is presented on the graph.

The load was applied using a load control pattern. The loads were increased in 10 kN intervals.

The following bending moment convention was used. Positive bending moment is occurring when the outside part of the connection is under tension emulating the frame loaded with gravity loads. The specimen was loaded in compression. Negative bending moment is present when the inside part of the joint is under tension analogous to the earthquake or wind loads. The specimen was loaded in tension.

The moment displacement relation was linear only during the first loading, when the bending moment reached 10 kNm under compression and 5 kNm under tension. During the next, higher loadings a much stiffer behavior was observed under compression than under tension. The reason was the development of a hinge at the weld between the interior straps. This was an oversight, it should have had a stiffener.

During the second to last loading wood crushing started at the peak loads (98% of the ultimate load) on the exterior part of the joint. Specimen 1 reached its ultimate strength, when extensive wood crushing causing large decrease in the distance between the pins ; the end of stroke was reached in the actuator. The maximum positive bending moment was 148 kNm, which was 90% of design glulam resistance, assuming a bending stress in the glulam of 30.6 kNm. (Stress in glulam during testing - 27.5 MPa)

The specimen was then loaded in tension to failure. The failure was located at the weld connecting the re-bars and the steel plate on the interior part of the joint. It was caused by the mentioned development of the hinge at the weld joining the straps, since stiffener had not been used. See Photograph 7.3. The maximum negative bending moment was 49 kNm. The relation between the bending moment at joint and the displacement between pins is presented on Figure 7.5. Displacement between pins is caused by joint deformation

and members deformations.

The specimen after failure in shown on Photograph 7.3. Note the wood bearing failure on the exterior part of the connection and the weld failure on the interior part of the joint.

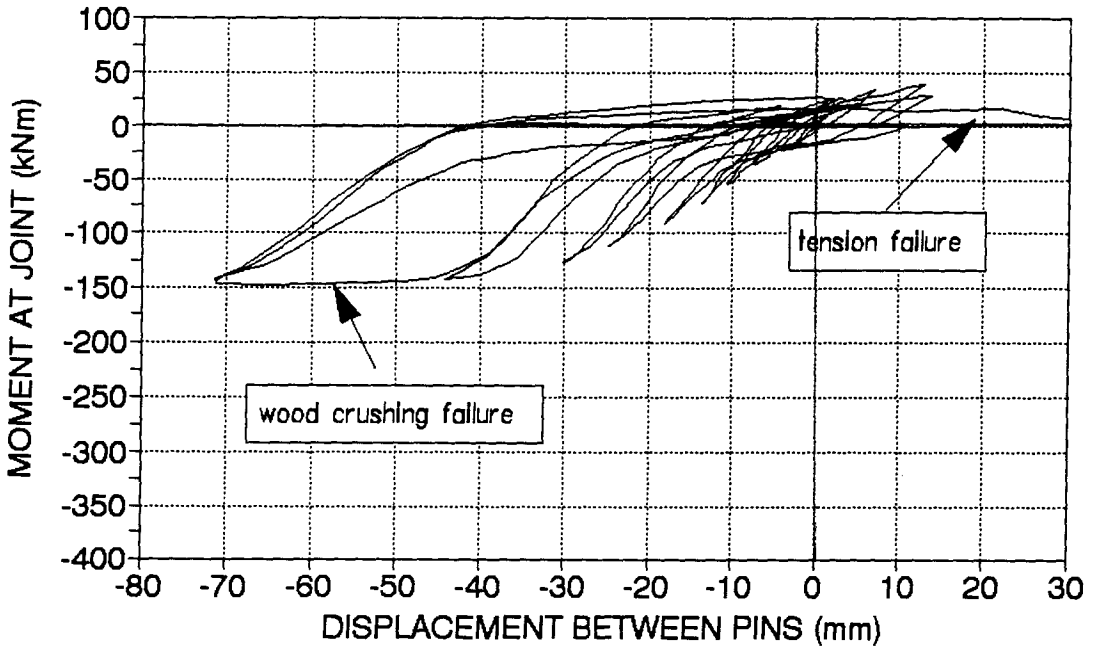

Figure 7.5 Displacement and bending moment relation for Specimen 1.

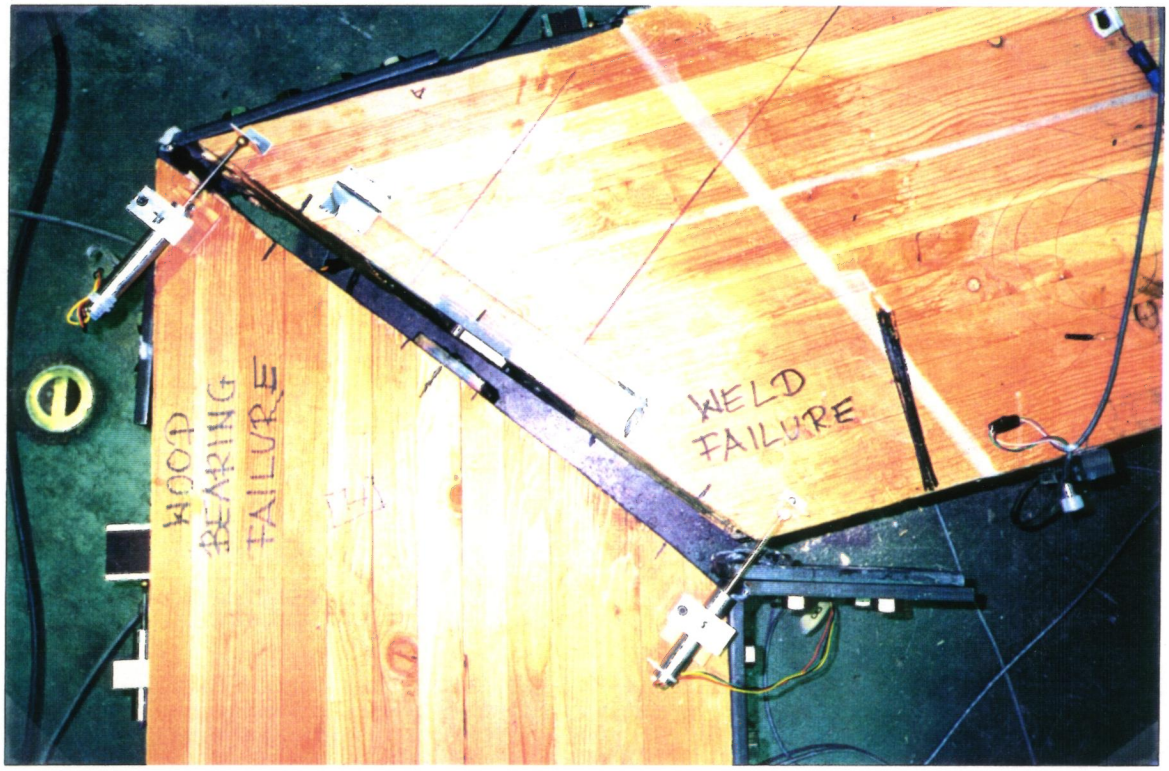

Photograph 7.3 Specimen 1 after failure.

This was as mentioned a preliminary test, and should not be considered in the overall analysis of the joints.

7.6.1.2 SPECIMEN 2

Beginning with specimen 2 the geometry of the glulam was specially designed for the purpose of testing knee joints, to satisfy the conditions described in Chapter 2.

Specimen 2 had four #20 re-bars on the external side, and two #20 re-bars on the internal part of the joint, in each of the members. The straps were welded to the inside plates. Specimen 2 was the only one where this welding was used. The purpose of this was to check the behavior of the welded strap, and compare it with that of bolted straps.

The interior part of the joint was equipped with two steel plate stiffeners, which were in the same planes as the re-bars. (See Photograph 7.2.) This was designed to prevent the development of a hinge at weld connecting the outside plates, which was observed, during Specimen 1 experiments.

The relations between the bending moment at the joint and the change of the distance between two pins were very linear for all the loadings except the final one. See Figure 7.6. The linear character was lost under loads creating bending moments grater then 275 kNm.

The maximum bending moment at failure was 302 kNm. The specimen failed by re-bar tension failure on the exterior part of the joint. The two outside re-bars failed in tension, and then the front part of the steel plate crushed into the wood. See Photograph 7.4 and 7.5.

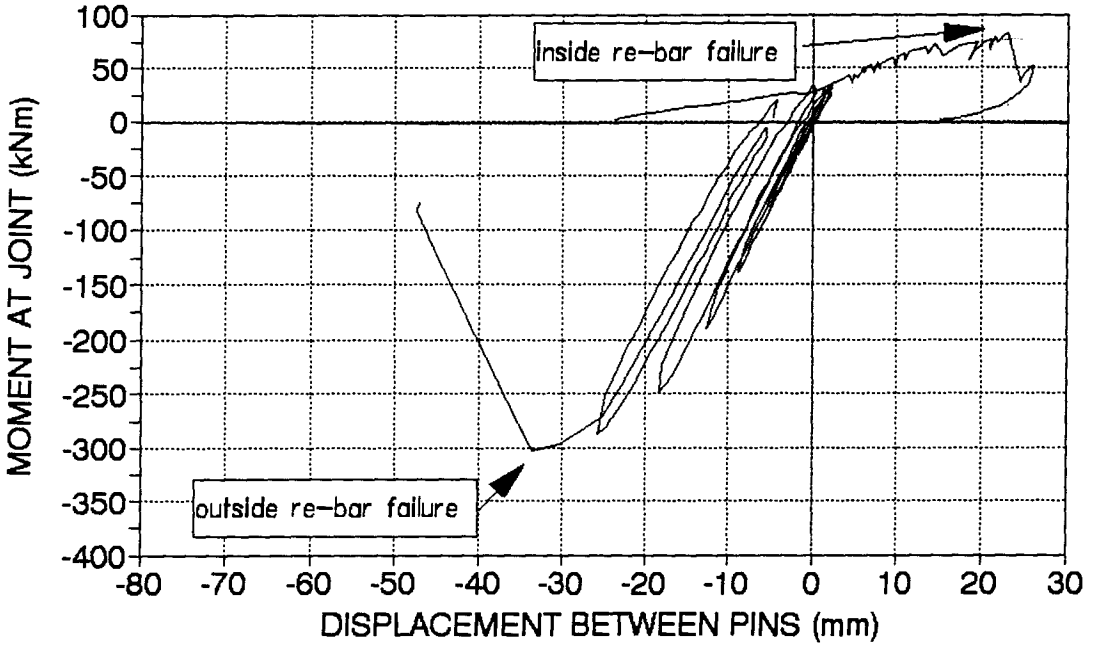

Figure 7.6 Displacement and bending moment relation for Specimen 2.

Specimen #	2
Bending moment - positive (kNm)	302
Bending moment - negative (kNm)	80
Glulam capacity - Mr (kNm)	314

Table 7.1 Ultimate bending moments at joint for Specimen 2.

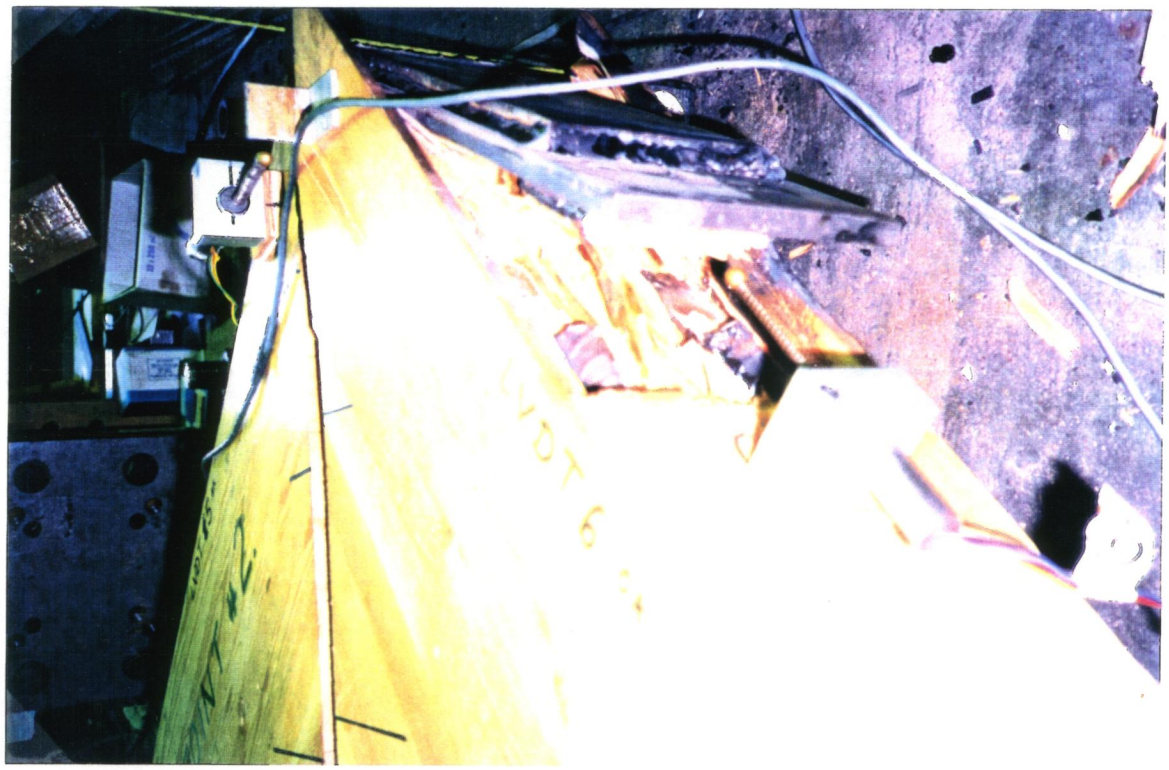

Photograph 7.4 Specimen 1 after failure. Re-bar failure - phase 1. (above)

Photograph 7.5 Specimen 1 after failure. Wood crushing failure - phase 2. (below)

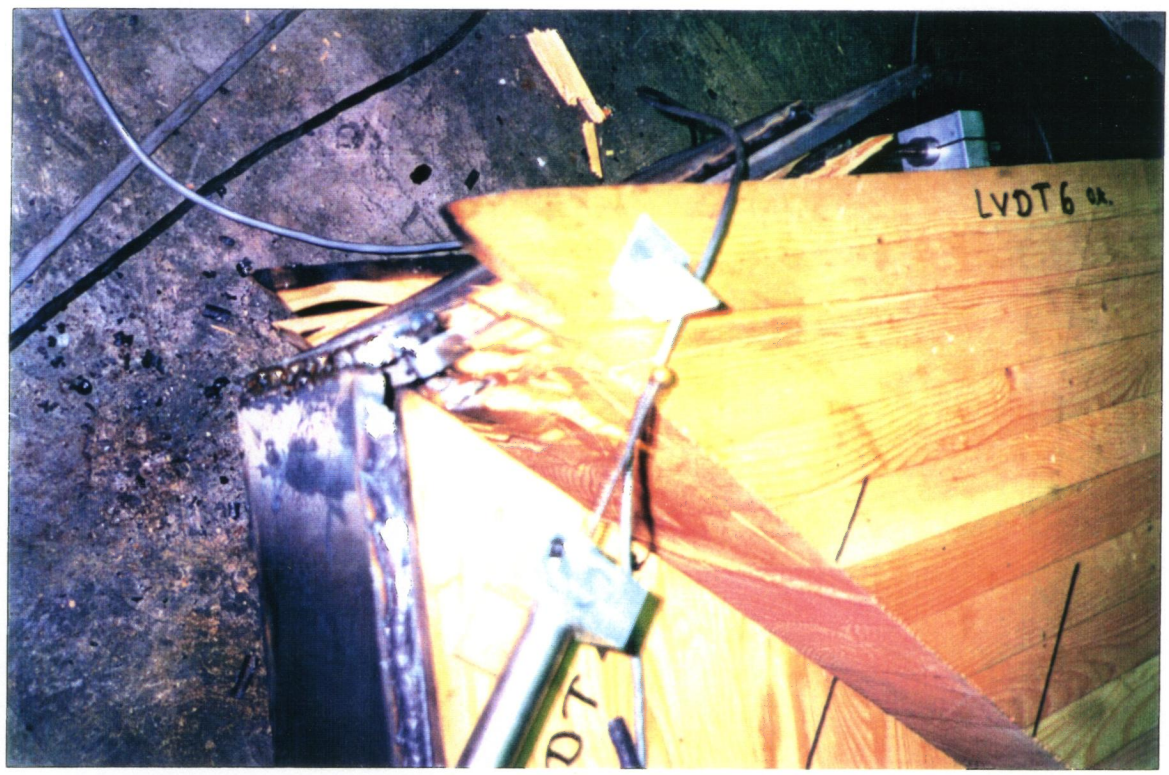

7.6.1.3 SPECIMENS 3,4 and 5

Specimens 3,4 and 5 were identical. They were equipped with four #20 re-bars on the external side of the joint and two #20 re-bars on the internal side. The strap and the steel plates were connected by bolts. (Eight 16 mm bolts were used on the exterior side and four bolts on the interior side, in each part of the connection) The connections had the stiffener similar to that of Specimen 2.

The relations between the bending moment in the joint and the displacement between pins was very similar for all three specimens. See Figures 7.7,7.8 and 7.9. For the loadings resulting in the moments less than 300 kNm, the relation is almost linear and identical for all four cycles of each loading. The failure was tension failure in the re-bars, for all specimens except Specimen 5 which failed under positive moment by wood crushing. In the other specimens two exterior re-bars failed in tension. Then the front part of the steel plate crushed into wood. After the failure under positive bending moment the specimens were loaded to failure under negative moment. In all three specimens the failure was tension failure in the re-bars. The failure modes are presented on Photographs 7.6,7.7 an 7.8.

The ultimate bending moments at joint for Specimens 3,4 and 5 are presented in Table 7.2. Specimen 4 failed in tension under a smaller moment than the other two because of a large displacement after failure on the outside of the joint, which bent the re-bars on the inside part of the connection.

Specimen #	3	4	5	AVERAGE
Bending moment - positive (kNm)	349.2	346.4	358.0	351.2
Bending moment - negative (kNm)	71.7	41.0	68.0	60.0
Glulam capacity - Mr (kNm)	314	314	314	314

Table 7.2. Ultimate bending moments at joint for Specimens 3,4 and 5.

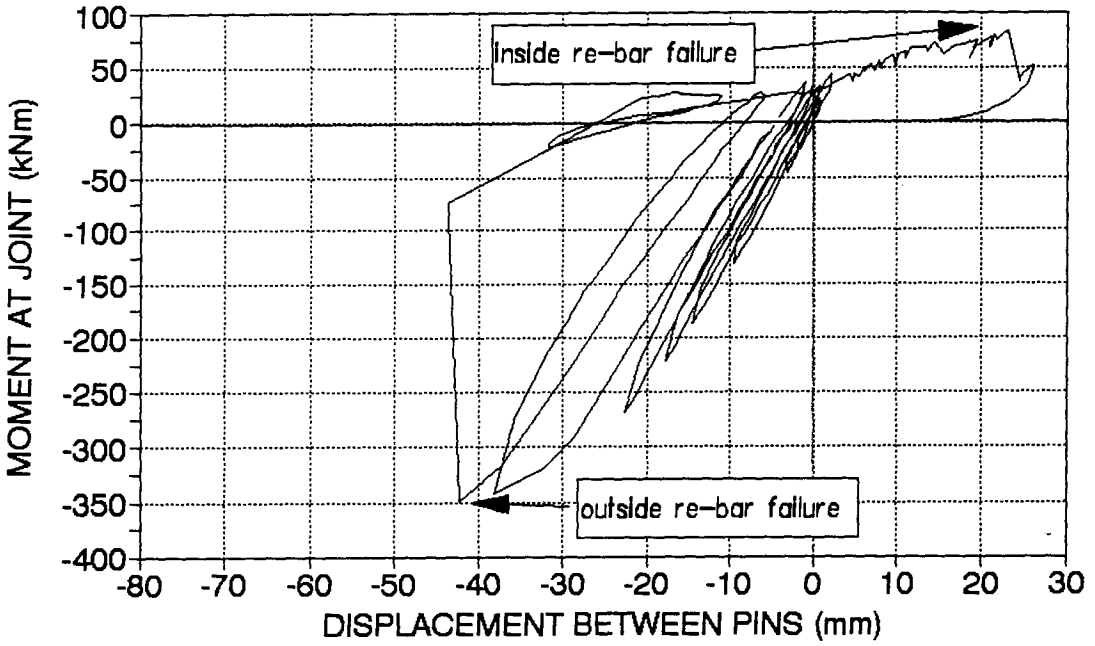

Figure 7.7 Displacement and bending moment relation for Specimen 3.

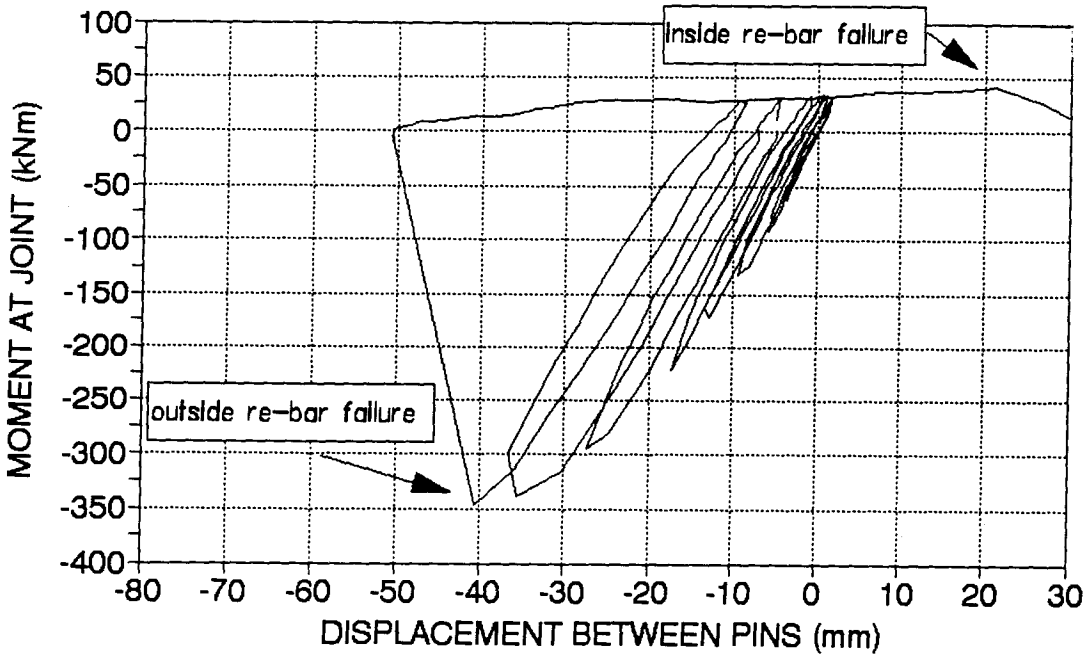

Figure 7.8 Displacement and bending moment relation for Specimen 4.

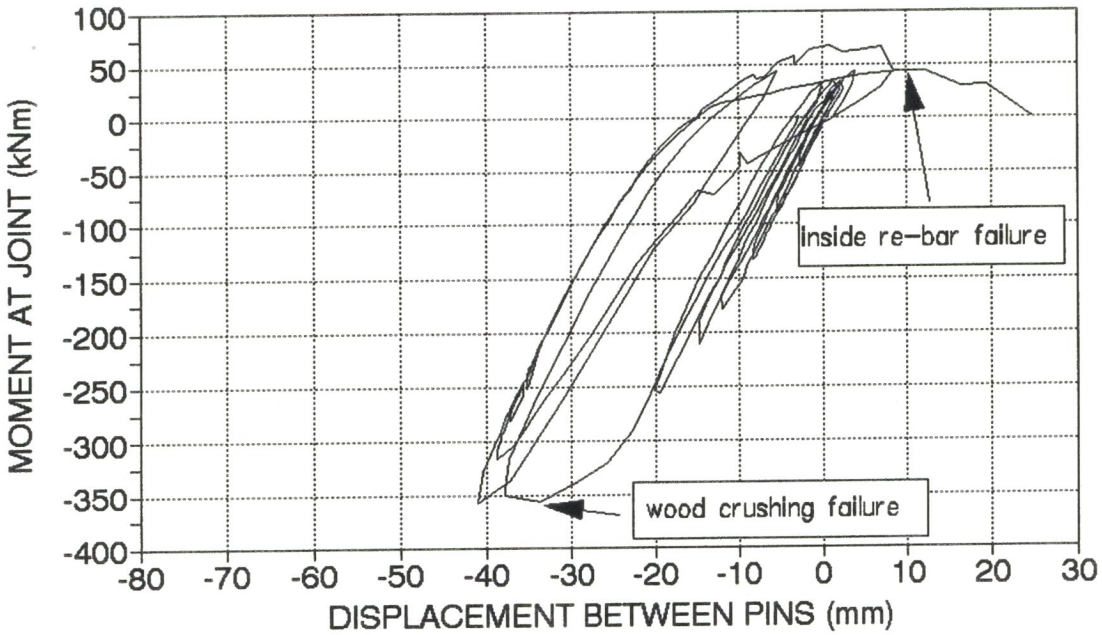

Figure 7.9 Displacement and bending moment relation for Specimen 5.

Photograph 7.6 Specimen 3 after failure.

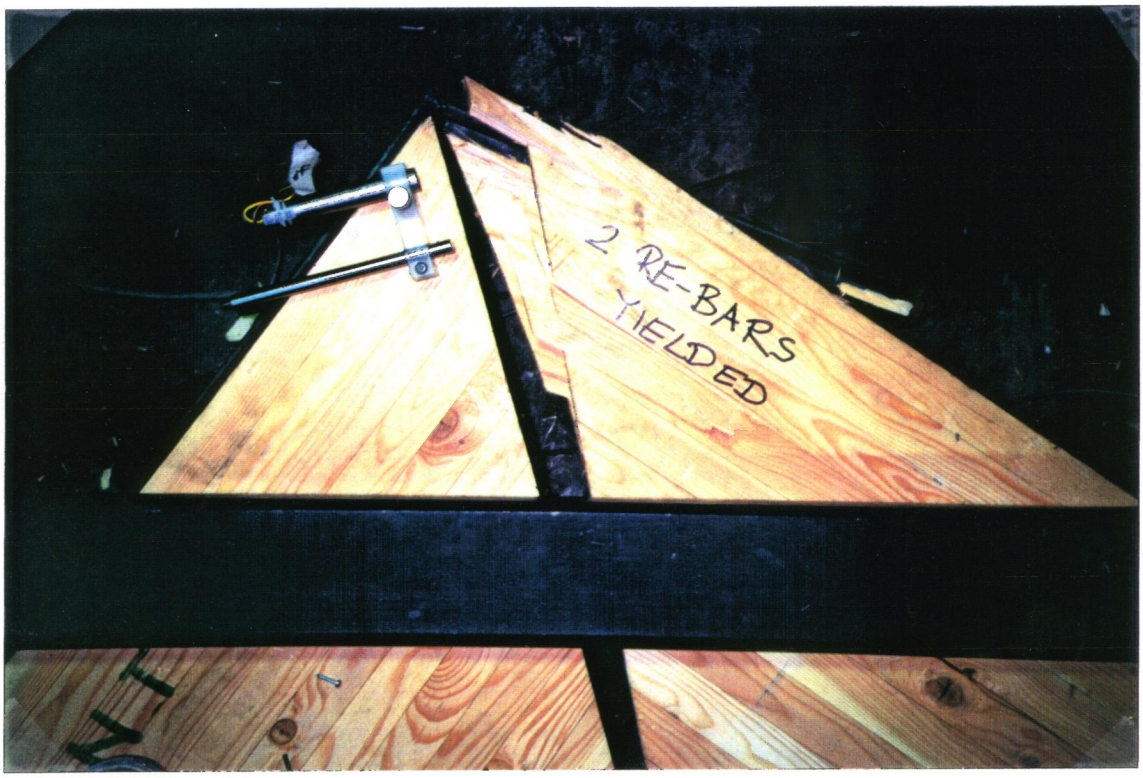

Photograph 7.7 Specimen 4 after failure. (above)

Photograph 7.8 Specimen 5 after failure. (below)

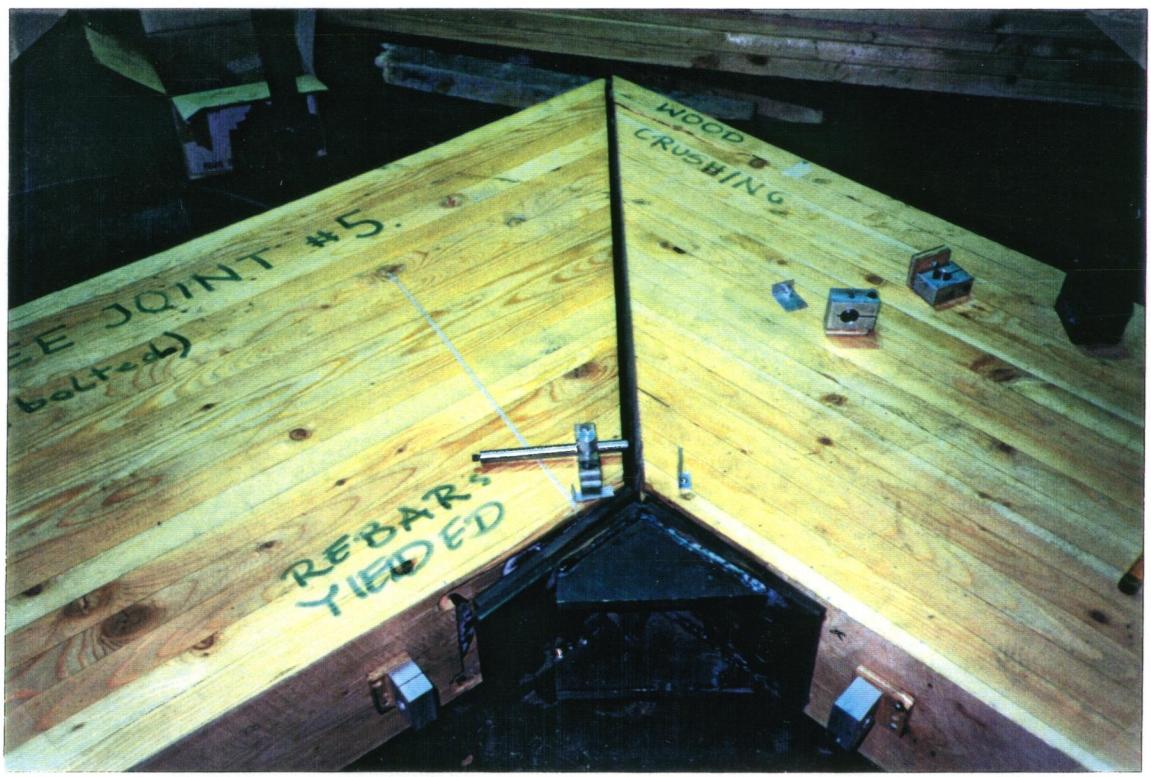

7.6.1.4 SUMMARY

1. Stiffeners, at the interior of the joint, are needed to eliminate the formation of a hinge in the strap on the interior part of the joint.

2. The welded joint failed at a bending moment 50 kNm less than the average of the bolted joints.

The reason may be that under the peak loads the two welded plates transferred the whole force to the back row of re-bars. Specimens 3,4 and 5, where the plates where bolted, failed at slightly higher loads because the interior and the exterior plates yielded, and the bolts moved in the oversized holes so more load was transferred to the front row of re-bars. The bolted specimens allowed more play in the joint region and were more flexible.

The indication of this can be shown on the moment displacement graphs presented in this section. Under failure the displacement between the pins for the welded specimen was 33 mm, while for the bolted ones it was between 41 and 43 mm.

3. The maximum positive bending moments for bolted specimens were close to each other. (Ultimate negative moment was measured after failure at the exterior of the joint)

4. Bolted joint moment resistance, measured during tests, was 10% higher than nominal glulam capacity.

7.6.2 THE ROTATION OF THE JOINT

The rotation of the joint was measured by two LVDT's : one situated at the exterior corner of the joint, and the other near the interior corner. The LVDT's were attached to the side of the glulam members, with one part on the column and the other on the rafter. The instrumentation of Specimen 5, typical for all tests, is presented on Photograph 7.9.

The bending moment at the knee, obtained from the analysis, under specified loads was 150 kNm. Since the deflections are checked under specified loads the gap openings caused by this moment are presented. See Table 7.3.

The relations between the bending moment in the joint and the gap openings at the locations of LVDT's are presented on graphs 7.8 to 7.11. The solid line on the graph represents the movement of the interior placed LVDT. The dotted line shows the exterior gap opening.

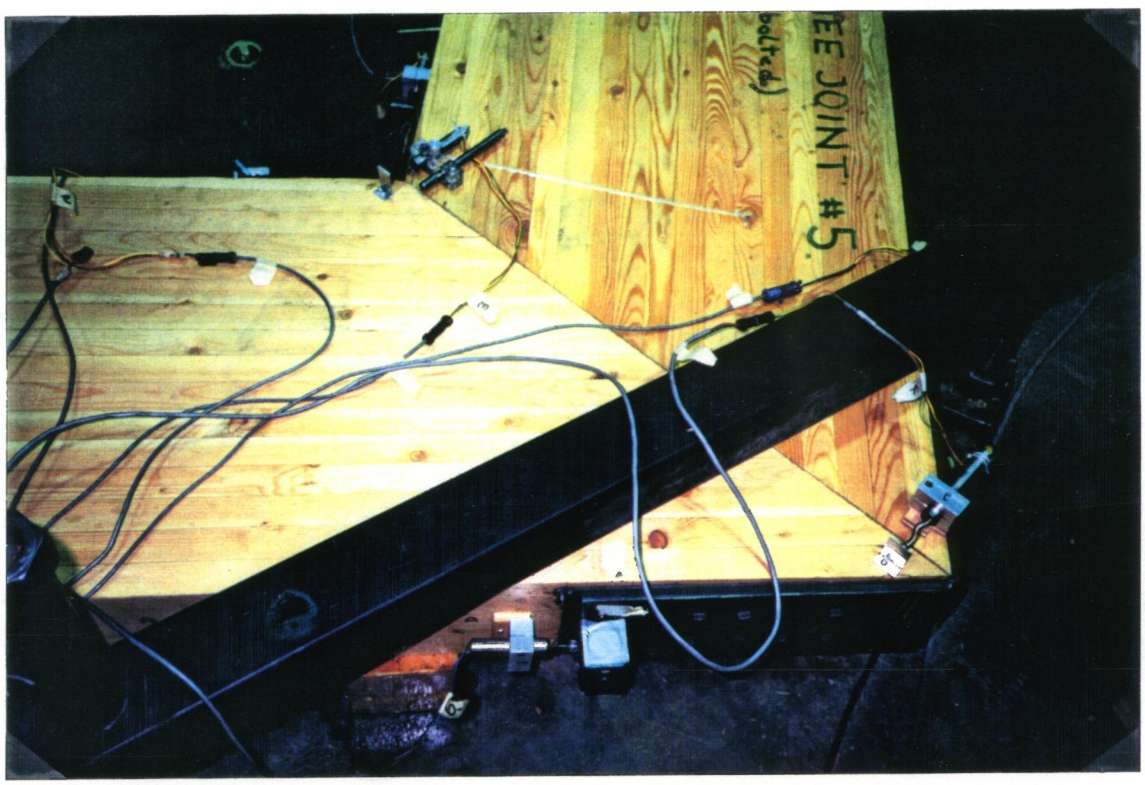

Photograph 7.9 Instrumentation of the specimen to measure the joint rotation.

7.6.2.1 SPECIMEN 2 (welded connection)

There was very little movement at the interior part of the joint. At ultimate loadings, the inside displacement was less than 1 mm. The exterior Lvdt's showed much more movements. Under specified loads the gap opened 3.5 mm, Åndunder ultimate loads the opening reached 12 mm at the exterior side. This deformation was caused by compression perpendicular to grain on the exterior part of the joint, as well as stretching of the straps. The relation between the bending moment at the joint and the gap opening is almost linear for all loadings, with exception of the final one. See Figure 7.10.

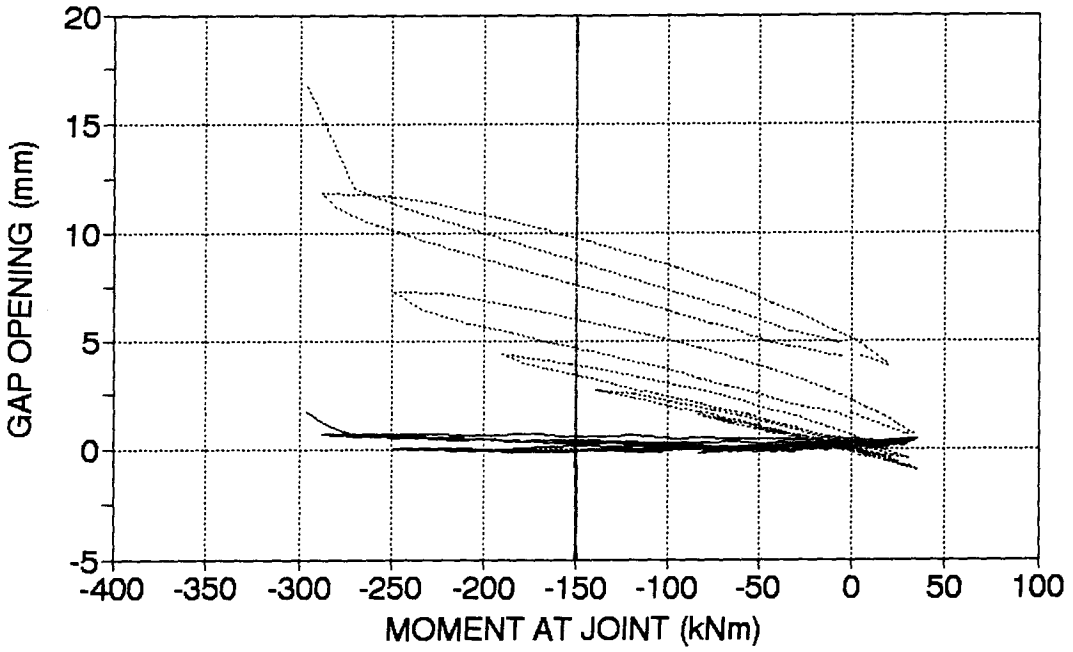

Figure 7.10 Gap opening in Specimen 2. (dotted line - exterior, solid line interior)

7.6.2.2 SPECIMEN 3,4 and 5 (bolted connection)

The movements on the interior of the joint were larger for the specimens equipped with bolted connections. The biggest increase can be observed on Figure 7.10 showing the behavior of Specimen 4. However under specified loads the interior movements are less then 3 mm for all three specimens.

The exterior gap opening for the bolted specimens, under specified loads, was in the same range as for the welded joint. It varied from 1.7 mm in Specimen 3, through 2.4 mm in Specimen 5, up to 3 mm in Specimen 4. The relation between the gap opening and the bending moment at joint is similar to that of Specimen 2, linear for all the loadings excluding the failure ones. See Figures 7.11, 7.12, and 7.13.

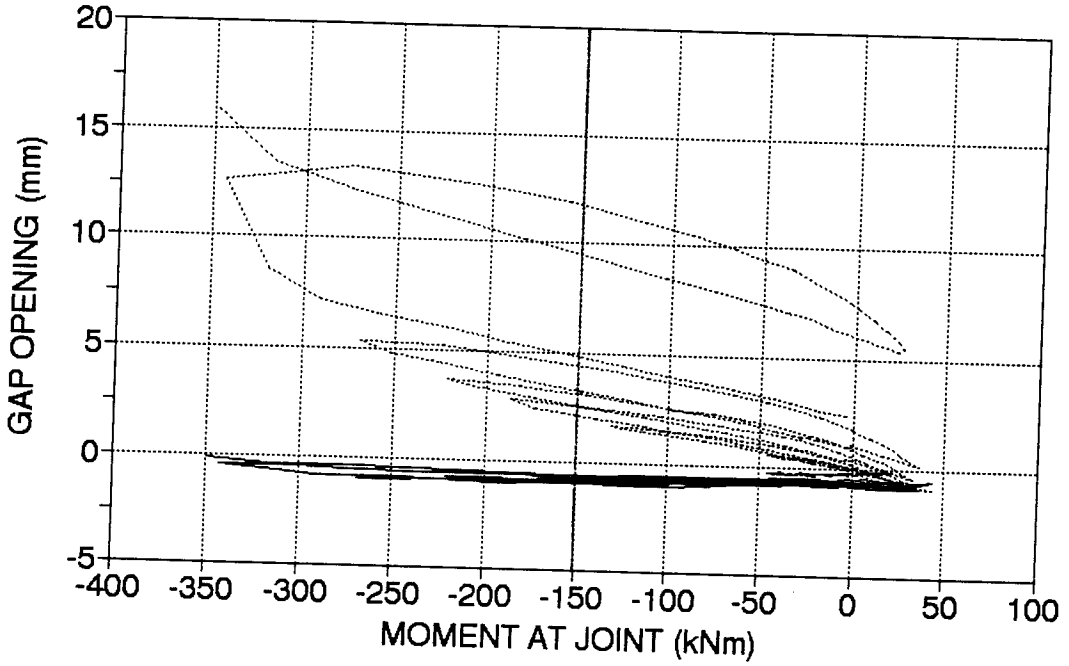

Figure 7.11 Gap opening in Specimen 3. (dotted line - exterior, solid line interior)

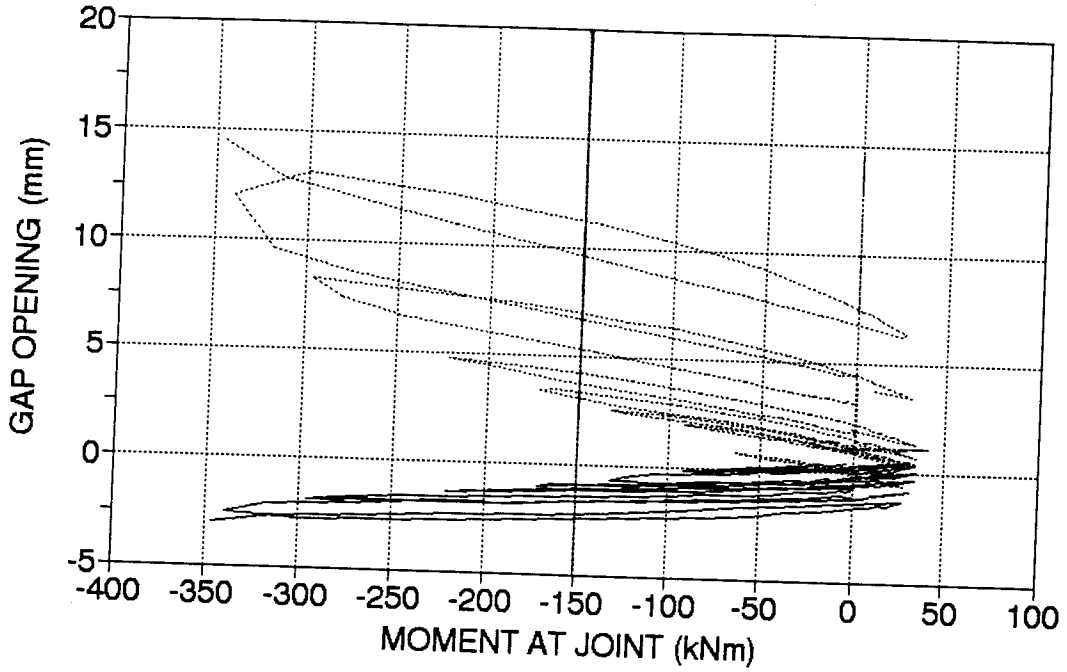

Figure 7.12 Gap opening in Specimen 4. (dotted line - exterior, solid line interior)

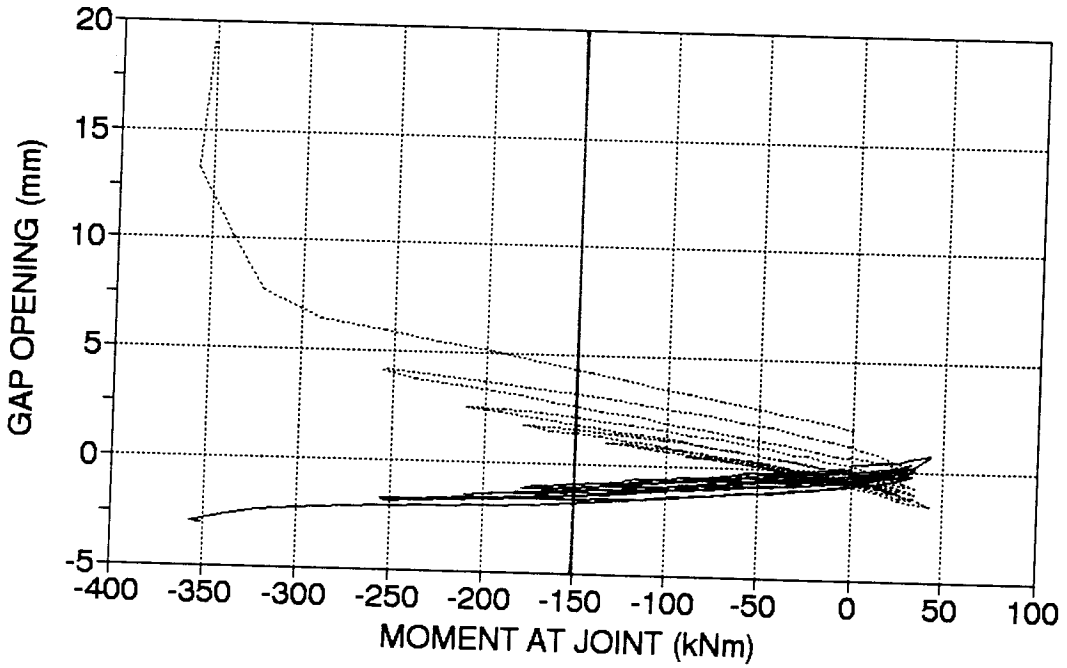

Figure 7.13 Gap opening in Specimen 5. (dotted line - exterior, solid line interior)

The following table summarizes the results

Spec	GAP OPENING - (mm)					
#	At specified load			At ultimate load		
	external	internal	total	external	internal	total
2	2	1	3	13	1	14
3	2.5	1	3.5	12	1	13
4	3	1.5	4.5	12	3	15
5	1.5	1	2.5	10	2	12

Table 7.3 Gap opening results.

7.6.2.3 SUMMARY

1. Gap opening analysis showed the difference between welded and bolted joints. For the welded connection, the inside crushing of wood was less than 1 mm up to failure load. For the bolted joints, the inside crushing of wood reached 3 mm in Specimen 4. On the outside, gap opening was similar for welded and bolted joints. Under failure the joint opened around 15 mm for all four specimens. This translates to a deflection of the real structure of 36 mm and 150 mm for the service load and ultimate load respectively, caused by rotation alone.

2. For the design and specified load range, the relations between the gap opening and the bending moment at joint are very linear and consistent for all four cycles of each loading.

7.6.3 MOVEMENT IN THE STEEL PLATES

The performance of the glued-in rod connection depends on the bond between the re-bars and the wood. One of the methods to monitor this behavior is to check how much the steel plates move relatively to glulam surface under loading.

During this series of tests, movement of all four steel plates was recorded. Four LVDT's were fixed to the wood with its moving parts rested on magnets attached to the plates. The following analysis uses the relation between the displacement of all four plates and bending moment at joint for selected loadings. (each loop represents different loading)

7.6.3.1 SPECIMEN 2

Very little movement was observed on the interior part of the joint for the welded connection of Specimen 2. The displacement under designed loads was less than 1 mm. On the exterior side of the joint a non-symmetrical behavior was observed.

A much bigger movement was noticed in the steel plate fixed to the rafter than the one attached to the column, what is indicated by the location of failure which took place in the outside bars of the rafter plate. The other plate moved less than 1 mm even under peak loads. For the relation between the steel plate movements and the bending moment at knee see Figure 7.14. Solid lines on the graph represent the movements of the interior plates, while the dotted lines represent the movements of the exterior plates.

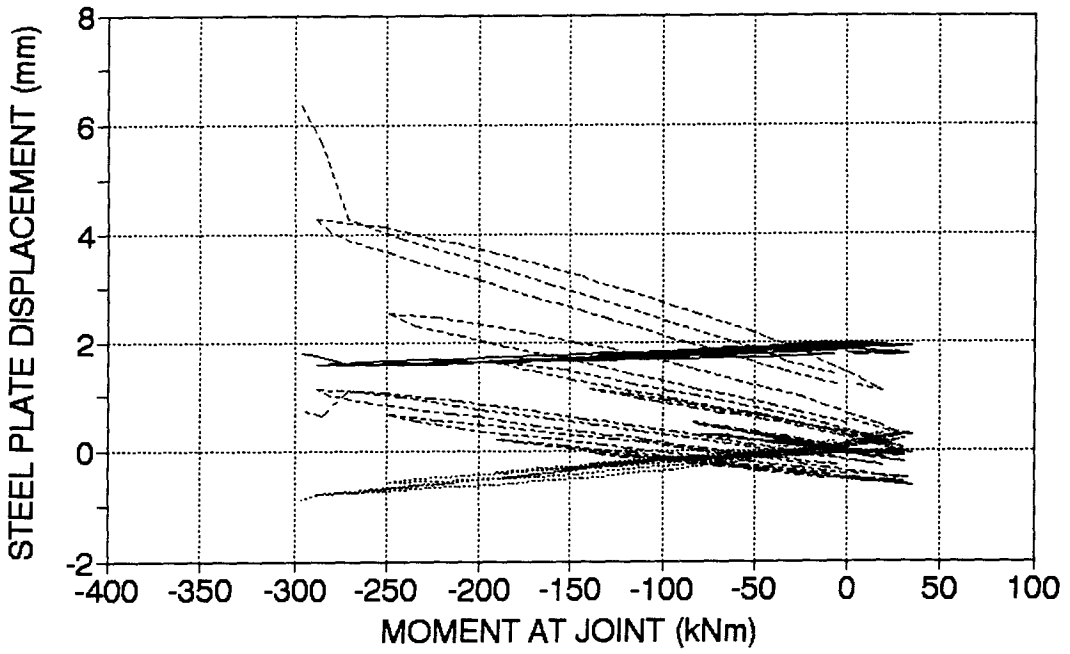

Figure 7.14 Steel plate movements of Specimen 2. (dotted line - exterior, solid line interior)

7.6.3.2 SPECIMEN 3,4 and 5

The steel plates displaced much more in the bolted specimens, than in the welded joint. This can be observed on the interior part of the joint where the movement of the plates under peak loads reached 3 mm (Specimen 3), comparing with less than 1 mm for the welded connection.

On the exterior part the similar behavior as for the welded joint was observed. The steel plate attached to the rafter moved much more than the one attached to the beam, where displacement and moment relation remained linear during all loadings including the peak ones. For the relations of the steel plate movement and the bending moment at joint see Figures 7.15, 7.16.

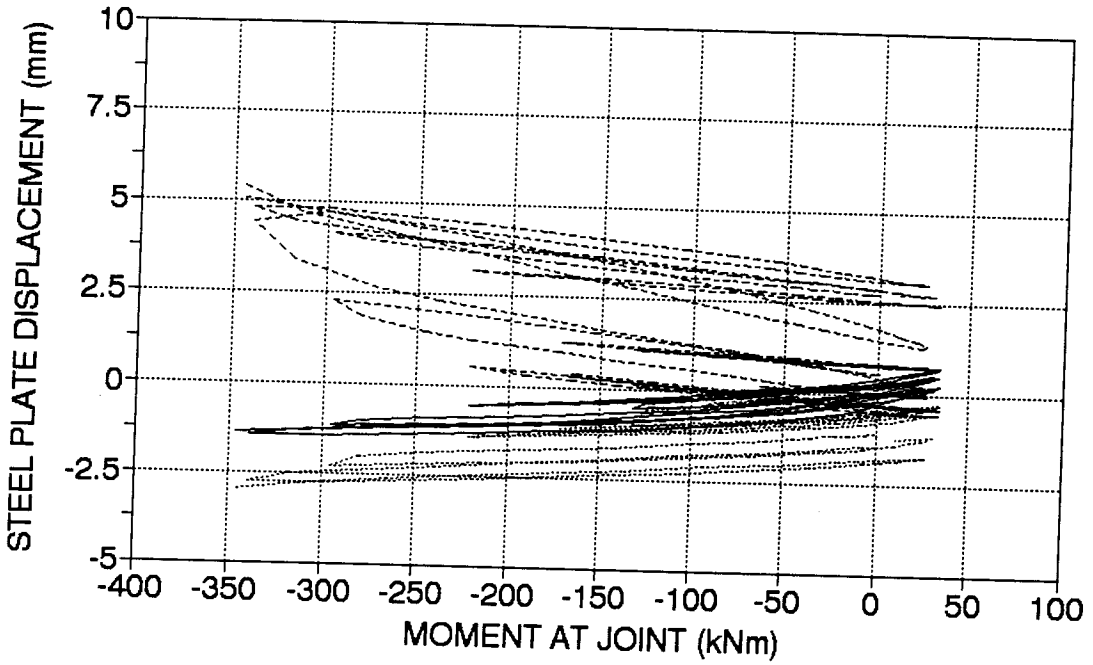

Figure 7.15 Steel plate movements of Specimen 4. (dotted line - exterior, solid line interior)

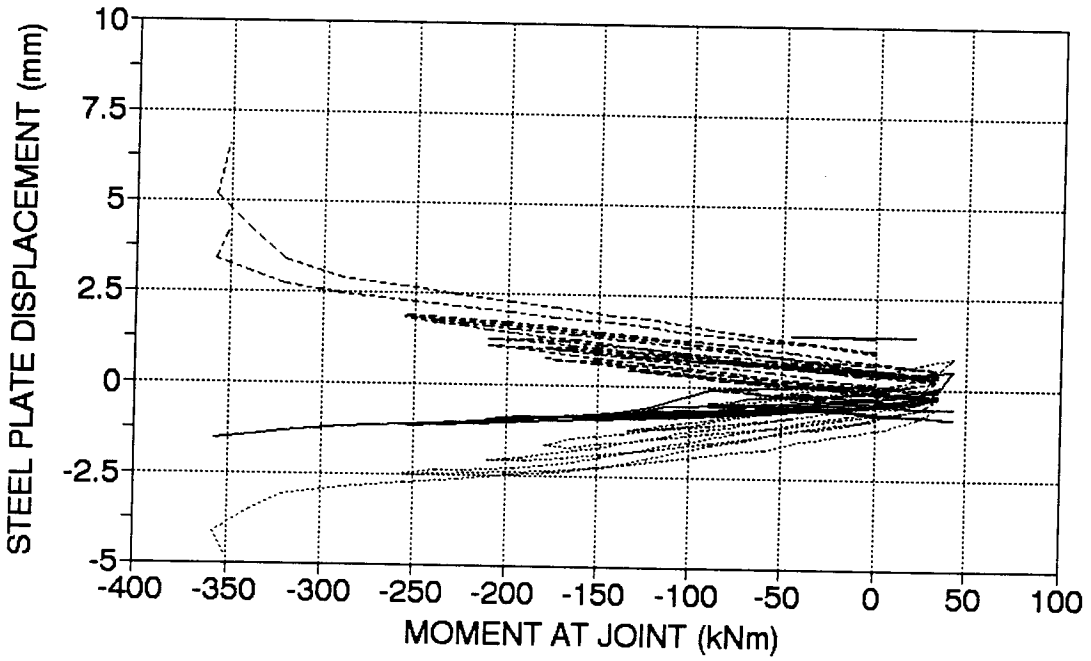

Figure 7.16 Steel plate movements of Specimen 5. (dotted line - exterior, solid line interior)

7.6.3.3 SUMMARY

1. The analysis of the steel plate movement showed the linear relationship and very small deformations during specified and design loads. The re-bar tension failure can be tracked more precise looking at the movement of the steel plate attached to the rafter, where the re-bars failed.

2. The steel plate displacement indicates very stiff bond between glulam and embedded re-bars, which is a desired requirement for the glued-in rod joint.

7.7 CONCLUSIONS FROM THE KNEE JOINT TESTS

1. The knee joint tests demonstrated a balanced designed glued-in rod knee joint. The bending moment resistance of the connection was 10% higher than the nominal glulam cross-section capacity.

2. Knee joints failed by tension failure in the re-bars in the interior and exterior of the connection except the preliminary joint #1 and Specimen 5 which failed by wood crushing under positive moment. The ultimate resistance of Specimen 5, despite different failure mode was in the same range as for the specimens which failed under re-bar tension failure.

3. The positive bending moment resistance - 350 kNm, was very consistent for all bolted specimens and 50 kNm higher than the resistance of the welded joint - 300 kNm.

4. The preliminary test showed the need of using a stiffener on the inside part of the connection.

5. The gap opening analysis showed that under specified loads the opening of the gap on the exterior of the joint was less than 3.6 mm, which translates to 51 mm deflection in the real structure. For the ultimate load the deflection caused by the joint rotation will be around 215 mm.

6. The steel plate movement analysis showed the existence of a strong bond between the re-bars and the glulam, which allowed less than 1 mm movement of the steel plates.

CHAPTER 8

DESIGN OF GLUED-IN RE-BAR JOINTS

8.1 INTRODUCTION

Based on the test results and an engineering analysis a proposed, approximate design method for glued-in rod joints is presented. Two configurations are considered :

1. A symmetrical joint such as would be used in a column to foundation connection, or in a splice joint for a beam, where the moments are resisted by the forces in the steel rods.
2. An unsymmetrical knee joint as in a portal frame.

8.2 DESIGN STEPS

A design of a glued-in rod joint may consist of the following steps :

A) STRENGTH LIMIT STATE.

STEP 1. Moment resistance - Mr of the joint. Knowing the external bending moment Mf from analysis determine the area of re-bars needed to carry the moment, according to the geometry of the joint.

STEP 2. Bearing capacity of the steel plate. Force perpendicular to grain has to be transferred to glulam by compression perpendicular to grain.

STEP 3. Steel plate resistance.

A. Tension resistance of the steel plates: inside plate and straps.

B. Bending resistance of the steel plates.

C. Tension and bending combined.

STEP 5. Bolts or studs.

Calculate the number of bolts and check them for shear.

STEP 6. Welds : Strap weld.

Re-bar to steel plate weld.

STEP 7. Shear resistance.

Interior stiffener, design for shear.

B.) SERVICEABILITY LIMIT STATE.

STEP 8. Check deflections under specified loads.

DESIGN ASSUMPTIONS

1. Failure of glued-in rod joint takes place in re-bars - failure mode is bar tension failure.
2. Bending moment is carried by tension in re-bars and compression by re-bars in conjunction with compression in the glulam.
3. Shear resistance is provided by outside straps and inside stiffener.
4. Shear force V2 (See Figure 8.1) is assumed small in comparison to Fr and it was neglected.

The testing was performed for the angle of re-bar inclination to grain equal to 30 degrees. In the design steps a general angle alpha is used.

8.3 SPLICE JOINT AND FOUNDATION JOINT

8.3.1 STEP 1. - CALCULATE BENDING RESISTANCE OF THE JOINT.

During Step 1 of the design process the re-bar area needed to transfer the moment is determined.

The geometry of the joint is presented on Figure 8.1 .

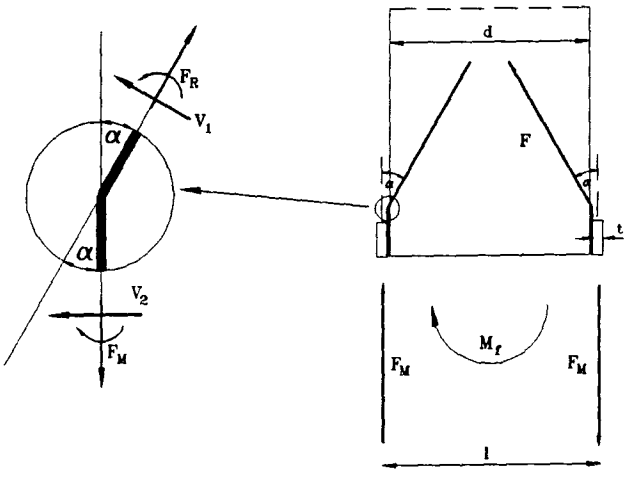

Figure 8.1 Geometry of the splice or foundation joint.

Knowing the geometry of the glulam cross-section and external forces : bending

moment and shear force, the number of re-bars needed to transfer the moment can be calculated.

To calculate lever arm l we add steel plate thickness to the height of the glulam member.

$$l = d + t \tag{1}$$

where:

d - depth of the member.

t - thickness of the strap.

Force Fm acting in the strap can be calculated from the following formula.

$$F_M = \frac{M_f}{l} \tag{2}$$

Knowing Fm axial force in the re-bars Fr and shear force in the re-bars V1 can be obtained from the following formulas, neglecting V2. (See Figure 8.1):

$$F_R = F_M \times \cos(\alpha) \tag{3}$$

$$V_1 = F_M \times \sin(\alpha) \tag{4}$$

To determine the required re-bar area, force Fr should be dived by the characteristic yielding stress in the re-bars.

$$A_{reb}^{req} = \frac{F_R}{F_v} \tag{5}$$

where : Fv is a yielding stress, according to CAN/CSA-S16.1-M89

After determining the required re-bar area the number of re-bars can be established. Weldable re-bars must be specified.

Shear resistance of the re-bars can now be compared with shear force V1 :

$$V_r = \phi \times A_{reb} \times F_s \tag{6}$$

where :

Fs = 0.66 Fv

Areb - area of the re-bars.

The moment capacity of the joint can be calculated:

$$M_r = \frac{\phi F_v A_{reb} l}{\cos(\alpha)} \tag{7}$$

where : phi = 0.67 (number used in design of testing specimen)

8.3.2 STEP 2 - DETERMINE BEARING CAPACITY OF THE STEEL PLATE.

Calculate the dimensions of steel plate needed to carry compression perpendicular to grain.

1. Find compression perpendicular to grain :

Compression force can be calculated as follows (See Figure 8.1):

$$F_c = F_M \tan(\alpha) - \frac{V_1}{\cos(\alpha)} \tag{8}$$

For the design purposes the worst case should be checked so the compression perpendicular to grain should be checked for the following force:

$$F_c = F_M \tan(\alpha) \tag{9}$$

where : Fm = Mf/l

2. Assume steel plate dimensions l1, b.
3. Find the bearing resistance assuming the stress distribution according to Figure 8.2

$$F_{rc} = 0.5 \times (0.5 l_1 \times f_{cp} \times b) \tag{10}$$

Where fcp is obtained from CAN/CSA-089.

4. Check if Frc > Fc - if not increase length l1 and go back to 3.

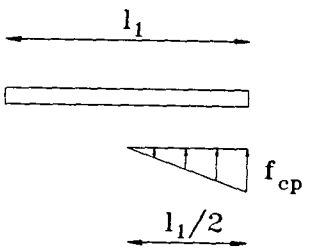

Figure 8.2 Assumed compression perpendicular to grain distribution.

8.3.3 STEP 3 - CHECK COMBINED TENSION AND BENDING RESISTANCE OF STEEL PLATES.

A. CHECK STEEL PLATES FOR TENSION.

The inside steel plates and straps must be checked for tension. The minimum nett cross-sections should be calculated according to the following formula :

$$A_{nett}^{req} = \frac{F_M}{0.85\phi f_u} \qquad (10)$$

Where : steel properties according to CAN/CSA-S16.1-M89

In this research program 12 mm thick steel plate was used.

B. CHECK STEEL PLATES FOR BENDING.

The strap and the interior steel plate must be checked for the bending moment M1 see Figure 8.3.

Assumption : wood bearing is neglected.

$$M_1 = F_R x_R + V_1 x_v \qquad (11)$$

Where :

$x_r = l\sin(\alpha)$

$x_v = l\cos(\alpha)$

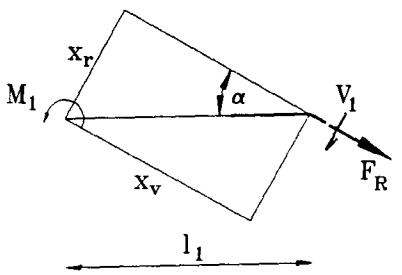

Figure 8.3 Forces acting on the steel plate.

Bending resistance Mr should be calculated according to CAN/CSA-S16.1-M89,

considering that, the cross-section consists of two steel plates, re-bars and welds.

C. CHECK STEEL PLATES FOR TENSION AND BENDING COMBINED.

The steel strap should be checked for tension and bending. Tensile resistance should be calculated using total cross-section (no holes for bolts should be placed over the first re-bar row).

Resistance to bending and tension should be checked according to the following formula :

$$\frac{F_M}{T_r} + \frac{M_1}{M_r} < 1.0 \qquad (11)$$

8.3.4 STEP 4 - CHECK BOLTS (STUDS) FOR SHEAR

In this step the number of studs needed to carry the force from the strap to the inside plate is calculated. The inside plate has tapped holes, National Fine thread is recommended. The studs should be checked for shear for force - Fm.

Shear resistance of the studs, and bearing resistance of the steel plates should be checked according to CAN/CSA-S16.1-M89.

In this testing program 5/8 NF high strength alloy studs were used.

8.3.5 STEP 5 - CHECK WELDS.

RE-BAR TO STEEL PLATE WELD

The weld between steel plates and re-bars should be calculated for the force Fm according to CAN/CSA-S16.1-M89.

8.3.6 STEP 6

Not applicable.

8.3.7 STEP 7

Not applicable.

8.4 KNEE JOINT

8.4.1 CALCULATION OF THE BENDING MOMENT RESISTANCE OF THE JOINT.

1. CALCULATION OF RE-BAR AREA AT THE OUTSIDE PART OF THE JOINT.

Figure 8.4 shows a typical geometry of a knee joint. The cut bisects the angle between column and rafter in to equal parts. The force Fr (tension in re-bars) is assumed to act half way between the two rows of re-bars, if two rows are used.

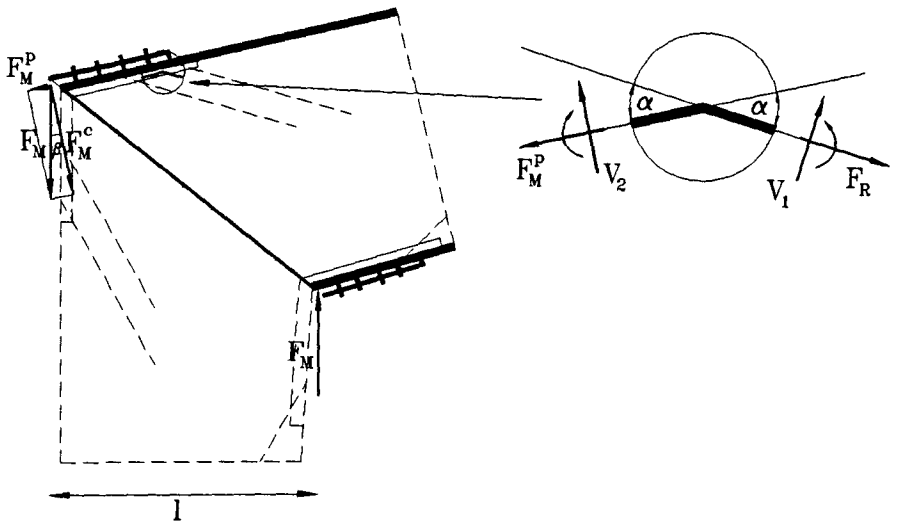

Figure 8.4 Forces in the knee joint.

Knowing the positive bending moment - Mf, at the knee from gravity load, force Fm can be determined from the formula :

$$F_M = \frac{M_f}{l} \qquad (12)$$

where : l - lever arm according to Figure 8.4

Knowing the angle beta the following components can be calculated :

$$F_M^c = F_M \times \cos(\beta) \qquad (13)$$

$$F_M^p = F_M \times \sin(\beta) \qquad (14)$$

The force Fmp travels through the steel plate and then is transferred to the re-bars.

Knowing Fmp axial force in the re-bars and shear force in the re-bars can be obtained from the following formulas :

$$F_R = F_M^p \times \cos(\alpha) \tag{15}$$

$$V_1 = F_m^p \times \sin(\alpha) \tag{16}$$

The required area of re-bars can be now found :

$$A_{reb}^{req} = \frac{F_R}{F_v} \tag{17}$$

where : Fv according to CAN/CSA-S16.1-M89

After determining the required area of the re-bars, the number of re-bars is established. Only weldable re-bars must be specified.

Shear resistance of the re-bars can now be compared with shear force V1 :

$$V_r = \phi \times A_{reb} \times F_s \tag{6}$$

where :

Fs = 0.66 Fv

Areb - area of the re-bars.

Now the positive moment capacity of the joint can be calculated:

$$M_r = \frac{\phi F_v A_{reb} l}{\cos(\alpha)\sin(\beta)} \tag{19}$$

where : phi = 0.67 (as for the steel connections to assure that the connection will not break before the member.)

2. CALCULATION OF THE RE-BAR AREA ON THE INSIDE PART OF THE JOINT.

The geometry of the inside area of joint is presented on Figure 8.5.

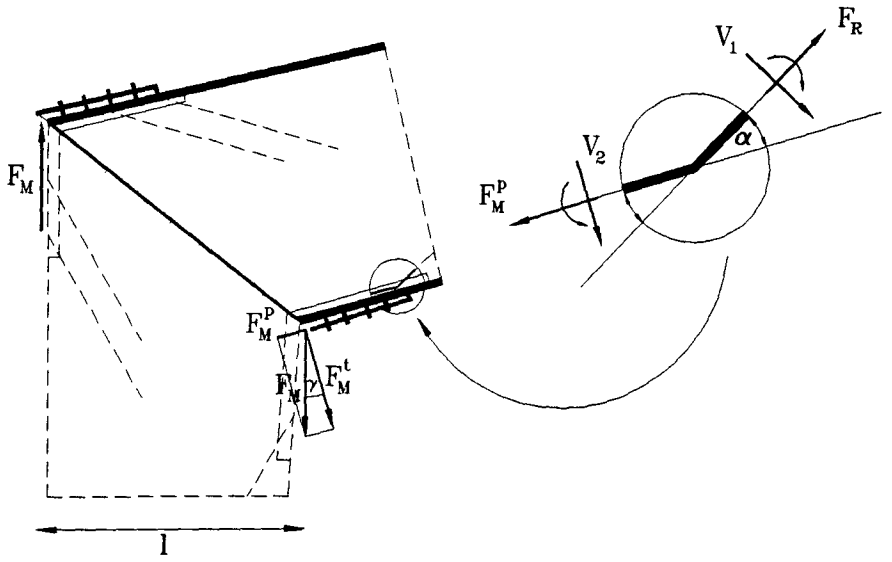

Figure 8.5 Forces on the inside part of the knee joint.

Knowing the maximum negative bending moment value from wind or earthquake load, force Fm can be calculated from the following formula.

$$F_M = \frac{M_f}{l}$$

where : l - lever arm according to Figure 8.5

Knowing the angle gamma the following components can be calculated :

$$F_M^t = F_M \times \cos(\gamma) \qquad (18)$$

$$F_M^p = F_M \times \sin(\gamma) \qquad (19)$$

The force Fmp travels through the steel plate and then is transferred to the re-bars. Knowing Fmp axial force in the re-bars Fr and shear force in the re-bars V1 can be obtained from the following formulas (See Figure 8.5):

$$F_R = F_M^p \times \cos(\alpha) \qquad (3)$$

$$V_1 = F_M^p \times \sin(\alpha) \qquad (4)$$

To determine the required re-bar area, force Fr should be dived by the characteristic yielding stress in the re-bars.

$$A_{reb}^{req} = \frac{F_r}{F_v} \tag{5}$$

where : Fv is a yielding stress, according to CAN/CSA-S16.1-M89

After determining the required re-bar area the number of re-bars can be established. Weldable re-bars must be specified.

Shear resistance of the re-bars can now be compared with shear force V1 :

$$V_r = \phi \times A_{reb} \times F_s \tag{6}$$

where :

Fs = 0.66 Fv

Areb - area of the re-bars.

The moment capacity of the joint can be calculated:

$$M_r = \frac{\phi F_v A_{reb} l}{\cos(\alpha)} \tag{7}$$

where : phi = 0.67 (number used in design of testing specimen)

8.4.2 STEP 2 - DETERMINE BEARING CAPACITY OF THE STEEL PLATE.

Calculate the dimensions of steel plate needed to carry compression perpendicular to grain. Compression perpendicular to grain has to be checked for at two ends of the steel plate :

A. At the end of the plate where the re-bars are welded. Compression check same as for the foundation joint.

B. At the peak of the knee joint. Compression perpendicular to grain has to be checked for the force Fmc (See Figure 8.4)

A. Check compression perpendicular to grain at the end of the plate where the re-bars are welded:

Compression force can be calculated as follows (See Figure 8.4):

$$F_c = F_M^p \tan(\alpha) - \frac{V_1}{\cos(\alpha)} \qquad (8)$$

For the design purposes the worst case should be checked so the compression perpendicular to grain should be checked for the following force:

$$F_c = F_M^p \tan(\alpha) \qquad (9)$$

1. Assume steel plate dimensions l1, b.
2. Find the bearing resistance assuming the stress distribution according to Figure 8.6

$$F_{rc} = 0.5 \times (0.5 l_1 \times f_{cp} \times b) \qquad (10)$$

3. Check if Frc > Fc - if not increase length l1 and go back to 3.

Where fcp is obtained from CAN/CSA-089.

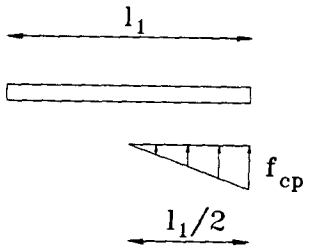

Figure 8.6 Assumed compression perpendicular to grain distribution.

B. Check compression perpendicular to grain at the peak of the joint.

Compression perpendicular to grain at the peak of the joint has to be equal to force Fmc calculated from the following formula :

$$F_M^c = F_M \times \cos(\beta) \qquad (13)$$

1. Assume steel plate dimensions l1, b.
2. Find the bearing resistance assuming the stress distribution according to Figure 8.7

$$F_{rc} = 0.5 \times (0.5 l_1 \times f_{cp} \times b) \qquad (10)$$

3. Check if Frc > Fmc - if not increase length l1 and go back to 3.

Where fcp is obtained from CAN/CSA-089.

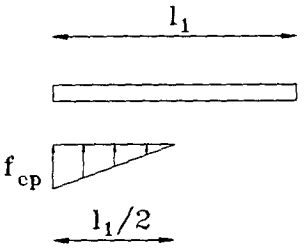

Figure 8.7 Assumed compression perpendicular to grain distribution.

8.4.3 STEP 3 - CHECK TENSION AND BENDING RESISTANCE OF STEEL PLATES.

A. CHECK STEEL PLATES FOR TENSION.

The inside steel plates and straps must be checked for tension. The minimum nett cross-sections should be calculated according to the following formula :

$$A_{nett}^{req} = \frac{F_m^p}{0.85\phi F_v} \qquad (10)$$

Where : steel properties according to CAN/CSA-S16.1-M89

In this research program 12 mm thick steel plate was used.

B. CHECK STEEL PLATES FOR BENDING.

The strap and the interior steel plate must be checked for :

A. Bending moment M1

B. Bending moment M2.

A. Check for bending moment M1.

For the location of bending moment M1 see Figure 8.8

Assumption : wood bearing is neglected.

$$M_1 = F_R x_R + V_1 x_v \qquad (11)$$

Where :

$x_r = l_1 \sin(\alpha)$

$x_v = l_1 \cos(\alpha)$

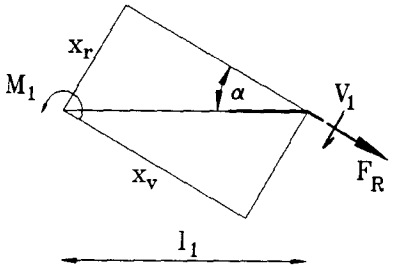

Figure 8.8 Forces acting on the steel plate.

Bending resistance Mr should be calculated according to CAN/CSA-S16.1-M89, considering that, the cross-section consists of two steel plates, re-bars and welds.

B. Check for bending moment M2.

For the location of bending moment M2 see Figure 8.9

Assumption : wood bearing is neglected.

$$M_2 = F_M^c \times l_1 \qquad (12)$$

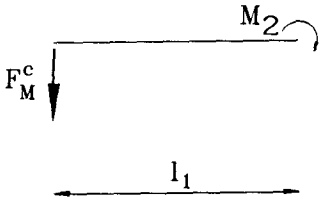

Figure 8.9 Forces acting on the steel plate.

Bending resistance Mr should be calculated according to CAN/CSA-S16.1-M89, considering that, the cross-section consists of two steel plates, re-bars and welds.

C. CHECK STEEL PLATES FOR TENSION AND BENDING COMBINED.

The steel strap should be checked for tension and bending. Tensile resistance should be calculated using total cross-section (no holes for bolts should be placed over the first re-bar row).

Resistance to bending and tension should be checked according to the following formula :

$$\frac{F_M^p}{T_r} + \frac{M_{1,2}}{M_r} < 1.0 \qquad (11)$$

8.4.4 STEP 4 - CHECK BOLTS FOR SHEAR

In this step the number of bolts needed to carry the force from the strap to the steel plate is calculated. The steel plate must have tapped holes. National Fine thread is recommended. Bolts should be checked for shear for force - Fmp.

Bolts for shear and steel plate bearing should be checked according to CAN/CSA-S16.1-M89.

In this testing program 5/8 NF high strength bolts were used.

8.4.5 STEP 5 - CHECK WELDS.

WELDING OF RE-BAR TO STEEL PLATE.

Weld between steel plates and re-bars should be calculated for force Fmp according to CAN/CSA-S16.1-M89.

WELDING OF STRAP

Check weld thickness for strap and inside stiffener.

Weld should be checked for force Fm according to CAN/CSA-S16.1-M89

8.4.6 STEP 6 - DESIGN INTERIOR STIFFENER - SHEAR RESISTANCE

The shear resistance of the knee joint is provided by the interior stiffener.

Interior stiffener should be checked for shear since the shear resistance provided by the straps is limited. For the interior stiffener geometry see Figure 8.9.

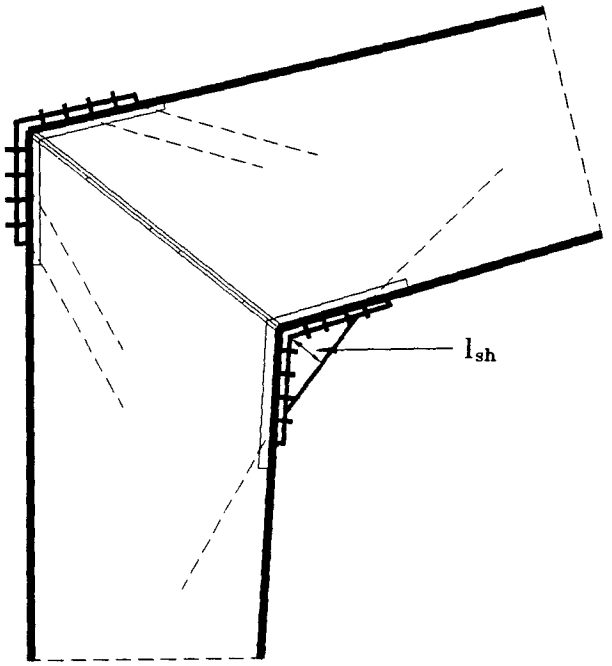

Figure 8.10 Interior stiffener.

Shear force obtained from analysis - Vf should be less then shear resistance Vr

$$V_r = \phi A F s \qquad (27)$$

$$F_s = 0.66 F y$$

The shear area required can be found as follows :

$$A^{req} = \frac{V_f}{\phi 0.66 F_u} \qquad (28)$$

So the height of the stiffener is :

$$l_{sh}^{req} = \frac{A^{req}}{2t} \qquad (30)$$

where t - thickness of stiffener (use 2 stiffeners for two rows of re-bars)

In this testing program t=12 mm lsh=95 mm.

The interior stiffener plates should allow direct transfer of the force from one member to the other for negative moments. Therefore the alignment of the re-bars, should coincide with the outside edge of the stiffeners, and the plane of the stiffeners. See Figure 8.10

8.4.7 STEP 7 - CHECK DEFLECTIONS UNDER SPECIFIED LOADS.

The deflection check of a structure equipped with glued-in rod connections can be performed using all frame analysis computer programs, which are able to simulate joints as rotational springs. Glued-in rod joints are modelled as rotational springs with known stiffness. The average rotational stiffness of the knee joints tested was c= 46900 kNm/rad. The stiffness was calculated from joint opening data, the rotational change of two members and the readings under specified load were used.

CONCLUSIONS

1. A stiffer connection method has been developed that will enable the industry to design and build statically indetermined structural systems. This in turn will permit the industry to expand its' markets to include the structures which they could not build previously due to a lack of connection methods.

This connection is based upon the use of glued-in reinforcing bars inserted at a 30 degree angle to the length of the glulam member, thus engaging the whole cross-section to participate in the transfer of the forces.

2. The required minimum embedment length was established but it is recommended that the reinforcing bars be inserted so some of them cross in order to improve the shear carrying capacity of the glulam in addition to forming the anchor for transferring tension and compression forces.

3. A simple manufacturing method was derived to produce test specimens but a more sophisticated production methods should be developed for commercial manufacturing.

4. The type of structural connections used in this experiment includes connections for : beam splice, column foundation, knee joints for frames.

5. Suggested design methods for these connections are outlined in the thesis.

6. The appearance of the connection was of primary concern. By attaching the reinfor-

cing bars to the underside of a dapped in steel plate the appearance was found to be acceptable.

7. The connection is designed so the failure takes place as ductile steel failures without affecting the timber. The timber connection thus has a reliability equal to that of a steel joint.

FUTURE RESEARCH

The tests described in this thesis have been limited to short term tests. However since the failure takes place as yielding in the reinforcing bars it could be argued that the experience with steel connections can be transferred directly.

It would never the less be prudent to conduct additional tests aimed at investigate the effect of varying temperature and moisture content might have on the interface between the glue and the wood.

Glued-in rods with the rods placed parallel to grain have been used in practice in Europe for more than 25 years without apparent trouble, but despite this it would be prudent to conduct additional experiments.

The creep behaviour of the joint would also be useful information.

SUMMARY OF TEST DATA

Test type	Connection type	Number of bars bar dia. (mm)	Failure mode	Stress in bars at failure (MPa)	Max. force in steel plates (kN)	Max. bending moment (kNm)
Pull-out	Preliminary	1x20	Re-bar tension failure	495	171	
Pull-out	Pre-welded	1x20	Re-bar tension failure	517	189	
Pull-out	Pre-welded	2x20	Re-bar tension failure	478	345	
Beam test	Pre-welded	2x20	Re-bar tension failure	344	237	92
Racking tests:						
Spec-1	Pre-welded	2x20	Re-bar tension failure	336	231	90
Spec-2	Pre-welded	3x20	Re-bar tension failure	378	341	175
Spec-3	Pre-welded	4x20	Re-bar tension failure	325	390	200
Spec-4	Pre-welded	4x20	Shear stud failure	398	478	245

Test type	Connection type	Number of bars bar dia.	Failure mode	Stress in bars at failure (MPa)	Max. force in steel plates (kN)	Max. bending moment (kNm)
Knee joint tests:						
Spec-1	Pre-welded	4x20	Compr. perp. failure	276	381	148
Spec-2	Pre-welded	4x20	Re-bar tension failure	342	472	302
Spec-3	Pre-welded	4x20	Re-bar tension failure	395	545	349
Spec-4	Pre-welded	4x20	Re-bar tension failure	392	541	346
Spec-5	Pre-welded	4x20	Compr. perp. failure	405	559	358

Bibliography

Baird, J.A., Ozelton, E.C.,1990

Timber designers' manual, Collins, London, U.K.

Buchanan, A.H., Moss, P.J., Townsend, P.K., 1990

Reinforced bars epoxy bonded in glue laminated timber, Proceedings of the 1990 International Conference on Timber Engineering, Tokyo, Japan.

Canadian Institute of Steel Construction, 1992

Handbook of steel construction, Canadian Institute of Steel Construction, Willowdale, Ontario, Canada.

Canadian Wood Council, 1990

Wood designers manual, Canadian Wood Council, Ottawa, Ontario, Canada.

Crews, K.J., 1991

Joints and connections: Timber engineered structures, Australian Forest Industries Journal, November 1991.

Fairweather, R.H., Buchanan, A.H., 1992

Beam column connections for multi-storey timber buildings, Research report, Department of Civil Engineering, University of Canterbury, Christchurch, New Zealand.

Foschi, R.O., Folz, B.R., Yao, F.Z., 1990

Reliability based design of wood structures, Report No. 34, Department of Civil Engineering, University of British Columbia, Vancouver, Canada.

Keenan, F.J.,1986

Limit states design of wood structures, Morrison Hershfield Ltd, Toronto, Ontario, Canada.

Madsen, B., 1992

Structural behaviour of timber, Timber Engineering Ltd., Vancouver, BC,Canada.

McIntosh, K.A., 1989

From theory to reality - 30 years in glulam manufacture, Proceedings
of the second pacific timber engineering conference, Auckland, New Zealand.

Riberholt, H.,1980

Steel bolts glued into glulam, Proceedings, Meeting of IUFRO Wood Engineering Group, Oxford, U.K.

Riberholt, H.,1986

Glued bolts in glulam, Department of Structural Engineering, Technical University of Denmark, Series R, Number 210.

Riberholt, H.,1988

Glued bolts in glulam. Proposals for CIB code, Proceedings, CIB Meeting 21, Parksville, BC, Canada.

Townsend, P.K., Buchanan, A.H., 1990

Steel dowels epoxy bonded in glue laminated timber, Research report, Department of Civil Engineering, University of Canterbury, Christchurch, New Zealand.

Turkowskij, S., 1991

Prefabricated joints of timber structures on inclined glued-in bars, Proceedings of the 1991 International Timber Engineering Conference, Volume 3, Trada, London, U.K.

Turkowskij, S., Lukyanow, E.I., Pogoreltsew, A.A., 1991

Use of glued-in bars for reinforcement of wood structures, Proceedings of the 1991 International Timber Engineering Conference, Volume 3, Trada, London, U.K.

APPENDIX A.

FRAME ANALYSIS

1.1 DESIGN OF TWO HINGE PORTAL FRAME.

A two hinge glulam frame of the geometry shown on Figure A.1 was designed for an industrial building in Vancouver. The following sections present the loads, and the design of decking and purlins, as well as design of the frame.

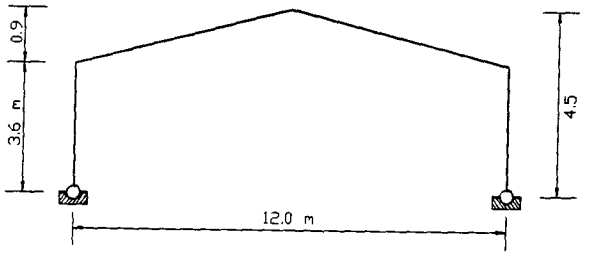

Figure A1. Two hinge glulam frame.

1.2 SNOW LOAD

The snow load was calculated for Vancouver (Granville and 41).

The specified loading, S, due to snow accumulation on a roof is

$$S = S_s(C_b C_w C_s C_a) + S_r$$

Ss - ground snow load in kPa	Ss = 2.5 kPa
Sr - associated rain load in kPa	Sr = 0.3 kPa
Cb - basic roof snow load factor	Cb = 0.8
Cw - wind exposure factor	Cw = 1.0
Cs - slope factor	Cs = 1.0 when roof slope alpha < 15 deg
	alpha = 8 deg
Ca - accumulation factor	Ca = 1.0

$$S = 2.5 \times 0.8 \times 1.0 \times 1.0 \times 1.0 + 0.3$$

$$S = 2.3 kPa$$

Spacing range - 3.0 to 6.0 m

Smax is the snow load for the maximum spacing - 6.0 m.

$$S_{max} = 2.3 \times 6 = 13.8 \left(\frac{kN}{m} \right)$$

The code requires checking of two loading modes.

1. Full load on entire span.
2. Full load on half of the span, and half load on the other part.

$$\frac{S_{max}}{2} = 6.9 \frac{kN}{m} = 6.9 \frac{N}{mm}$$

1.3 WIND LOAD

EXTERNAL WIND PRESSURE

The specified external pressure or suction due to wind is:

$$p = q \times C_e \times C_g \times C_p$$

p - the specified external pressure acting statically and in the direction normal to the surface.

q - the reference velocity pressure (probability of being exceeded in any one year in 30 for the design of structural members

q = 0.55 kPa

Ce - exposure factor Ce = 0.9 for height < 6 m

Cg - the gust effect factor

Cp - the external pressure coefficient

Cp Cg - used together for low buildings

	Direction of pressure			
Roof slope deg	1 front	2 roof	3 roof	4 back
8	0.84	-1.3	-0.78	-0.65

Table 2.1 External wind pressures.

INTERNAL WIND PRESSURE

The following three cases have been checked:

CASE 1. Openings in wall at which wind is blowing.

CASE 2. Openings in wall opposite the wall wind is blowing.

CASE 3. Wind parallel to ridge.

Table 2.2 presents internal wind pressure coefficients.

	Direction of pressure			
CASE #	1 front	2 roof	3 roof	4 back
1	-0.7	-0.7	-0.7	-0.7
2	0.5	0.5	0.5	0.5
3	0.7	0.7	0.7	0.7

Table 2.2 Internal wind pressures.

TOTAL WIND PRESSURES

The following table presents the total wind pressures.

	Direction of pressure Total wind pressures (kPa)			
CASE #	1 front	2 roof	3 roof	4 back
1	0.07	-0.99	-0.73	-0.67
2	0.66	-0.64	-0.39	-0.07
3	0.76	-0.64	-0.39	-0.02

Table 2.3 Total wind pressures.

Figure 2.6 illustrates the directions of wind pressures.

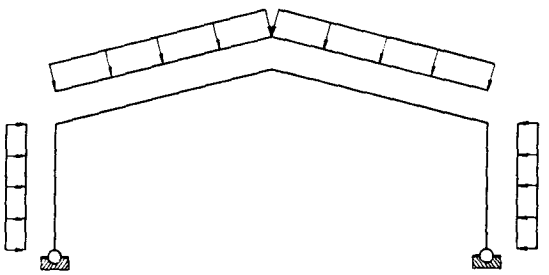

Figure 2.6 Directions of wind pressures. (Positive values)

1.4 EARTHQUAKE LOAD

The minimum lateral seismic force, V, shall be calculated in accordance with the following formula.

$$V = \left(\frac{V_e}{R}\right)U$$

Where :

U = 0.6

R - force modification factor

R = 2.0 (moment resisting wood space frame with ductile connections)

In the present code it is assumed that the commercially available types of fasteners are used. The force modification factor R should reach 3, depending on the actual stiffness, for the glued-in rod joints. The actual stiffness is discussed in the chapters describing experimental results. (Chapter 8).

Presently used connection methods do not provide rigid joints. Assuming rigidity and failure in steel for glued in rod joint this structure should be treated as a steel structure. The equivalent lateral seismic force, representing elastic response, Ve :

$$V_e = v \times s \times I \times F \times w$$

v - zonal velocity ratio

v = 2.0 for Vancouver

Za = Zv = 4.0

Za/Zv = 1.0

s - seismic response factor

T - fundamental period

$$T = \frac{0.09 \times h_n}{\sqrt{D_s}}$$

Ds = 12.0 m hn = 3.6 m

$$T = \frac{0.09 \times 3.6}{\sqrt{12}} = 0.093s$$

From Table 4.1.9.A (National Building Code) S = 3.0

I - seismic importance factor I = 1.5

F - foundation factor - assume F = 1.5

W - the weight of the structure

$$w = w_{roof} + w_{purlins} + w_{frame} + w_{snow}$$

$$w_{roof} = 0.27 \times 6.0 \times 12.0 = 19.4kN$$

$$w_{purlins} = 0.24 \times 6.0 \times 7 = 10.1kN$$

$$w_{frame} = (2 \times 3.6 + 12.0) \times 0.63 = 12.1kN$$

$$w_{snow} = 2.3 \times 6 \times 12 \times 0.25 = 41.4kN$$

$$w = 83.0kN$$

$$V_e = 0.2 \times 3 \times 1.0 \times 1.5 \times 83.0 = 74.7kN$$

$$V = \left(\frac{74.7}{2}\right) \times 0.6 = 22.4kN$$

Force V = 22.4 kN is applied at node 2 during finite element analysis

1.5 DESIGN OF MEMBERS

1.5.1 MATERIALS

The following materials were used for design :

1. Commercial grade decking.
2. Purlins - glulam, D.Fir-L, 20f-E.
3. Frame - glulam, D.Fir-L, 20f-E.

1.5.2 DECKING DESIGN

- Roof deck

- Specified Dead Load =	- wood decking self weight	= 0.13 kPa
	- felt	= 0.14 kPa
	Total load	**= 0.27 kPa**

- Specified Live Load = - snow load = 2.3 kPa

- Purlin spacing = 2.0 m

- Dry service condition

- untreated

- deflection limitation of L/180 based on total specified load

- use controlled random pattern western red cedar

- commercial grade

Factored loading = Wf = 1.25x0.27 + 1.5x2.3 = 3.8 kPa

Total specified loading = W = 0.27 + 2.3 = 2.6 kPa

From Decking Selection Tables (Wood Design Manual) select 38 mm thickness

Wfr = 11.0 kPa > 3.8 kPa O.K.

Wdr = 3.95 kPa > 2.6 kPa O.K.

1.5.3 PURLIN DESIGN

Purlin spacing = 2.0 m

Purlin span = 6.0 m

Specified Dead Load = 0.27 kPa (decking + felt)

Specified Live Load = 2.3 kPa (snow)

Standard load duration

Dry service condition

Untreated

CALCULATION

Tributary area = 2.0 x 6.0 = 12.0 m^2

Factored load = 1.25x0.27 + 1.5x2.3 = 3.8 kPa

Specified load = 0.27 + 2.3 = 2.6 kPa

Self weight = 5.3x0.13x0.342 = 0.24 kN/m - try 130x342 glulam

Wf = 3.8x2.0 + 0.24x1.25 = 7.9 kN/m

W = 2.6x2 + 0.24 = 5.4 kN/m

Wl = 2.3x2.0 = 4.6 kN/m

$$M_f = \frac{w_f L^2}{8} = \frac{7.9 \times 6.0^2}{8} = 35.6 kNm$$

$$V_f = \frac{w_f \times L}{2} = \frac{7.9 \times 6.0}{2} = 23.7 kN$$

For L/180 deflection limit based on total load:

$$E_s I_{Reqd} = 180 \frac{5wL^3}{384} Nmm^2 = 180 \times \frac{5 \times 5.4 \times 6000^3}{384} = 2734 \times 10^9 Nmm^2$$

For L/360 deflection limit based on live load:

$$E_s I_{Reqd} = 360 \frac{5wL^3}{384} Nmm^2 = 360 \times \frac{5 \times 4.6 \times 6000^3}{384} = 4656 \times 10^9 Nmm^2$$

From beam selection tables for glulam

use : cross-section 130 x 342 mm, D.Fir-L, 20f-E

Mr = 58.4 kNm

Vr = 53.4 kN

EsI = 5370*10^9 Nmm^2

1.5.4 TOTAL LOADS

Several load combinations were checked during the analysis. See 1.11.4.2.

According to the CAN/CSA-O861-M89 Clause 4.2.4.1 the factored load combination shall be taken as:

$$\alpha_D D + \gamma\psi(\alpha_L L + \alpha_Q Q + \alpha_T T)$$

where:

D - dead load due to load of members

L - live load due to snow and rain

Q - live load due to wind and earthquake

T - loads due to contractions or expansion caused by temperature changes

LOAD FACTORS

$\alpha_D = 1.25, \vee 0.85 \epsilon .cases.of.stress.reversal$

$\alpha_L = 1.5$

$\alpha_Q = 1.5 for wind$

$\alpha_Q = 1.0 for earthquake$

$\alpha_T = 1.25$

$\psi = 0.7 when.two.L, Q.act$

1.5.5 LOADING ON THE FRAME

All load values presented in this section are unfactored.

1. ROOF DEAD LOAD

Ws = 0.27 + 0.1 = 0.37 kPa

Wsp = 2 x 0.37 = 0.74 kN/m

Vp = 0.74 x 6 = 4.4 kN - reaction from 2 purlins

2. SNOW LOAD

Ws = 2.3 kPa

Wsp = 2.3 x 2 = 4.6 kN/m

Vp = 4.6 x 6 = 27.6 kN - reaction from 2 purlins

3. WIND LOAD

Wind loads :

CASE 1:

P1 = 0.42 kN/m P2 = -5.94 kN/m P3 = -4.38 kN/m P4 = -4.02 kN/m

CASE 2:

P1 = 3.96 kN/m P2 = -3.84 kN/m P3 = -2.34 kN/m P4 = -0.42 kN/m

CASE 3:

P1 = 4.56 kN/m P2 = -3.84 kN/m P3 = -2.34 kN/m P4 = -0.12 kN/m

4. EARTHQUAKE LOAD

V = 22.4 (earthquake load applied at node 2)

1.5.5.1 LOAD CASES

1. Frame self weight
2. Roof dead load
3. Full snow load
4. Earthquake load
5. Half snow load
6. Wind load - case 1
7. Wind load - case 2
8. Wind load - case 3

1.5.5.2 LOAD COMBINATIONS

1. (Roof dead load + frame self weight) x 1.25 + (full snow load) x 1.5
2. (Roof dead load + frame self weight) x 0.85 + (wind load) x 1.5
3. (Roof dead load + frame self weight) x 0.85 + (earthquake load) x 1.0
4. (Roof dead load + frame self weight) x 0.85 + ((wind load - case 1) x 1.5 + (half snow load) x 1.5) x 0.7

1.6 MATERIAL PROPERTIES

Modulus of elasticity for 20 f-EX glulam according to the code is E = 12400 MPa. Shear modulus G = 852 MPa. Glulam density = 5.3 kN/m ^ 3.

1.7 ANALYSIS RESULTS

The following table presents the internal forces obtained during analysis at knee joint for all load combinations.

Load combination	Bending moment kNm	Shear force kN	Axial force kN
1. Full snow	219.5	111.4	147.9
2. Wind	51.6	26.5	18.5
3. Earthquake	-22.6	3.3	22.9
4. Wind + half snow	76.6	24.4	25.3

Table 2.4 Internal forces obtained during analysis.

The maximum bending moment occurred during full snow load - positive moment resulting in tension on outside of the frame, and during earthquake load - negative bending moment resulting in tension on the inside part of the knee joint area. Negative moment from earthquake load was around 10% of the positive moment from full snow load. Maximum shear and axial forces were found during full snow load.

1.7.1 DESIGN OF CROSS-SECTION

Try glulam 175 x 646 mm 20f-EX, D.Fir-L.

The following design was done according to CAN/CSA-O86.1-M89

1.7.1.1 BENDING MOMENT RESISTANCE

The factored bending moment resistance shall be taken as :

$M_r = \phi F_b S K_L K_x$

where :

$$\phi = 0.9$$

$$F_b = f_b(K_D K_H K_{Sb} K_T)$$

$$K_D = 1 ; K_H = 1 ; K_{Sb} = 1 ; K_T = 1 ; K_L = 1 ; K_x = 1$$

$$f_b = 25.6 Mpa$$

$$S = \frac{175 \times 646^2}{6} = 12.2 \times 10^6 mm^3$$

$$M_r = 0.9 \times 25.6 \times 12.2 \times 10^6 \times 1 \times 1 = 280.4 kNm > M_f = 219.5 kNm . O.K.$$

1.7.1.2 SHEAR RESISTANCE

The factored shear resistance shall be taken as :

$$V_r = \phi F_v \frac{2A}{3} K_N$$

where :

$$\phi = 0.9$$

$$F_v = f_v (K_D K_N K_{Sv} K_T)$$

$$f_v = 2.0 Mpa$$

$$K_D = 1 ; K_H = 1 : K_{Sv} = 1 ; K_T = 1 K_N = 1$$

$$A = 175 \times 646 = 11.3 \times 10^4 mm^2$$

$$V_r = 0.9 \times 2.0 \times 11.3 \times 10^4 \times \frac{2}{3} \times 1 = 135.7 kN > V_f = 111.4 kN . O.K.$$

1.7.1.3 COMPRESSIVE RESISTANCE

The factored compressive resistance parallel to grain shall be taken as:

$$P_r = \phi F_c A K_c$$

where :

$$\phi = 0.9$$

$$F_c = f_c (K_D K_H K_{Sc} K_T)$$

$$f_c = 20.4 Mpa$$

$$K_D = 1 ; K_H = 1 : K_{Sc} = 1 ; K_T = 1$$

$$A = 175 \times 646 = 11.3 \times 10^4 mm^2$$

$$C_c = \frac{3.6}{0.175} = 20.6$$

$$C_k = \sqrt{\frac{0.76 \times 0.87 \times 12400 \times 1 \times 1}{20.4}} = 20.0$$

$$K_c = \frac{1}{2 \times 20.6^2} \frac{0.87 \times 12400 \times 1 \times 1}{20.4} = 0.62$$

$$P_r = 0.9 \times 20.4 \times 11.3 \times 10^4 \times 0.62 = 1293.3kN > P_f = 146.9kN \, .O.K.$$

1.7.1.4 RESISTANCE TO COMBINED BENDING MOMENT AND AXIAL LOAD

Members subject to combined bending and axial loads shall be designed to satisfy the following interaction equation

$$\frac{P_f}{P_r} + \frac{M_f}{M_r} < 1.0$$

$$\frac{147.9}{1293.3} + \frac{219.5}{280.4} = 0.11 + 0.78 = 0.89 < 1.0 . O.K.$$

Use 175 x 646 mm glulam 20f-EX D.Fir-L